Investigation of Diazapyrones in the Context of Bioorthogonal Chemistry

Kaitlyn Morrill

A thesis submitted in partial fulfillment of the requirements for the Masters degree in Chemistry and Biomolecular Sciences

Department of Chemistry and Biomolecular Sciences

Faculty of Science

University of Ottawa

Abstract

The field of bioorthogonal chemistry uses click chemistry as a tool to further understand cellular function. The tools of bioorthogonal chemistry include cell and metabolic probes, fluorescent probes with varying bioorthogonal handles that can be used for cell labelling, and gauging metabolic function. This is done by using non-toxic, orthogonal, and selective chemical probes that do not interfere with the complex environment of the cell (termed bioorthogonal). An example of a bioorthogonal reaction is the tetrazine ligation, which occurs via an Inverse Electron Demand Diels Alder (IEDDA) reaction with the 4π and 2π orbitals of a tetrazine and an alkyne/alkene, respectively. This reaction is considered bioorthogonal due to the reagents' high selectivity, quick kinetic rates of reaction, and the reaction's high yield, all of which do not disturb the native cellular environment. The key advantage of this reaction is its extremely fast rate, with second-order rate constants ranging from 10^3 to 10^6 $M^{-1}s^{-1}$ with the exergonic release of $N_{2\ (g)}$ as the sole by-product which causes the reaction to be irreversible. However, tetrazines are easily hydrolyzed and are redox-sensitive.

In this work, we describe herein an alternative bioorthogonal reagent to tetrazine in an IEDDA reaction with cyclooctynes or trans-cyclooctene (TCO). Currently, the tetrazine ligation, with an alkene/alkyne is the fastest bioorthogonal reaction known. Based on this, we investigated the synthesis of diazapyrones as an alternative heterocycle to tetrazine. We also investigated the synthesis of trans-cyclooctenes using a photochemical flow reactor developed by Dr. Fox *et al*. From this we aimed to develop two cycloaddition reactions, the first one using bicyclononyne (BCN) and the second using strained trans-cyclooctenes (sTCO). Both of these reagents act as the dienophiles. Evaluation of reactions between diazapyrones, cyclooctynes, and trans-cyclooctenes was done through kinetic studies using UV-Vis spectroscopy under pseudo-first-order conditions.

Different diazapyrones were tested accordingly with BCN and sTCO dienophiles. The effects of varying substituents on the diazapyrones were also studied. From the results, it was determined that electron-poor diazapyrones react the fastest with BCN and sTCO. Kinetic studies also indicated that diazapyrones are unstable in aqueous environments and are prone to hydrolysis. However, this primarily poses issues for electron poor diazapyrone. The reactions between diazapyrones and cyclooctynes or trans-cyclooctenes are slower than the established tetrazine ligation (k2 ~ 1 – 10^4 $M^{-1}s^{-1}$). The k2 values are 10^{-2} $M^{-1}s^{-1}$ and 10 $M^{-1}s^{-1}$ respectively. However, reaction rates are comparable to other established bioorthogonal reactions such as SPACC (k~ 10^{-2} – 10 $M^{-1}s^{-1}$) or SPANC (k~ 10 – 60 $M^{-1}s^{-1}$). Thus, this reaction is a useful addition to the bioorthogonal toolbox and can be applied in cell labelling experiments.

Statement of Work

The work presented in this thesis was completed on my own and I take full responsibility for its content. All experiments, research, and analysis were completed by me. The trans-cyclooctene molecule used in chapter 3 was synthesized by Colette Makara of the Fox lab.

Acknowledgments

I would like to express my sincerest gratitude to Dr. John Pezacki for his guidance, insights, and encouragement. You took me under your wing the moment I met you and I would not be the scientist I am today without your support and guidance. The things I have learned during my time in the Pezacki lab have been invaluable and will help me in my future endeavors. Thank you to my committee members Dr. Jeffrey Keillor and Dr. Andre Beauchemin for your insight and for reading my thesis.

Much of this work would not have been possible without the support and help from all the Pezacki members. Specifically, I would like to thank David Lefebvre, Christine Hum, Gabe Sullivan, and Jordan Brazeau-Henrie (Boddy lab). You four made me laugh every day especially when it came to piquant. I wouldn't have made it to this point without you. I would like to thank Didier Bilodeau for mentoring me 4 years ago and helping me become the chemist I am. Thank you for your guidance, training, support, and mentorship. I have learned many valuable chemical techniques from you and would not have been able to complete this project without all of your help and troubleshooting. I would also like to thank Dr. Shadi Sedghi Masoud. You made every day on the chem side a blast with all of your sassy comments and it has been a pleasure working with you. Thank you for reading my thesis, helping with troubleshooting, and putting up with me. I would also like to thank Kaitlyn Margison for her support and her assistance with obtaining and analyzing the kinetic data.

I would like to thank my friends and family for all their love and support over the years. To my mother and father, I wouldn't have made it here without you. Thank you for making me laugh, for your endless support, and for always being there for me. To my siblings Adam, Tamara, and Ethan

you are annoying but I guess I like you. To Annette Cook you're amazing. Thank you for making me take a break to have a craft night or to go climbing and all your sarcasm. To Maisie thank you for walking all over my laptop and adding some kitty magic to my thesis – you are the best little co-author I could ask for (even after you deleted half my thesis). Last, but certainly not least, thank you Orie, for all your cuddles and your sassy attitude. I wouldn't have made it this far without you. You were the best friend I ever had, and I cherish the 16 years I had with you. I miss you very much, This one's for you Babaloon.

Table of Contents

List of Figures

List of Tables

List of Schemes

List of Abbreviations

ACN	-	Acetonitrile
BARAC	-	Biarylazacyclooctynone
BCN	-	Bicyclo[6.1.0]non-4-yne
CuAAC	-	Cu(I)-catalyzed 1,3-dipolar azide-alkyne cycloaddition
DAP	-	Diazapyrone
DIBO	-	Dibenzocyclooctynol
DIFO	-	Difluorinated cyclooctyne
DMSO	-	Dimethyl sulfoxide
EDG	-	Electron-donating group
EWG	-	Electron-withdrawing group
FMOT	-	Frontier molecular orbital theory
HOMO	-	Highest occupied molecular orbital
IEDDA	-	Inverse-electron demand Diels Alder
LC-MS/ESI$^+$	-	Liquid chromatography-mass spectroscopy/electrospray ionization
LUMO	-	Lowest unoccupied molecular orbital
m	-	Meta
MW	-	Molecular weight
NMR	-	Nuclear magnetic resonance
o	-	Ortho
OCT	-	Cyclooctyne
p	-	Para
Py	-	Pyridine

RDS	-	Rate determining step
SPAAC	-	Strain-promoted azide-alkyne cycloaddition
SPANC	-	Strain-promoted alkyne-nitrone cycloaddition
s-TCO	-	Strained – trans-cyclooctene
tet	-	Tetrazine
TLC	-	Thin-layer chromatography
UV- Vis	-	Ultra Violet- visible

Chapter 1 – Introduction

1.1 Bioorthogonal Chemistry

It is an understatement to say that the biology of cells and organisms are complex. Cells contain an exorbitantly large number of functional groups and have several parts working in tandem with one another. For instance, cells contain macromolecules such as lipids, proteins, and sugars all with important and complex cellular roles, which makes studying these difficult. This is particularly evident when trying to study a system without damaging or interfering with its native function. A vital tool to overcome these problems is the use of the bioorthogonal chemistry toolbox, which aims to solve biological problems through the use of chemical tools.

Bioorthogonal chemistry is a set of chemical reactions that can occur within a cell without interfering with its native function or environment. This allows for the inner workings of a cell to be studied by modifying particular cellular components in real-time.[1] This is generally done using small-molecule probes such as cycloalkenes and cycloalkynes, often referred to as minitags.[2] These probes can selectively bind to a target protein via an amino acid to monitor or modify its function, allowing us to gain a deeper understanding of biochemical pathways and processes occurring within the cell. To be considered bioorthogonal, a stringent set of criteria need to be met, resulting in very few reactions being classified as such. These criteria are split amongst the starting materials (1), the reaction (2), and the product (3) of a given chemical reaction. (1) The starting materials for these reactions must be stable and cannot interact with the native chemicals of the cell (i.e. orthogonal). (2) The reaction must also be metabolically stable while simultaneously being non-toxic.[3] Furthermore, the reaction should proceed in a high yield while being spontaneous, irreversible, and specific, with little to no side products.[4,5] (3) The final products

must also be stable under physiological conditions. Historically, the first reaction to fit these criteria was the Staudinger ligation.

1.2 Click chemistry -Staudinger Ligation

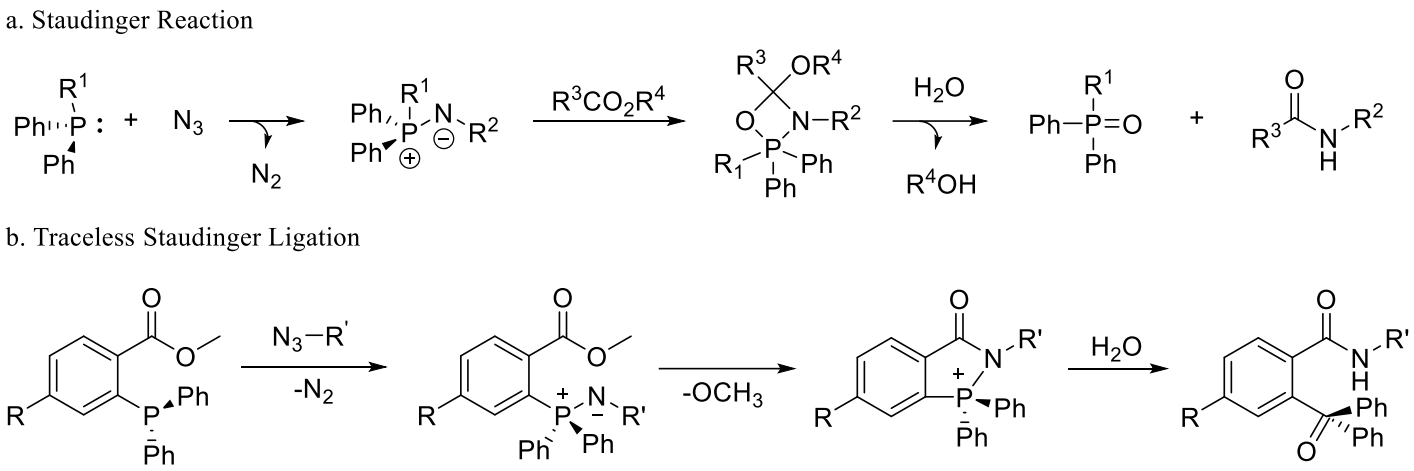

Scheme 1.1 The Staudinger ligation.

The first bioorthogonal click reaction was the Traceless Staudinger ligation which was discovered by Bertozzi and Raines in 2000,[6,7] based on the Staudinger reaction discovered in 1919 by Hermann Staudinger.[8] In the Staudinger reaction (**Scheme 1.1a**), a phosphane and azide react together to form an iminophosphorane intermediate which can react with a carboxylic acid derivative to form an amide bond. This reaction is a good basis for bioorthogonal chemistry due to the molecule's small size and the fact that it is not naturally occurring in cells and cannot cross-react with any functionalities found in the cell. In 2000, Bertozzi and Raines discovered the traceless Staudinger ligation (**Scheme 1.1b**)[6,7]. This reaction was deemed "traceless" due to the loss of the phosphane-containing by-product. An azide and acylated phosphane react together via a nucleophilic attack to form the iminophosphorane intermediate. This intermediate contains an

electron trap where the carbonyl group from the acylated phosphane pulls the electron density away from the N atom thereby "trapping" it.[6] The imnophosphorane is then easily hydrolyzed in an aqueous environment forming an amide bond. This is significant because amides are a key functional group found within the cellular environments and are involved in the formation of peptide bonds which opens the door to modifying biomolecules in a living system.[9] The benefits of this reaction over the Staudinger reaction are that it combines bioorthogonality while being non-toxic, selective, fast, and high yielding.

1.3 Copper-Catalyzed Azide Alkyne Cycloaddition (CuAAC)

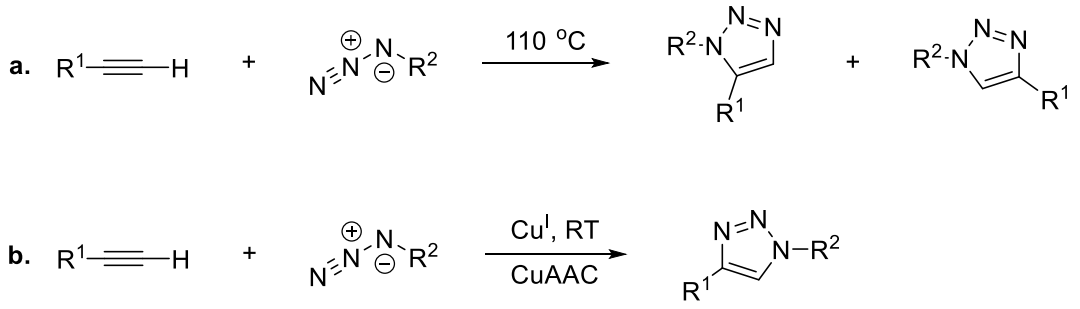

Scheme 1.2 Cycloaddition between a terminal alkyne and azide via a. the 1,3-dipolar cycloaddition and b. CuAAC.

The copper-catalyzed Azide-Alkyne Cycloaddition (CuAAC) is an expansion of the Huisgen 1,3-dipolar cycloaddition discovered by Meldal and Sharpless, which is a Cu(I) catalyzed reaction between an azide and a terminal alkyne (**Scheme. 1.2**).[10,11,12] The addition of the Cu(I) catalyst allows the reaction to have k_2 values between 10-200 $M^{-1}s^{-1}$.[13] This means that the CuAAC reaction is approximately 5 times faster than the Staudinger ligation and approximately 10-100 times faster than the copper-free azide-alkyne cycloaddition.[14,15] Besides increasing the rate of the reaction through the Cu(I) catalyst, using CuAAC allows us to decrease the temperature of this

bioorthogonal reaction as well as being regioselective. This makes the reaction more applicable to bioorthogonal chemistry compared to the 1,3-dipolar cycloadditions. However, at high concentrations, the Cu(I) catalyst is toxic to cells. This is because the Cu(I) catalyst gets oxidized in the presence of O_2 or H_2O_2 into Cu(II) via Fenton chemistry (**Scheme 1.3**),[16] which form superoxides and hydroxyl radicals, respectively, causing oxidative stress and damage to the biological system. Despite this, CuAAC is still one of the most used click reactions due to its versatility for labelling and capturing native bio-functionalities.[17]

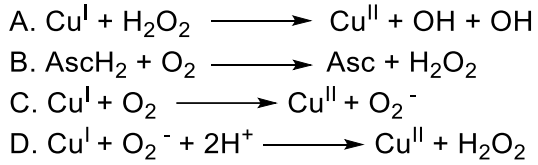

Scheme 1.3 Copper catalyzed development of reactive oxygen species.[18]

1.4 Strain Promoted Azide Alkyne Cycloaddition (SPAAC)

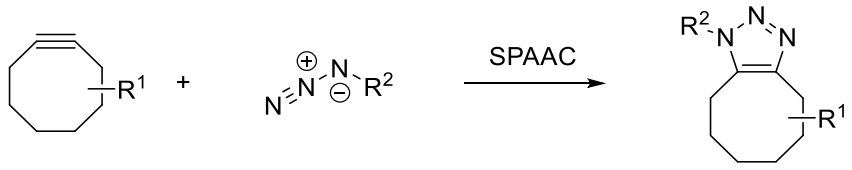

Scheme 1.4 Cycloaddition reaction between a cyclooctyne and azide via the SPAAC reaction.

The Strain Promoted Azide Alkyne Cycloaddition (SPAAC) (**Scheme 1.4**) takes the basis of the CuAAC reaction and eliminates the need for a Cu(I) catalyst. This is accomplished by using a strained alkyne, typically a cyclooctyne, the smallest cycloalkyne that can accommodate a triple bond. Ideally, the bond angles for alkynes are 180°; however, the cyclic nature of a cyclooctyne causes the bond angle to be 163°.[19] This decrease in the bond angle provides ~18 kcal/mol of energy of ring strain and drives the reaction forward.[3] The overall second-order rate for the SPAAC

reaction is ~ 10^{-2} – 1 $M^{-1}s^{-1}$. While CuAAC is ~100 times faster than SPAAC, the lack of a Cu(I) eliminates cellular toxicity and allows for SPAAC to be used *in vivo* for live-cell imaging of glycoproteins tagged with azides.[20] The most effective way to increase the rate of the SPAAC reaction is to change the structure of the cyclooctyne by either manipulating the electronics or its hybridization. By making the cyclooctyne electron-deficient, the HOMO-LUMO gap decreases through reduction in the LUMO energy level.[9] This increases the rate of reaction 60-fold compared to the reaction between an azide with an unsubstituted cyclooctyne (OCT) and with a difluorinated cyclooctyne (DIBO, **Figure 1.1**).[21] Another way to increase the rate of reaction is to use benzoannulated cyclooctynes. This increases the rate of reaction by adding strain through the sp^2 hybridized carbons from the phenyl rings.[19,22] The more sp^2 hybridized orbitals present in a cyclooctyne, the more strained the molecule becomes. This is because the sp^2 orbitals force the cyclooctyne to be planar in two directions and consequently, increases the rate of the reaction by introducing additional strain to the system (**Figure 1.1**). In the case of BARAC, DIBAC or DIBO, the forced planar conformation of the molecule causes one of the sp^2 orbitals to be aligned with one of the conjugated phenyl rings which further increases the ring strain. Overall, this results in the diphenyl cyclooctynes having faster rates than the OCT or DIFO.

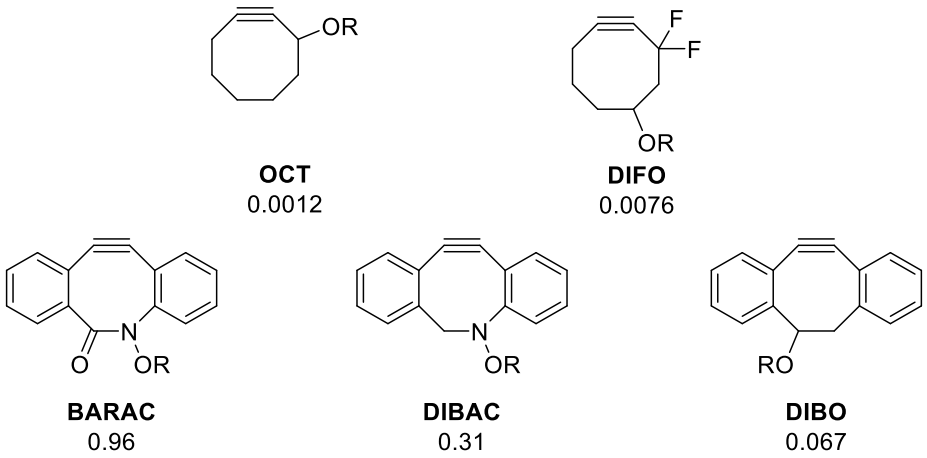

Figure 1.1 Respective second-order rate constants ($M^{-1}s^{-1}$) of different cyclooctynes reacting with azides.

1.5 Strain Promoted Alkyne Nitrone Cycloaddition (SPANC)

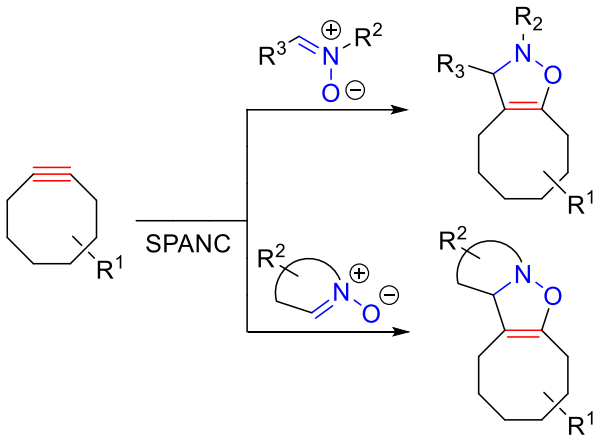

Scheme 1.5 SPANC reaction between a generic cyclooctyne and an acyclic and cyclic nitrone.

The Strain Promoted Alkyne Nitrone Cycloaddition (SPANC) reaction takes the SPAAC reaction and replaces the azide with a nitrone which reacts via a [3+2] cycloaddition. A nitrone is a 1,3-dipole between N and O atoms.[23] Nitrones have the added benefit of increasing reaction tunability through modification of the molecules' electronics, strain and sterics via its three modification sites, compared to their azide counterparts.[24] In addition, nitrones can be acyclic or cyclic, increasing the scope of this type of reaction in bioorthogonal chemistry. However, acyclic nitrones

are not very stable in an aqueous environment.[25] When in the presence of an acid or base, the acyclic nitrone will hydrolyze into an aldehyde and a hydroxylamine, making their use in biology difficult.[26] Cyclic nitrones tend to be preferred as they are stable in aqueous environments while being more reactive than their acyclic counterparts. This is because the cycloaddition reaction is driven by the strain from both the cycloalkynes and the cyclic nitrone. In fact, the reaction between DIBO and a cyclic nitrone has a second-order rate constant that is 25 times larger than the same reaction between DIBO and a phenyl azide.[27] Another way to enhance the rate is to fuse a cyclopropene ring to the cyclooctyne to further add strain to the molecule. An example of this would be bicyclo[6.1.0]nonyne (BCN). A reaction using a cyclic nitrone has a second-order rate constant that is ~11 times larger than the reaction with an azide.[28] The large range in reactivity and tunability of this reaction makes it ideal for a variety of biological applications such as incorporation into N-based biomolecules for cell labelling. Nitrones are also key starting materials for synthesizing β-lactams and isoxazolidines.[29] Overall, the diverse reactivity makes this reaction ideal for bioorthogonal chemistry.

Table 1.1 Second-order rate constant comparison between SPAAC and SPANC reactions.[26,14,28]

	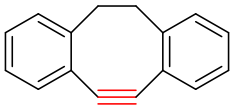 DIBO	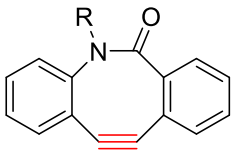 BARAC	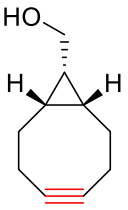 BCN
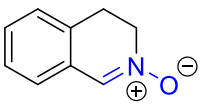 SPANC	1.5 $M^{-1}s^{-1}$	47.3 $M^{-1}s^{-1}$	1.5 $M^{-1}s^{-1}$
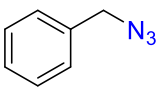 SPAAC	0.062 $M^{-1}s^{-1}$	0.96 $M^{-1}s^{-1}$	0.14 $M^{-1}s^{-1}$

1.6 Tetrazine Ligation

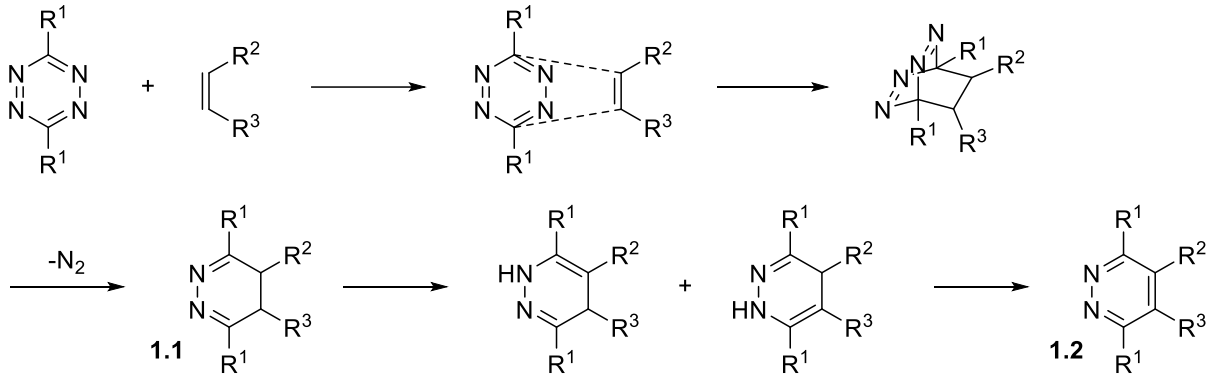

Scheme 1.6 Mechanism of the tetrazine ligation reaction.

The tetrazine ligation, the reaction between a strained alkene/alkyne and a tetrazine, was first applied to bioorthogonal chemistry in 2008 by Fox and Weissleder.[18] In this reaction, tetrazine (diene) and an alkene (dienophile) react via a [4+2] cycloaddition followed by a retro [4+2] cycloaddition to afford a dihydropyridine (**1.1**) or pyridazine (**1.2**) product (**Scheme 1.6**). This reaction occurs via an inverse electron demand Diels-Alder, where the diene is electron-poor and the dienophile is electron-rich. This is the opposite of a typical Diels-Alder reaction where the diene is electron-rich and the dienophile is electron-poor.

Table 1.2 Second-order rate constants of the reaction between tetrazine and various dienophiles.

Dienophile	Second-order rate constant ($M^{-1}s^{-1}$)	Reference
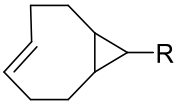	10^4-10^6	30
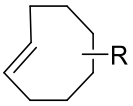	10^3-10^4	31
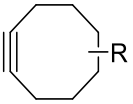	1-10^1	32
	10^{-1}-10^1	33
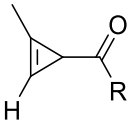	10^{-2}-10^1	34, 35
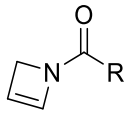	10^{-1}	36

This reaction meets the bioorthogonal criteria better than other established bioorthogonal reactions such as CuAAC, SPAAC and SPANC. Firstly, the tetrazine ligation does not require a catalyst which eliminates the toxicity issues of the CuAAC reaction. Since the reaction does not involve metal and occurs at a physiological pH, the reaction does not affect the function of the cell. The tetrazine ligation is also selective and only produces one by-product, nitrogen gas, making the reaction irreversible. Also, the tetrazine ligation surpasses the rates of all other bioorthogonal reactions ensuring a concentration of reactant comparable to those of physiological components

(e.g., proteins) present in the cell. Since the tetrazine ligation is an exceptional bioorthogonal reaction, it has been the subject of great interest over the past 10 years in the field of bioorthogonal chemistry and has been studied with a number of reaction partners (**Table 1.3**). This allowed the tetrazine ligation to be optimized for bioorthogonal chemistry by enhancing the reagent's cell permeability, stability, and reaction kinetics.[37] Ultimately, this allows the reaction to be used for a variety of applications or as an alternative to other bioorthogonal reactions.

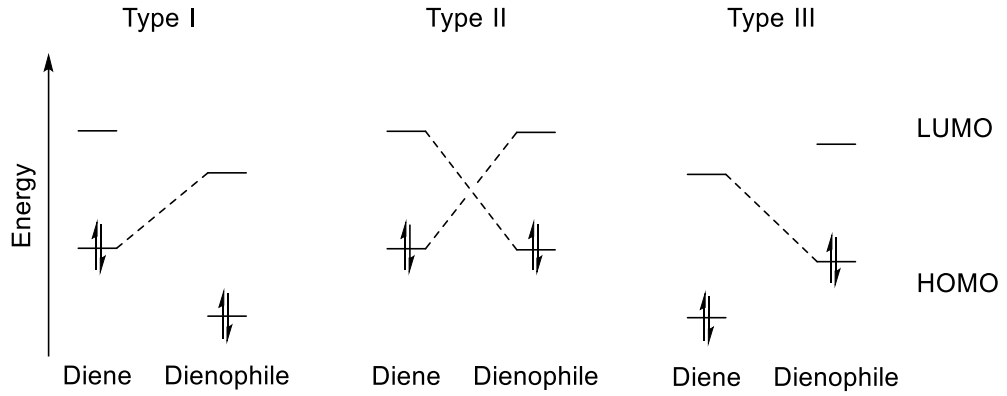

Figure 1.2 Frontier molecular orbital theory diagram describing the interaction between the diene and dienophile for the three types of Diels-Alder cycloaddition. Figure was adapted from Sustmann.[24]

The reaction dynamics of the tetrazine ligation are governed by the highest occupied molecular orbital (HOMO) and lowest unoccupied molecular orbital (LUMO) gap which is described by frontier molecular orbital theory (FMOT). According to FMOT, having a smaller HOMO-LUMO energy gap increases the reactivity.[38] Electron-donating groups add electron density into the rest of the molecule, ideally the reaction center. While electron withdrawing groups do the opposite. When electron density is added into a molecule, the enhanced repulsion increases the HOMO molecular energy level. This brings the energy level of the diene's HOMO closer to that of the dienophile's LUMO.[39]

Therefore, the reactivity can be tuned through the manipulation of the electronics of both the diene and dienophile. This will allow for the energy gap between the $HOMO_{diene}$ and $LUMO_{dienophile}$ to be decreased. The FMOT of Diels-Alder cycloadditions can be described in three ways (**Figure 1.2**). The first type of cycloaddition is termed "normal" where the diene is electron-rich, and the dienophile is electron-poor.[24] In terms of FMOT, increasing the rate of the reaction is then determined by the $HOMO_{diene}$-$LUMO_{dienophile}$. In this case, the $HOMO_{diene}$ needs to be electron-rich and the $LUMO_{dienophile}$ needs to be electron-poor. Type II cycloadditions are dependent on both the HOMO and LUMO.[24] However, in this case, the change of electronics of either reagent will affect both the HOMO and LUMO. The third type of cycloaddition is the inverse electron demand Diels-Alder (IEDDA) where to increase the rate of reaction, either the $HOMO_{dienophile}$ needs to be electron-rich, or the $LUMO_{diene}$ needs to be electron-poor.[40] The increase in reactivity, when the previous conditions are met, is what qualifies this as the third type of cycloaddition.[41,42]

1.6.1 Tetrazine

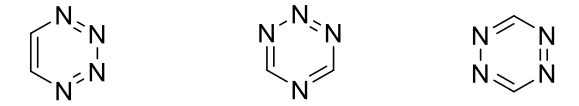

Figure 1.3 Isomers of tetrazine.

Tetrazines are aromatic heterocycles containing four nitrogens in a six-membered ring. There are three isomers of tetrazine (**Figure 1.3**) which are dictated by the position of the nitrogen atoms in the molecule. The first isomer is 1,2,3,4-tetrazine (v-tetrazine), the second is 1,2,3,5-tetrazine (as-tetrazine), and the third is 1,2,4,5-tetrazine (s-tetrazine).[43] S-tetrazine is the most commonly used isomer in bioorthogonal chemistry due to its symmetry and comparatively simple synthesis (**Scheme 1.7**). Tetrazines are typically synthesized via the condensation of nitriles or Pinner salts

using a thiol, sulfur-based catalyst, or a Lewis acid.[44,45,46] Tetrazines can also be synthesized using organometallic chemistry through the use of a Pd, Zn, or Ni catalyst which couples to aryl halides or boronic acids to form the desired tetrazine.[47,48]

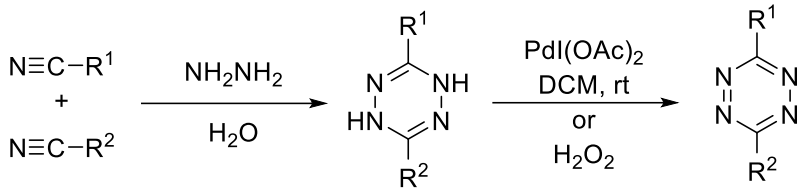

Scheme 1.7 Synthesis of tetrazine.

1.6.2 Trans-cyclooctene

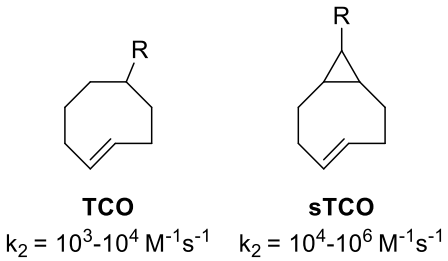

Figure 1.4 Structure of trans-cyclooctene (TCO) and strained trans-cyclooctene (sTCO) and their relative second-order rate constants.[49,50,30]

There is a great interest in the tetrazine ligation involving trans-cyclooctenes (TCO), specifically, strained trans-cyclooctene (s-TCO, **Figure 1.4**).[51] This is because the fused cyclopropene ring on s-TCO causes the rate of reaction to increase 50-fold compared to the reaction using TCO.[52,53] TCOs are easily made using a photochemical flow reactor developed by Fox *et al.* (**Figure 1.5**).[54] In the past, TCO was synthesized via a Hoffman elimination of trimethylcyclooctyl ammonium iodide for cis-cyclooctene.[49] However, this synthesis could not prepare other TCOs derivatives, which limits the potential of this reagent in chemical applications. The reactor converts the cis-

isomer to the trans via UV light and a photosynthesizer, methyl benzoate. The set up of the reactor and how it works are described in chapter 2.

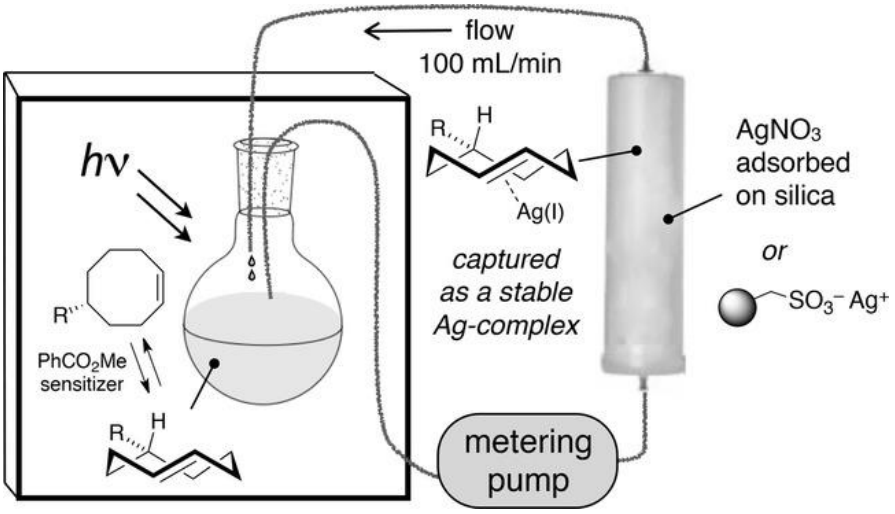

Figure 1.5 Photochemical flow reactor developed by Fox *et al*. The figure was obtained from Pegga *et al*, 2020 and reproduced with permission.[54]

1.7 Outline of Work

The purpose of the work demonstrated here is to develop an alternative bioorthogonal reaction based on the tetrazine ligation. The tetrazine ligation, known to be the fastest bioorthogonal reaction occurs via and Inverse Electron Demand Diels Alder. The tetrazine ligation exhibits extremely fast rates when tetrazines are reacted with strained dienophiles, such as trans-cyclooctenes and cyclooctynes. Our "new" bioorthogonal reaction is achieved by replacing tetrazine with diazapyrones, which are an analog of tetrazine. This reaction will be studied under pseudo first-order conditions to determine the second-order rate constants of the reaction. Which is achieved by reacting diazapyrones with cyclooctynes an trans-cyclooctenes. The cyclooctyne used in this reaction are synthesized with known procedures. While trans-cyclooctenes are synthesized using the photochemical reaction developed by Fox *et al*.

References

(1) Prescher, J. A.; Bertozzi, C. R. Chemistry in living systems. *Nature Chemical Biology* **2005**, *1* (1), 13-21. DOI: 10.1038/nchembio0605-13

(2) Yang, J.; Liang, Y.; Šečkutė, J.; Houk, K. N.; Devaraj, N. K. Synthesis and Reactivity Comparisons of 1-Methyl-3-Substituted Cyclopropene Mini-tags for Tetrazine Bioorthogonal Reactions. *Chemistry – A European Journal* **2014**, *20* (12), 3365-3375. DOI: 10.1002/chem.201304225.

(3) Sletten, E. M.; Bertozzi, C. R. From mechanism to mouse: a tale of two bioorthogonal reactions. *Accounts of Chemical Research* **2011**, *44* (9), 666-676. DOI: 10.1021/ar200148z PubMed.

(4) Sletten, E. M.; Bertozzi, C. R. Bioorthogonal chemistry: fishing for selectivity in a sea of functionality. *Angewandte Chemie (International ed. in English)* **2009**, *48* (38), 6974-6998. DOI: 10.1002/anie.

(5) Devaraj, N. K. The Future of Bioorthogonal Chemistry. *American Chemical Society Central Science* **2018**, *4* (8), 952-959. DOI: 10.1021/acscentsci.8b00251.

(6) Saxon, E.; Bertozzi Carolyn, R. Cell Surface Engineering by a Modified Staudinger Reaction. *Science* **2000**, *287* (5460), 2007-2010. DOI: 10.1126/science.287.5460.2007.

(7) Nilsson, B. L.; Kiessling, L. L.; Raines, R. T. Staudinger Ligation: A Peptide from a Thioester and Azide. *Organic Letters* **2000**, *2* (13), 1939-1941. DOI: 10.1021/ol0060174.

(8) Staudinger, H.; Meyer, J. Ueber neue organische Phosphorverbindungen II. Phosphazine. *Helvetica Chimica Acta* **1919**, *2* (1), 619-635. DOI: 10.1002/hlca.19190020163.

(9) Agard, N. J.; Baskin, J. M.; Prescher, J. A.; Lo, A.; Bertozzi, C. R. A Comparative Study of Bioorthogonal Reactions with Azides. *American Chemical Society Chemical Biology* **2006**, *1* (10), 644-648. DOI: 10.1021/cb6003228.

(10) Huisgen, R. Kinetics and reaction mechanisms: selected examples from the experience of forty years. *Pure and Applied Chemistry* **1989**, *61* (4), 613-628. DOI:10.1351/pac198961040613.

(11) Meldal, M.; Tornøe, C. W. Cu-catalyzed azide-alkyne cycloaddition. *Chemical Review* **2008**, *108* (8), 2952-3015. DOI: 10.1021/cr0783479.

(12) Wu, P.; Feldman, A. K.; Nugent, A. K.; Hawker, C. J.; Scheel, A.; Voit, B.; Pyun, J.; Fréchet, J. M.; Sharpless, K. B.; Fokin, V. V. Efficiency and fidelity in a click-chemistry route to triazole dendrimers by the copper(i)-catalyzed ligation of azides and alkynes. *Angewandte Chemie International Edition* **2004**, *43* (30), 3928-3932. DOI: 10.1002/anie.200454078.

(13) Neumann, S.; Biewend, M.; Rana, S.; Binder, W. H. The CuAAC: Principles, Homogeneous and Heterogeneous Catalysts, and Novel Developments and Applications. *Macromolecular Rapid Communications* **2020**, *41* (1), 1900359. DOI: 10.1002/marc.201900359.

(14) Jewett, J. C.; Sletten, E. M.; Bertozzi, C. R. Rapid Cu-Free Click Chemistry with Readily Synthesized Biarylazacyclooctynones. *Journal of the American Chemical Society* **2010**, *132* (11), 3688-3690. DOI: 10.1021/ja100014q.

(15) Presolski, S. I.; Hong, V.; Cho, S.-H.; Finn, M. G. Tailored Ligand Acceleration of the Cu-Catalyzed Azide−Alkyne Cycloaddition Reaction: Practical and Mechanistic Implications. *Journal of the American Chemical Society* **2010**, *132* (41), 14570-14576. DOI: 10.1021/ja105743g.

(16) Wang, Q.; Chan, T. R.; Hilgraf, R.; Fokin, V. V.; Sharpless, K. B.; Finn, M. G. Bioconjugation by Copper(I)-Catalyzed Azide-Alkyne [3 + 2] Cycloaddition. *Journal of the American Chemical Society* **2003**, *125* (11), 3192-3193. DOI: 10.1021/ja021381e.

(17) Moses, J. E.; Moorhouse, A. D. The growing applications of click chemistry. *Chemical Society Reviews* **2007**, *36* (8), 1249-1262, 10.1039/B613014N. DOI: 10.1039/B613014N.

(18) McKay, Craig S.; Finn, M. G. Click Chemistry in Complex Mixtures: Bioorthogonal Bioconjugation. *Chemistry & Biology* **2014**, *21* (9), 1075-1101. DOI:10.1016/j.chembiol.2014.09.002.

(19) Dommerholt, F. J.; Rutjes, F.; Delft, F. C. Strain-Promoted 1,3-Dipolar Cycloaddition of Cycloalkynes and Organic Azides. *Topics in Current Chemistry* **2016**, *374* (2), 20-40. DOI: 10.1007/s41061-016-0016-4.

(20) Fokin, V.F. CuAAC: The Quintessential Click Reaction. **2012**, 247-277. DOI: 10.1002/9783527664801.ch7.

(21) Baskin, J. M.; Prescher, J. A.; Laughlin, S. T.; Agard, N. J.; Chang, P. V.; Miller, I. A.; Lo, A.; Codelli, J. A.; Bertozzi, C. R. Copper-Free Click Chemistry for Dynamic in vivo Imaging. *Proceedings of the National Academy of Sciences.* **2007**, *104* (43), 16793-16797. DOI: 10.1073/pnas.0707090104.

(22) Ramil, C. P.; Lin, Q. Bioorthogonal chemistry: strategies and recent developments. *Chemical Communications* **2013**, *49* (94), 11007-11022, 10.1039/C3CC44272A. DOI: 10.1039/C3CC44272A.

(23) Gothelf, K. V.; Jørgensen, K. A. Asymmetric 1,3-Dipolar Cycloaddition Reactions. *Chemical Reviews* **1998**, *98* (2), 863-910. DOI: 10.1021/cr970324e.

(24) Sustmann, R. Orbital energy control of cycloaddition reactivity. *Pure and Applied Chemistry* **1974**, *40* (4), 569-593. DOI: doi:10.1351/pac197440040569.

(25) McKay, C. S.; Blake, J. A.; Cheng, J.; Danielson, D. C.; Pezacki, J. P. Strain-promoted cycloadditions of cyclic nitrones with cyclooctynes for labeling human cancer cells. *Chemical Communications (Cambridge, England)* **2011**, *47* (36), 10040-10042. DOI: 10.1039/c1cc13808a.

(26) MacKenzie, D. A.; Sherratt, A. R.; Chigrinova, M.; Cheung, L. L. W.; Pezacki, J. P. Strain-promoted cycloadditions involving nitrones and alkynes—rapid tunable reactions for bioorthogonal labeling. *Current Opinion in Chemical Biology* **2014**, *21*, 81-88. DOI: doi.org/10.1016/j.cbpa.

(27) McKay, C. S.; Moran, J.; Pezacki, J. P. Nitrones as dipoles for rapid strain-promoted 1,3-dipolar cycloadditions with cyclooctynes. *Chemical Communications* **2010**, *46* (6), 931-933, DOI: 10.1039/B921630H.

(28) Dommerholt, J.; Schmidt, S.; Temming, R.; Hendriks, L. J. A.; Rutjes, F. P. J. T.; van Hest, J. C. M.; Lefeber, D. J.; Friedl, P.; van Delft, F. L. Readily Accessible Bicyclononynes for Bioorthogonal Labeling and Three-Dimensional Imaging of Living Cells. *Angewandte Chemie International Edition* **2010**, *49* (49), 9422-9425. DOI: 10.1002/anie.201003761.

(29) Bilodeau, D. A.; Margison, K. D.; Serhan, M.; Pezacki, J. P. Bioorthogonal Reactions Utilizing Nitrones as Versatile Dipoles in Cycloaddition Reactions. *Chemical Reviews* **2021**, *121* (12), 6699-6717. DOI: 10.1021/acs.chemrev.0c00832.

(30) Taylor, M. T.; Blackman, M. L.; Dmitrenko, O.; Fox, J. M. Design and Synthesis of Highly Reactive Dienophiles for the Tetrazine–trans-Cyclooctene Ligation. *Journal of the American Chemical Society* **2011**, *133* (25), 9646-9649. DOI: 10.1021/ja201844c.

(31) Blackman, M. L.; Royzen, M.; Fox, J. M. Tetrazine Ligation: Fast Bioconjugation Based on Inverse-Electron-Demand Diels−Alder Reactivity. *Journal of the American Chemical Society* **2008**, *130* (41), 13518-13519. DOI: 10.1021/ja8053805.

(32) Chen, W.; Wang, D.; Dai, C.; Hamelberg, D.; Wang, B. Clicking 1,2,4,5-tetrazine and cyclooctynes with tunable reaction rates. *Chemical Communications* **2012**, *48* (12), 1736-1738, DOI: 10.1039/C2CC16716F.

(33) Devaraj, N. K.; Weissleder, R.; Hilderbrand, S. A. Tetrazine-Based Cycloadditions: Application to Pretargeted Live Cell Imaging. *Bioconjugate Chemistry* **2008**, *19* (12), 2297-2299. DOI: 10.1021/bc8004446.

(34) Patterson, D. M.; Nazarova, L. A.; Xie, B.; Kamber, D. N.; Prescher, J. A. Functionalized cyclopropenes as bioorthogonal chemical reporters. *Journal of the American Chemical Society* **2012**, *134* (45), 18638. DOI: 10.1021/ja3060436.

(35) Yang, J.; Šečkutė, J.; Cole, C. M.; Devaraj, N. K. Live-Cell Imaging of Cyclopropene Tags with Fluorogenic Tetrazine Cycloadditions. *Angewandte Chemie International Edition* **2012**, *51* (30), 7476-7479. DOI: 10.1002/anie.201202122.

(36) Engelsma, S. B.; Willems, L. I.; van Paaschen, C. E.; van Kasteren, S. I.; van Der Marel, G. A.; Overkleeft, H. S.; Filippov, D. V. Acylazetine as a dienophile in bioorthogonal inverse electron-demand Diels-Alder ligation. *Organic letters* **2014**, *16* (10), 2744-2747. DOI: 10.1021/ol501049c.

(37) Karver, M. R.; Weissleder, R.; Hilderbrand, S. A. Synthesis and Evaluation of a Series of 1,2,4,5-Tetrazines for Bioorthogonal Conjugation. *Bioconjugate Chemistry* **2011**, *22* (11), 2263-2270. DOI: 10.1021/bc200295y.

(38) Oliveira, B. L.; Guo, Z.; Bernardes, G. J. L. Inverse electron demand Diels-Alder reactions in chemical biology. *Chemical Society Reviews* **2017**, *46* (16), 4895-4495. DOI: 10.1039/c7cs00184c.

(39) Stéen, E. J. L.; Edem, P. E.; Nørregaard, K.; Jørgensen, J. T.; Shalgunov, V.; Kjaer, A.; Herth, M. M. Pretargeting in nuclear imaging and radionuclide therapy: Improving efficacy of theranostics and nanomedicines. *Biomaterials* **2018**, *179*, 209-245. DOI: 10.1016/j.biomaterials.2018.06.021.

(40) Scinto, S. L.; Bilodeau, D. A.; Hincapie, R.; Lee, W.; Nguyen, S. S.; Xu, M.; am Ende, C. W.; Finn, M. G.; Lang, K.; Lin, Q.; et al. Bioorthogonal chemistry. *Nature Reviews Methods Primers* **2021**, *1* (1), 30. DOI: 10.1038/s43586-021-00028-z.

(41) Boger, D. L.; Schaum, R. P.; Garbaccio, R. M. Regioselective Inverse Electron Demand Diels−Alder Reactions of N-Acyl 6-Amino-3-(methylthio)-1,2,4,5-tetrazines. *The Journal of Organic Chemistry* **1998**, *63* (18), 6329-6337. DOI: 10.1021/jo980795g.

(42) Hamasaki, A.; Ducray, R.; Boger, D. L. Two Novel 1,2,4,5-Tetrazines that Participate in Inverse Electron Demand Diels−Alder Reactions with an Unexpected Regioselectivity. *The Journal of Organic Chemistry* **2006**, *71* (1), 185-193. DOI: 10.1021/jo051832o.

(43) *ADVANCES IN HETEROCYCLIC CHEMISTRY*; Vol. 132, Ch 3, pg135-239. *Elsevier Academic Press*, 2020.

(44) Mao, W.; Shi, W.; Li, J.; Su, D.; Wang, X.; Zhang, L.; Pan, L.; Wu, X.; Wu, H. Organocatalytic and Scalable Syntheses of Unsymmetrical 1,2,4,5-Tetrazines by Thiol-Containing Promotors. *Angewandte Chemie International Edition* **2019**, *131* (4), 1118-1121. DOI: 10.1002/ange.201812550.

(45) Qu, Y.; Sauvage, F. X.; Clavier, G.; Miomandre, F.; Audebert, P. Metal-Free Synthetic Approach to 3-Monosubstituted Unsymmetrical 1,2,4,5-Tetrazines Useful for Bioorthogonal Reactions. *Angewandte Chemie International Edition* **2018**, *57* (37), 12057-12061. DOI: 10.1002/anie.201804878.

(46) Yang, J.; Karver, M. R.; Li, W.; Sahu, S.; Devaraj, N. K. Metal-Catalyzed One-Pot Synthesis of Tetrazines Directly from Aliphatic Nitriles and Hydrazine. *Angewandte Chemie International Edition* **2012**, *51* (21), 5222-5225. DOI: 10.1002/anie.201201117.

(47) Lambert, W. D.; Fang, Y.; Mahapatra, S.; Huang, Z.; am Ende, C. W.; Fox, J. M. Installation of Minimal Tetrazines through Silver-Mediated Liebeskind–Srogl Coupling with Arylboronic Acids. *Journal of the American Chemical Society* **2019**, *141* (43), 17068-17074. DOI: 10.1021/jacs.9b08677.

(48) Wu, H.; Yang, J.; Šečkutė, J.; Devaraj, N. K. In Situ Synthesis of Alkenyl Tetrazines for Highly Fluorogenic Bioorthogonal Live-Cell Imaging Probes. *Angewandte Chemie International Edition* **2014**, *53* (23), 5805-5809. DOI: 10.1002/anie.201400135.

(49) Royzen, M.; Yap, G. P. A.; Fox, J. M. A Photochemical Synthesis of Functionalized trans-Cyclooctenes Driven by Metal Complexation. *Journal of the American Chemical Society* **2008**, *130* (12), 3760-3761. DOI: 10.1021/ja8001919.

(50) Darko, A.; Wallace, S.; Dmitrenko, O.; Machovina, M. M.; Mehl, R. A.; Chin, J. W.; Fox, J. M. Conformationally strained trans-cyclooctene with improved stability and excellent reactivity in tetrazine ligation. *Chemical Science* **2014**, *5* (10), 3770-3776, DOI: 10.1039/C4SC01348D.

(51) Pigga, J. E.; Rosenberger, J. E.; Jemas, A.; Boyd, S. J.; Dmitrenko, O.; Xie, Y.; Fox, J. M. General, Divergent Platform for Diastereoselective Synthesis of trans-Cyclooctenes with High Reactivity and Favorable Physiochemical Properties**. *Angewandte Chemie International Edition* **2021**, *60* (27), 14975-14980,. DOI: 10.1002/anie.202101483

(52) Lang, K.; Davis, L.; Wallace, S.; Mahesh, M.; Cox, D. J.; Blackman, M. L.; Fox, J. M.; Chin, J. W. Genetic Encoding of Bicyclononynes and trans-Cyclooctenes for Site-Specific Protein Labeling in Vitro and in Live Mammalian Cells via Rapid Fluorogenic Diels–Alder

Reactions. *Journal of the American Chemical Society* **2012**, *134* (25), 10317-10320. DOI: 10.1021/ja302832g.

(53) Seitchik, J. L.; Peeler, J. C.; Taylor, M. T.; Blackman, M. L.; Rhoads, T. W.; Cooley, R. B.; Refakis, C.; Fox, J. M.; Mehl, R. A. Genetically Encoded Tetrazine Amino Acid Directs Rapid Site-Specific in Vivo Bioorthogonal Ligation with trans-Cyclooctenes. *Journal of the American Chemical Society* **2012**, *134* (6), 2898-2901. DOI: 10.1021/ja2109745.

(54) Pigga, J. E.; Fox, J. M. Flow Photochemical Syntheses of trans-Cyclooctenes and trans-Cycloheptenes Driven by Metal Complexation. *Israel Journal of Chemistry* **2020**, *60* (3-4), 207-218, DOI: 10.1002/ijch.201900085.

Chapter 2 - Chemical synthesis of diazapyrones and trans-cyclooctenes

2.1 Introduction

With recent advancements in bioorthogonal chemistry, many reagents have been developed for use in biological systems; however, further optimization is required. Ideally, for bioorthogonal chemistry to reduce its interference with cells, k_2 is required to be larger than 1 $M^{-1}s^{-1}$ [1] to ensure bioorthogonal reagents are used at low concentrations. An issue with this requirement is that some reactions with large k_2 values are not selective and can react with the native components of the cellular environment. In addition, obtaining reliable diagnostic data is difficult without the simultaneous labelling of multiple functionalities within a cell.[2] We aim to develop alternative bioorthogonal reagents to expand the field of bioorthogonal chemistry and resolve these limitations.

2.1.1 Trans-Cyclooctenes

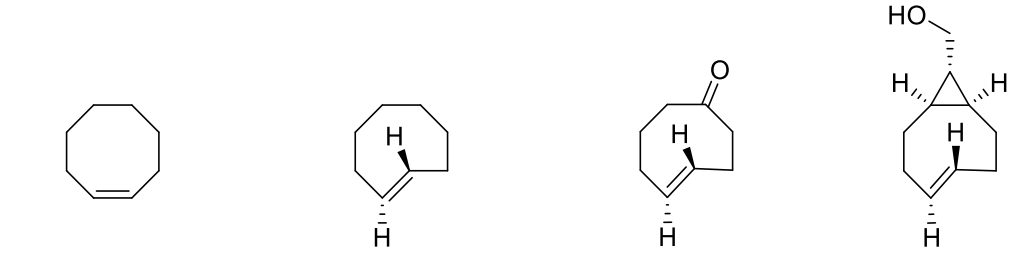

Figure 2.1 Comparison of the structure of cyclooctene and TCO/sTCO.

Trans-cyclooctenes are significantly less stable compared to the cis-configuration. This is in part due to the larger strain energy associated with the trans-conformers (16.7 kcal/mol), ~2 fold larger than the cis strain contribution of 7.4 kcal/mol (**Figure 2.1**).[3] To synthesize trans-cyclooctene derivatives, a method utilizing a photochemical flow reactor developed by the Fox group was

used.[4] The reactor works by using UV light to excite the photosynthesizer molecule which then transfers energy into cyclooctene to convert the cis-isomer into trans. The setup of the reactor is described in detail in **Section 2.3.2**. In which the cis-isomer is transformed into the trans-isomer using a UV-lamp and a FMI laboratory pump to create a continuous flow. The trans-isomer is "trapped" on a column filled with silver-impregnated silica via chelation. In terms of bioorthogonal chemistry, the use of TCO/s-TCO in reaction with tetrazine opened the door to the fastest known bioorthogonal reaction, the tetrazine ligation (with $k_2 \sim 10^4 - 10^6\ M^{-1}s^{-1}$).[5] The benefit of using TCO in this reaction is that the added strain provided by the molecule drives the reaction forward. This is further amplified when using s-TCO, which contains a fused cyclopropane ring (**Figure 2.1**). The added cyclopropene induces what is known as the double-strained effect which increases the k_2 160-fold compared to TCO.[6] The benefit of using TCO is that it is very easily modified, particularly when looking at trans-cycloct-4-enone (**Figure 2.1**). Trans-cycloct-4-enone can easily be modified at the carbonyl side into a multitude of functional groups, making it versatile for several different applications such as cellular incorporation. One major downfall of TCO is its high lipophilicity, which can cause issues when used in cells. The lipophilicity of TCO causes the biological environment to be disturbed when incorporated into the cell.[1]

2.1.2 Diazapyrones

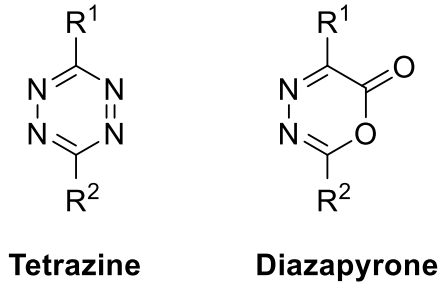

Figure 2.2 Comparison of the structure of tetrazine and diazapyrone.

Diazapyrones are a heterocycle, similar in structure to tetrazine, in which one of the N_2 groups has been replaced by a CO_2 group (**Figure 2.2**). The synthesis of diazapyrones occurs in two steps.[7] (1) The first step involves the condensation reaction between a glyoxylic acid and a hydrazine derivative followed by a second reaction (2) involving the cyclization of a hydrazone using EDC/HCl. However, diazapyrones have similar stability issues to tetrazine. In an aqueous environment, electron-deficient tetrazine and diazapyrones tend to hydrolyze which poses a significant issue for bioorthogonal applications.

2.2 Objective

Inspired by the synthesis of diazapyrones by Garg, we aimed to prepare various diazapyrones as an alternative diene to tetrazine. This was done by expanding on Garg's work with the development of new diazapyrones. We also aimed to prepare trans-cyclooctene reagents to be used for bioorthogonal chemistry based on Fox's work on the tetrazine ligation. These reagents were used later for the development of a new bioorthogonal reaction, as described in chapter 3.

2.3 Results and Discussion

2.3.1 Synthesis of Diazapyrones

General procedure of the synthesis of Diazapyrones

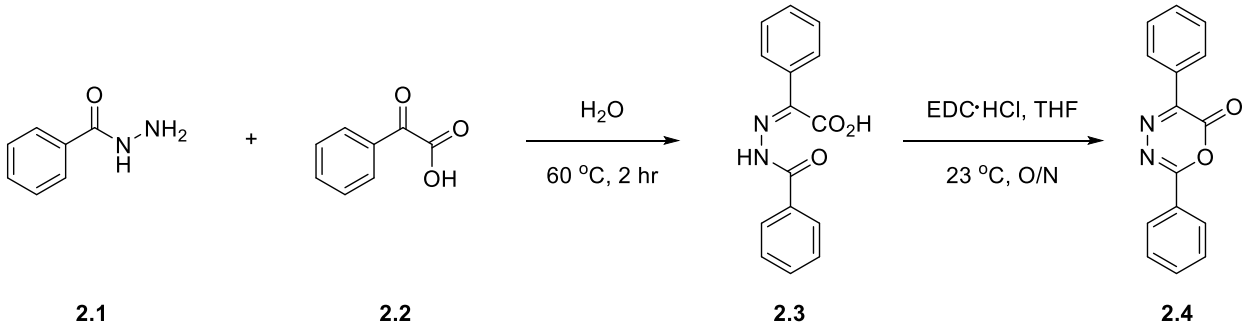

2.1 **2.2** **2.3** **2.4**

Scheme 2.1 Synthesis of a 2,5-Diphenyl-6H-1,3,4-oxadiazin-6-one (**2.4**). [13]

Diazapyrones are synthesized in two steps (**Scheme 2.1**). The first step of this synthesis involves a reaction between a phenylhydrazine (**2.1**) and a phenyl glyoxylic acid (**2.2**). These molecules react through a condensation reaction over two hours at 60 ^{o}C to form a hydrazone intermediate (**2.3)**. This hydrazone intermediate is a white powder and was obtained in a 70-90% yield. Before proceeding to the next reaction, the hydrazone must be very dry. This is accomplished by placing the hydrazone under reduced pressure using a high vac in a water bath at ~50 ^{o}C. The hydrazone intermediate (**2.3**) is then placed in a dry round bottom flask (RBF) with dry tetrahydrofuran (THF) and N-(3-dimethylaminopropyl)-N'-ethylcarbodiimide hydrochloride (EDC HCl). A cyclization reaction occurs in which EDC HCl is used to turn hydrazone (**2.3**) into a diazapyrone (**2.4**). The diazapyrone was obtained in a ~40-95 % yield (**Table 2.1**). The wide range of yields obtained for the diazapyrone is due to the purification process which involved recrystallization in acetone. This causes for a significant amount of product to be lost likely due to much solvent being used to dissolve the product. In some situations, where the cyclization reaction did not work, *N*,*N*′-dicyclohexylcarbodiimide (DCC) was used instead. In this case, the DCC hydrates to form dicyclourea. However, dicyclourea is difficult to remove from the diazapyrones as it is insoluble in aqueous solvents and barely soluble in organic solvents. To remove dicyclourea, the solution was concentrated under reduced pressure and filtered immediately as the dicyclourea crashes out. While this method worked, there is often still urea present in NMR making EDC HCl a better cyclization reagent.

Table 2.1 Synthetic results for diazapyrone synthesis. Diazapyrone 2.28 was synthesized using DDC HCl instead of EDC HCl. (The * represents the diazapyrones that were synthesized with DDC HCl)

Diazapyrone	Structure	% Yield
2.4	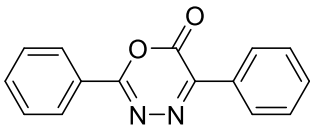	78
2.8	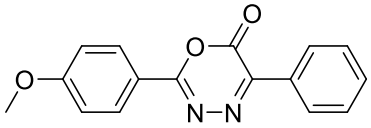	75
2.12	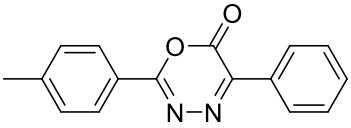	64
2.16	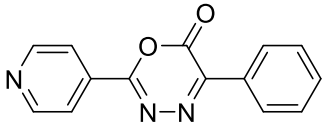	42
2.20	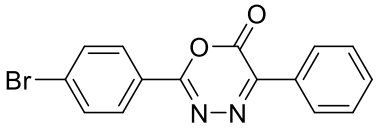	70
2.24	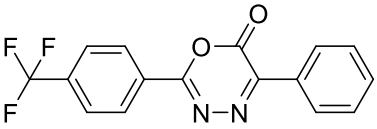	95
2.28*	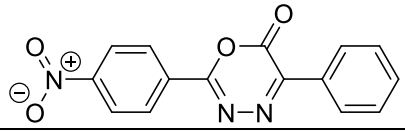	38

2.3.2 Synthesis of trans-cyclooctenes

General procedure B - Synthesis of trans-cyclooctene

Photochemistry is an elegant way to obtain cis and trans isomers. Through the use of a photochemical flow reactor developed by Fox *et al*, the trans isomer is photoisomerized from its cis counterpart and then trapped inside a silver impregnated silica column. Continuous cycling of the cis isomer through the reactor can fully convert all equivalents into the trans isomer.

Photochemical flow reactor

An FMI RP-QD lab pump was fitted with an end of tubing adapter and connected to PFTE tubing that was attached to a Biotage FSK0-1107 column (100 g) using a male Luer (1/4-28). The column was filled with ~10 cm of silica and then filled to the top with silver nitrate-impregnated silica. The column was attached to PFTE tubing using a female Luer (1/4-28) and the other end of the PFTE tubing was placed in one end of a Claisen adaptor and into a 500 mL quartz flask. Another PFTE tube was placed into the 21 flask leading back to the FMI lab pump. A Honeywell RUV Lamp 1/C UV air treatment system was used as the UV light source and was equipped with a RUV bulb 1/C. A photograph of the apparatus setup is presented in **Figure 2.3**. Once the reactor is set up, the reactor is flushed with 400 mL hexanes and diethyl ether and a reactor flask is attached containing the cis-isomer of cyclooctene, methyl benzoate, and 1% diethyl ether in hexanes. The FMI pump was set to 100 mL/min and the reactor was allowed to run for 12 hours for full conversion of cis to trans. The reaction flask was then removed, and the system was flushed with 200 mL of 1% diethyl ether in hexanes to flush out any remaining methyl benzoate and cis isomer.

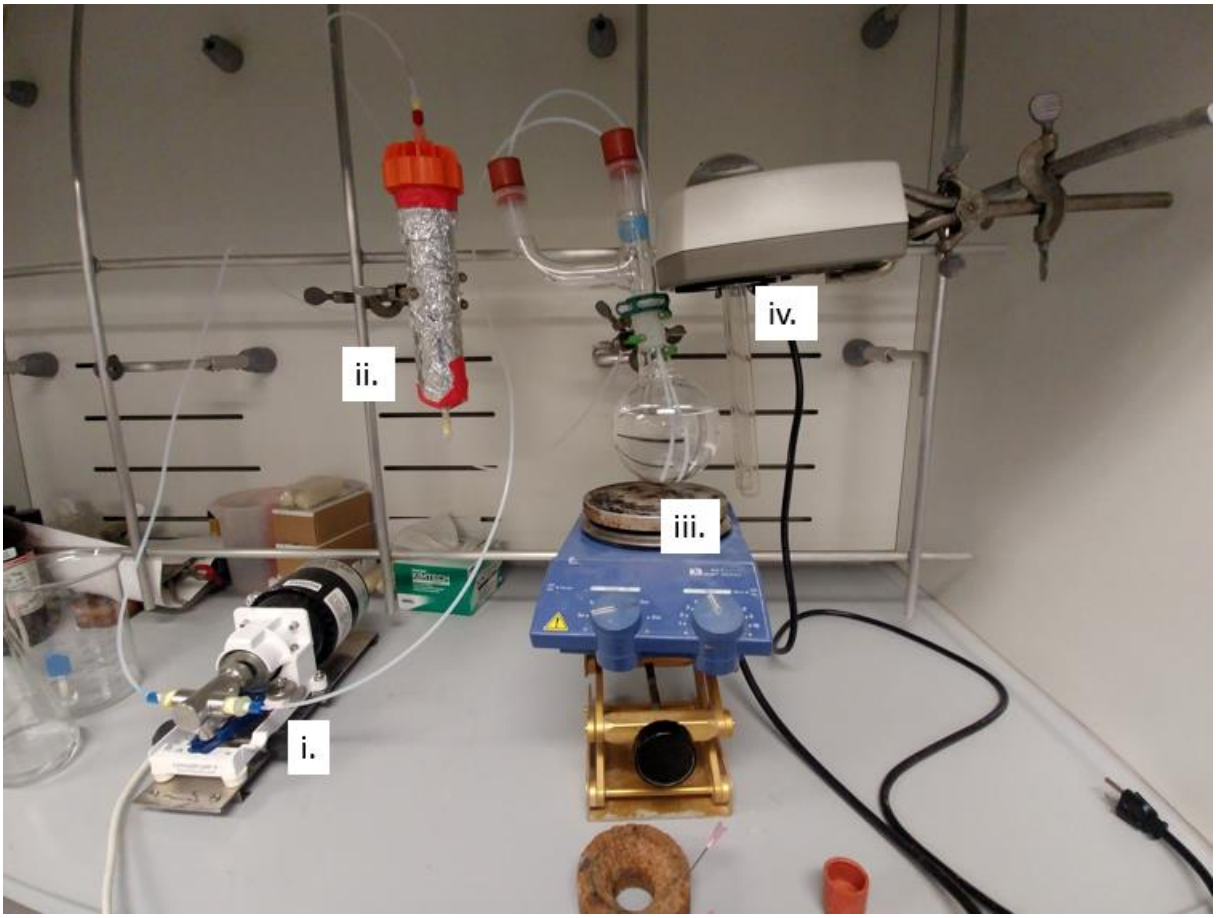

Figure 2.3 Photochemical flow reactor used to synthesize TCO where (i.) is the fluid pump, (ii.) is the column, (iii.) is the reaction flask, and (iv.) is the UV lamp.

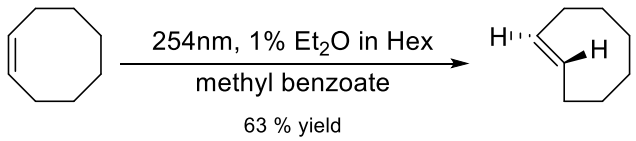

2.29 **2.30**

Scheme 2.2 Synthesis of TCO.[14]

Trans-cyclooctene is synthesized in one step (**Scheme 2.2**) using a photochemical flow reactor (**Figure 2.3**). To convert cyclooctene (**2.29**) into trans-cyclooctene (**2.30**) a photosynthesizer, methyl benzoate was placed in a quartz flask. Methyl benzoate absorbs UV light from the UV lamp which brings the molecule into the excited state. There is then an excited state transfer of

energy into the olefin of cyclooctene from the triplet excited state of methyl benzoate. The excited triplet state of cyclooctene is a diradical that breaks the double bond and allows frees rotation to be established. This transfer of energy causes the diradical bond of cyclooctene to twist 90 ^{o}. when the molecule relaxes to the ground state there is a probability for the molecule to become cis or trans. Therefore, once the trans-isomer is trapped on the column, the cis-isomer can continuously cycle through the reactor until it is fully converted into the trans-isomer. The silver nitrate acts as a coordinating reagent that exclusively chelates the trans-conformation, thereby isolating the trans-conformation. To separate the trans-conformation from the column, the column is first flushed excessively with the mobile phase. The column was then dried, and the silica was stirred with 200 mL ammonium hydroxide and 200 mL DCM for 10 minutes. The ammonium hydroxide releases the trans-conformation from the silica by displacement. The slurry was then filtered, and the resulting solution was extracted with 200 mL DCM x 3 and with 100 mL water x 2. The organic phase was then dried and concentrated under reduced pressure to isolate trans-cyclooctene.

In the end, trans-cyclooctene (**2.30**) was obtained in a 63% yield. There was a loss in the product due to stopping the flow reactor before the full conversion of the E isomers and due to leaks. To check if full conversion had been reached, a TLC was performed on the reaction flask to determine if any cis-cyclooctene remained. When the flow reactor was run for 8hrs very little cis-isomer remain according to TLC. When left overnight no cis-isomer remained. However, the reactor would leak. As well, during the workup phase, the column and filter were not flushed enough to ensure all the trans-isomer had eluted. A comparison between the ^{1}H NMR of the cis and trans-isomer can be seen in **Figure 2.4** previously**.** The key peak in **Figure 2.4** that indicates the conversion from cis to trans is the peak in the alkyl H region from 0-2.6 ppm. In the cis-conformation, there is one peak at ~1.4 ppm. The other peaks represent impurities such as water.

While in the trans-isomer, there are many peaks in the alkyl region representing that the chemical environment around the hydrogens are no longer uniform.

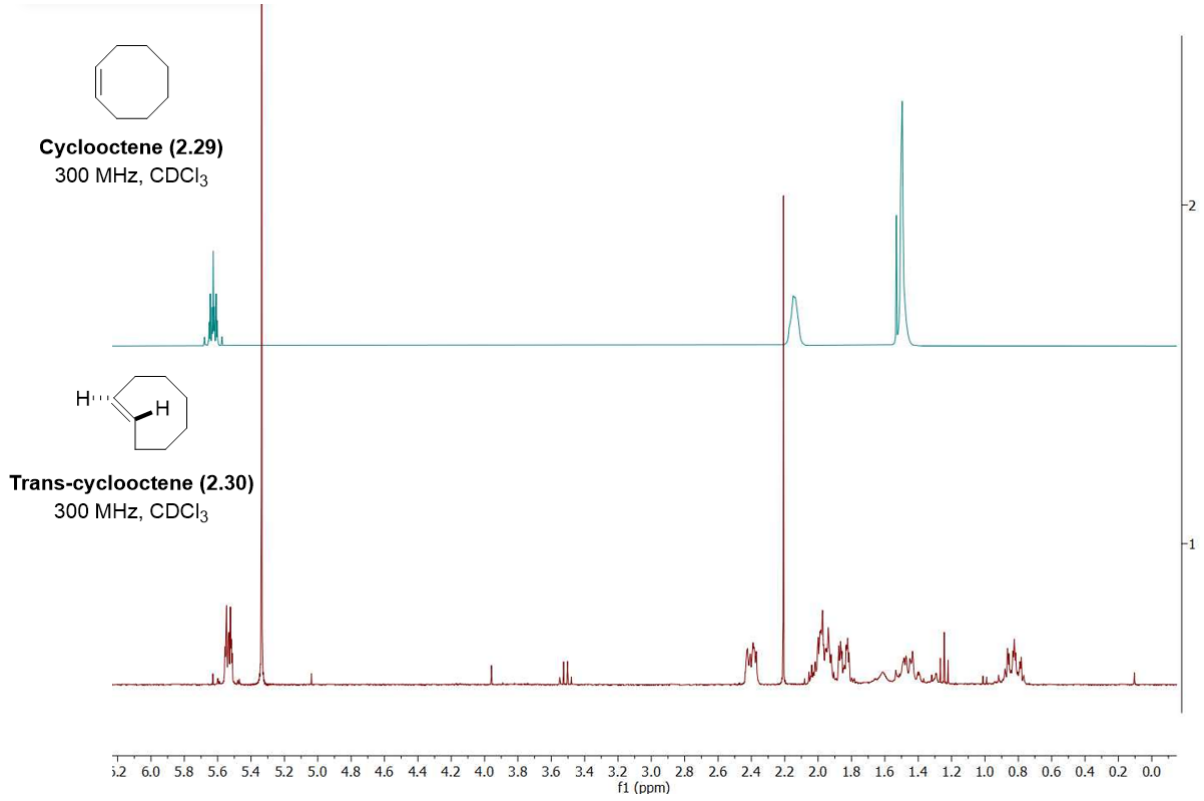

Figure 2.4 Comparison of the ^{1}H NMR of the conversion of cis-cyclooctene to trans-cyclooctene.

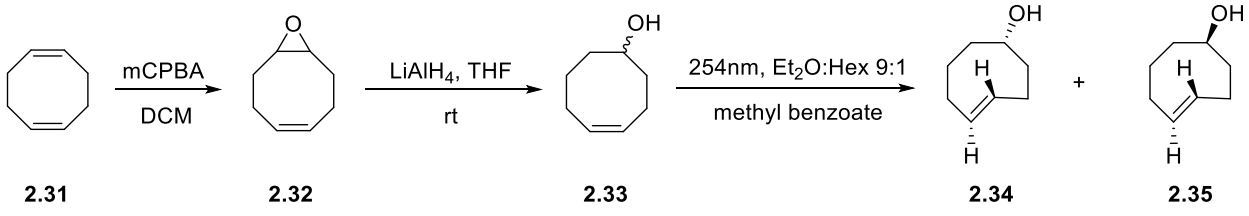

Scheme 2.3 Synthesis of TCO-OH. [14,15]

(Z)-cyclooctene-4-enol **(2.34)** was synthesized in three steps (**Scheme 2.3**). In the first step, 1,5-cyclooctadiene reacts with meta-chloroperoxybenzoic acid (mCPBA) via a Prilezhaev reaction resulting in the formation of 9-oxabicyclo[6.1.0]non-4-ene (**2.32**). The Prilezhaev reaction is an epoxidation reaction where an alkene reacts with mCPBA in dichloromethane (DCM) to form an epoxide. **2.32** was obtained in 51% yield which is lower than expected mainly due to the formation of the double epoxidation product The next reaction involves the reduction of **2.32** using lithium aluminum hydride ($LiAlH_4$). This reaction is done via a nucleophilic attack on the α-carbon which opens the ring and allows for the O^- to be protonated into an OH. The cyclooct-4-enol (**2.33**) intermediate was obtained in 66% yield. This reaction was also attempted with diisobutyl aluminum hydride (DIBAL-H), another strong reducing agent; however, the reaction was not as effective. The yield obtained for the DiBAL-H reaction was 13%. The final step of the synthesis is the conversion of **2.33** into (E)-cyclooct-4-enol (**2.34**) which was accomplished using the photochemical reactor (**Figure 2.3**) using methyl benzoate as the photosynthesizer and a 1:1 mixture of Et_2O:Hexane. The major product (**2.34)** was obtained in a 23% yield. These low yields are due to a leak in the photochemical reactor as the silicone seal at the top of the Biotage column expands over time when exposed to a high concentration of diethyl ether. To combat this, a new seal was placed in the column every time and the reactor was monitored every hour and stopped if a leak was observed. A comparison between the ^1H NMR of the cis and trans-isomer of cyclooctene-4-enol can be seen in **Figure 2.5.** The key peak in **Figure 2.5** that indicates the conversion from cis to trans is the peak at ~5.5 ppm. In the cis-isomer, there is one peak while in the trans-isomer there are two distinct peaks.

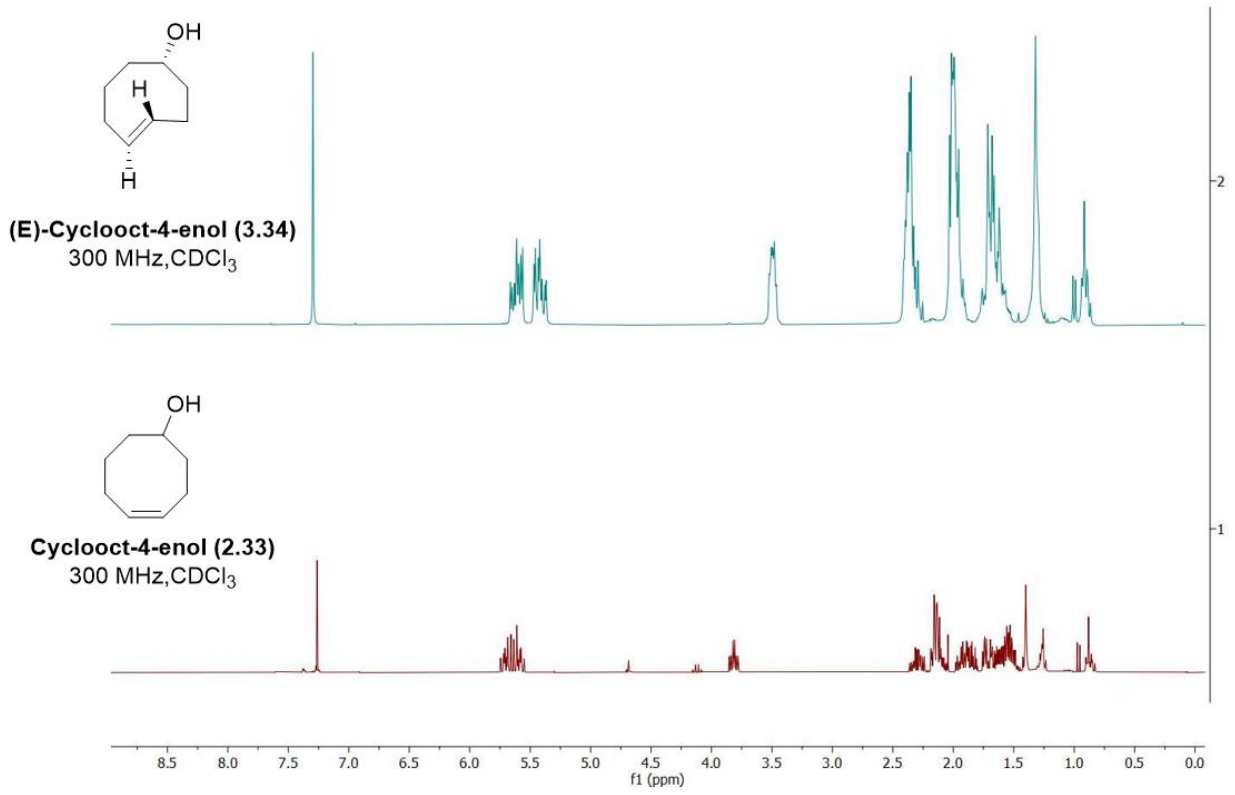

Figure 2.5 Comparison of the ^{1}H NMR of cis-4-cyclooctenol and trans-4-cyclooctenol.

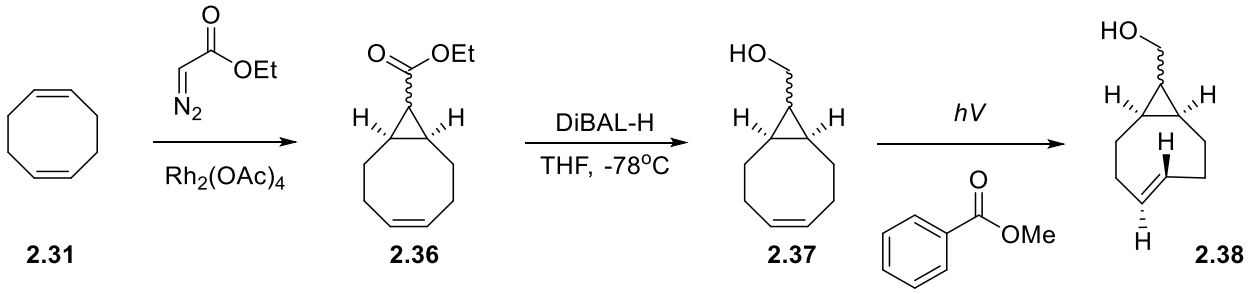

Scheme 2.4 Synthesis of s-TCO-OH. [6]

(rel-1R,8S,9R,4E)-bicyclo[6.1.0]non-4-ene-9-ylmethanol (**2.38**) was synthesized in three steps (**Scheme 2.4**). The first step involved reacting 1,5-cyclooctadiene with ethyl diazoacetate and Rh(II) acetate which allows for cyclopropanation to occur via the decomposition of ethyl diazoacetate to form the intermediate rel-(1R,8S,9S,Z)-ethyl bicyclo[6.1.0]non-4-ene-9-

carboxylate (**2.36**). Two isomers were obtained, the endo and exo, which had a 38% and 49% yield, respectively. Ester **2.36** was then reduced with DIBAL-H to obtain ((1R,8S,9S, Z)-Bicyclo[6.1.0]non-4-en-9-yl)methanol (**2.37**) and was obtained in a 94% yield. Alcohol **2.37** was then converted into (rel-1R,8S,9R,4E)-bicyclo[6.1.0]non-4-ene-9-ylmethanol (**2.38**) which was accomplished using the photochemical reactor (**Figure 2.3**), methyl benzoate as the photosynthesizer and a 1:10 mixture of Et_2O:Hexane. The yield obtained for the final product was 13% which was due to the leak in the reactor mentioned previously. In later attempts, the leaks were fixed by changing the silicon "O" ring before each run and by ensuring all the joints were wrapped in Teflon tape. Not only that, but by monitoring the reactor closely, very few leaks occurred. This increased the yield to 52%. A comparison between the ^{1}H NMR of the cis and trans-configurations of sTCO can be seen in **Figure 2.6** and all synthesized final products are shown in **Table 2.2.** The key peaks in **Figure 2.6** are the peaks at ~5.0-6.0 ppm which indicate the conversion from cis to trans. In the cis-isomer, the peak at ~5.5 ppm is 1 peak. However, in the trans-isomer, the peak at 5.5 splits into 2 peaks at ~ 6.0 ppm and 5.2 ppm.

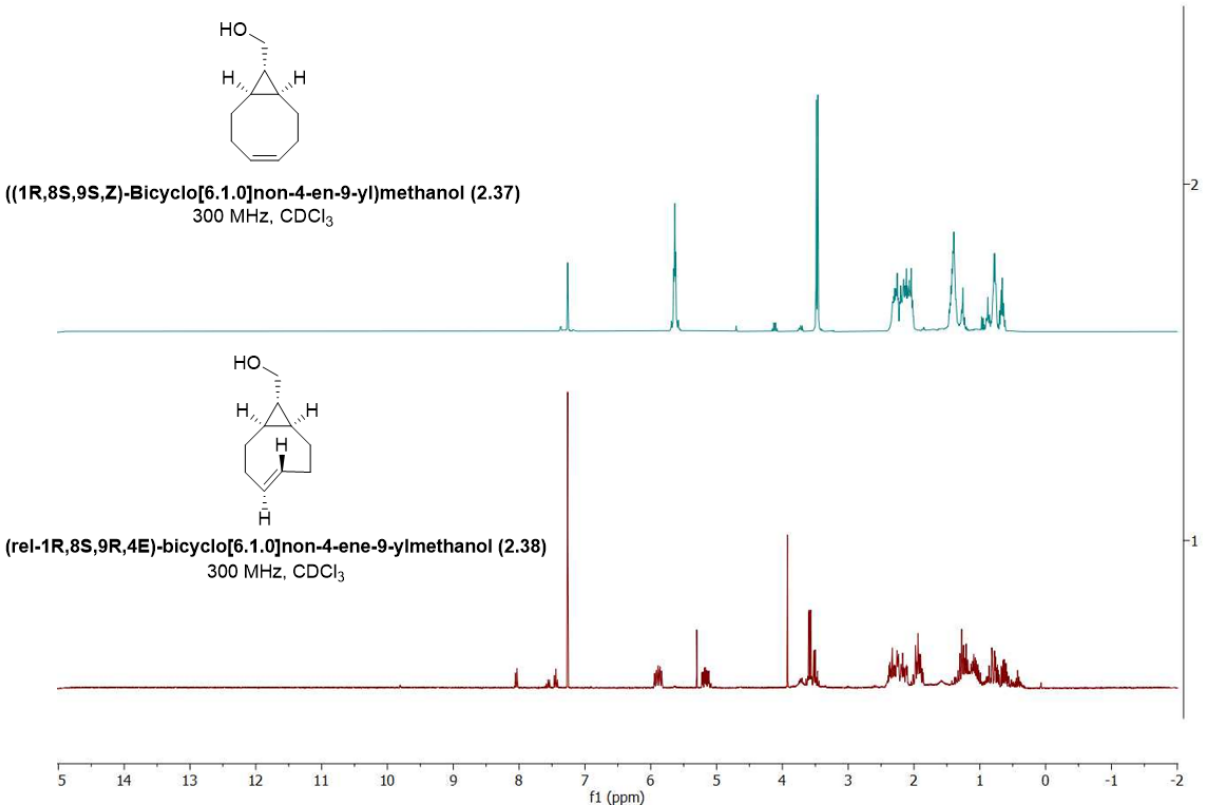

Figure 2.6 Comparison of the ^{1}H NMR of cis-4-cyclooctenol and trans-4-cyclooctenol.

Table 2.2 Synthetic results for TCO synthesis

Cyclooctene	Structure	% Yield
2.17	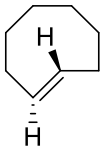	63
2.34	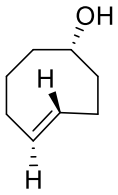	23
2.38	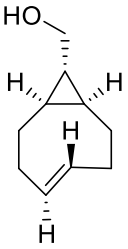	13/52

2.4 Conclusion

Overall, we have synthesized two classes of chemicals that can be applied to bioorthogonal chemistry. Diazapyrones (DAPs) are an alternative heterocycle to tetrazine and have been obtained with a yield ranging from 40-90%. We have also replicated the photochemical flow reactor developed by Fox *et al* and have shown that it works to turn cis-cyclooctenes into trans-cyclooctenes when irradiated with 254 nm light. The TCO molecules were obtained with a large span of yields ranging from 63% for TCO, 23% for TCO-OH, and 13% for s-TCO-OH. The loss of product was primarily due to the leak in the column of the reactor, and are fixed by replacing the column seal. These DAP and TCO molecules will be used in chapter 3 to study the kinetics of the reaction between DAP, BCN, and TCO for bioorthogonal reaction development.

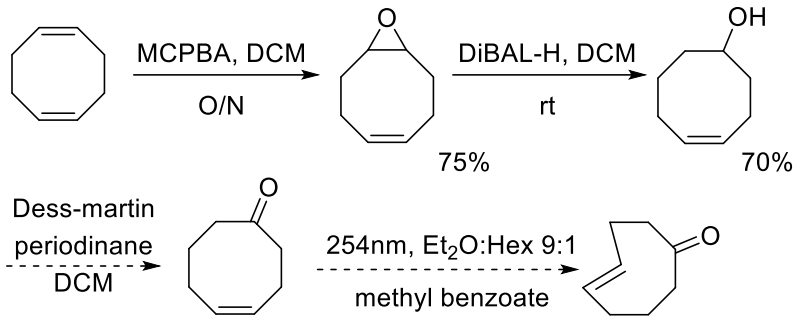

Scheme 2.5 Synthesis of trans-cyclooct-4-enone.

In future work, more TCO molecules will be synthesized, particularly trans-cyclooct-4-enone (**Scheme 2.**5) due to the easy addition of other substituents to the carbonyl. This allows for further analysis of the reactivity of reactions between DAP and TCO.

2.5 Materials and Methods

All commercially available reagents were purchased from Alfa Aesar and Sigma Aldrich and were used without further purification. Strained-trans cyclooctene rel-((1R,8S,9S, Z)-bicyclo[6.1.0]non-4-ene)-9-carboxylic acid) was received from the Fox group (Department of Chemistry at the University of Delaware, USA). All deuterated solvents were purchased from Cambridge Isotopes and were used as received, except for deuterated chloroform that was neutralized by passing through a pad of basic alumina (such treated $CDCl_3$ are indicated by an asterisk, i.e. '$CDCl_3$*'). Thin-layer chromatography (TLC) was performed on Analtech Uniplate® silica gel (60 A F254, layer thickness 250 μm). The TLC plates were visualized using a UV lamp and potassium permanganate. Flash chromatography was performed using silica gel (60 A, particle size 40-63 μm). Mass spectra were obtained using the John L. Holmes Mass Spectrometry facility at the University of Ottawa. A Waters Synapt High Definition Mass Spectrophotometer with TriWave which uses quadrupole time-of-flight mass spectrometry was used with positive

electrospray ionization (ESI+). The samples were prepared from a 4 mM stock solution in LCMS Optima grade ACN.

All ^{1}H and ^{13}C NMR spectra were obtained using 300 MHz, 400 MHz, and 600 MHz Bruker NMR spectrometers and processed using MestReNova iNMR 4.2.0 software. The units of the NMR spectra peaks are ppm and referenced against the residual solvent peak. Multiplicity of peaks are recorded as abbreviated: s = singlet, d = doublet, t = triplet, m = multiplet or unresolved, br = broad and J = coupling constants in Hz.

Experimental procedures

2.5.1 Synthesis of Diazapyrones
General Procedure A – Synthesis of Diazapyrones

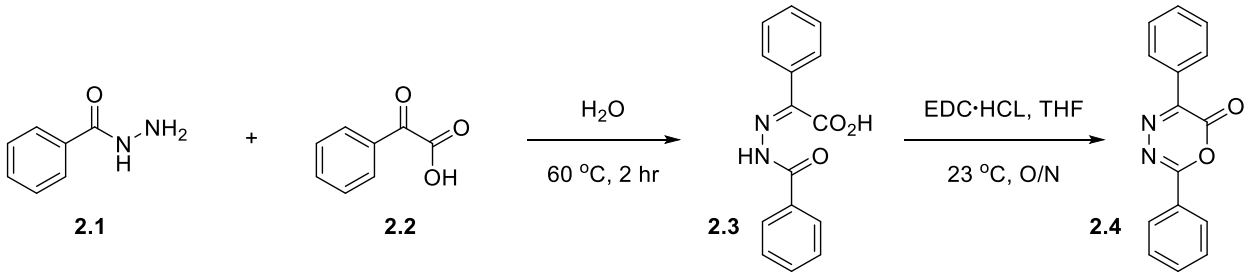

2.1 **2.2** **2.3** **2.4**

2-(2-phenylhydrazinylidene)-benzeneacetic acid (2.3) was synthesized by adding benzoic acid hydrazide (136 mg, 1 mmol) in 10 mL ddH_2O to an RBF under $Ar_{(g)}$ at 60 °C. Using a syringe pump, 150 mg of benzoylformic acid (1 mmol) was added to the RBF in 10 mL of water over 2 hours. The mixture was then stirred for an additional hour and placed in the 4 °C overnight to crystalize. The product was then filtered and dried to obtain a white solid in 48% yield. **^{1}H-NMR** (300 MHz; $CDCl_3$): δ 8.36–8.32 (m, 2H), 8.32–8.27 (m, 2H), 7.68–7.62 (m, 1H), 7.60–7.49 (m, 5H).

2,5-diphenyl-6H-1,3,4-oxadiazin-6-one (2.4) was synthesized by placing an RBF under $Ar_{(g)}$ and adding the hydrazone (300 mg, 1.11 mmol) from step A and EDC HCl (235 mg, 1.2 mmol, 1.1 eq) in 5 mL THF and allowing the mixture to stir overnight. The mixture was then extracted using 30 mL Et_2O three times and 30 mL H_2O twice. The solution was then filtered using $NaSO_4$ and concentrated. The resulting solid was then purified by crystallization with acetone to obtain a yellow crystal in 78% yield.[13] **^{1}H-NMR** (600 MHz, $CDCl_3$): δ 8.36 – 8.31 (m, 2H), 8.31 – 8.25 (m, 2H), 7.68 – 7.61 (m, 1H), 7.61 – 7.48 (m, 5H). **^{13}C-NMR** (150 MHz, $CDCl_3$): δ 157.6, 152.8, 148.2, 133.7, 132.1, 131.0, 129.1, 129.0, 128.7, 128.2, 127.5.

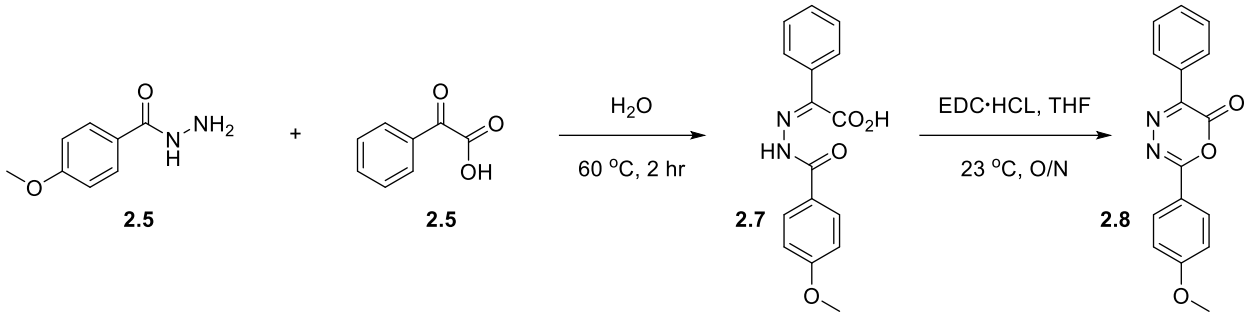

2-(2-phenylhydrazinylidene)-4-methoxy-benzeneacetic acid (2.7) was synthesized using a previously developed procedure described in general procedure A. The product was obtained in 76% yield. **^{1}H-NMR** (300 MHz, DMSO-d_6) δ 7.85 – 7.76 (m, 2H), 7.64 (dd, *J* = 6.6, 3.0 Hz, 2H), 7.44 – 7.35 (m, 3H), 7.08 (d, *J* = 8.9 Hz, 2H), 3.81 (s, 3H). Spectral data are as reported in literature.[13]

5-(4-Methoxyphenyl)-2-phenyl-6H-1,3,4-oxadiazin-6-one (2.8) was synthesized using a previously developed procedure described in general procedure A.[13] The product was obtained in 75% yield. **^{1}H-NMR** (600 MHz, $CDCl_3$): δ 8.34 – 8.29 (m, 2H), 8.27 – 8.23 (m, 2H), 7.58 – 7.50 (m, 3H), 7.07 – 7.02 (m, 2H), 3.92 (s, 3H). **^{13}C-NMR** (150 MHz, $CDCl_3$): δ 164.2, 157.7, 151.8, 148.4, 131.8, 131.3, 130.4, 128.9, 128.6, 119.6, 114.6, 55.6.

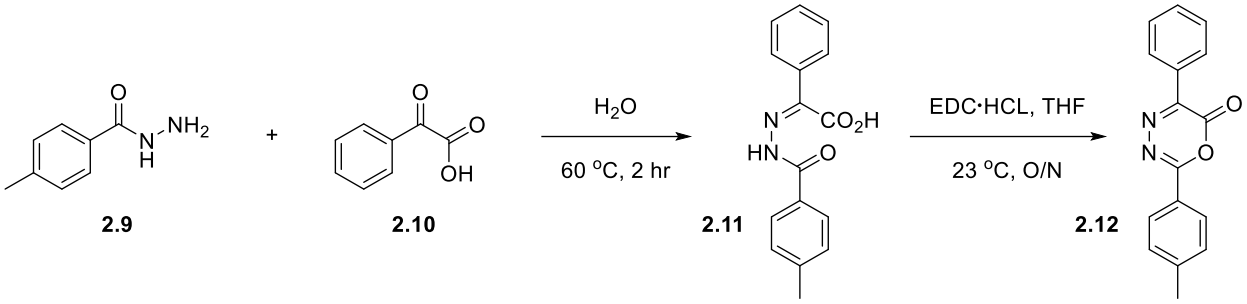

2.9 2.10 2.11 2.12

2-(2-phenylhydrazinylidene)-4-methyl-benzeneacetic acid (2.11) was synthesized using a previously developed procedure described in general procedure A[7]. The product was obtained in 64% yield. **^{1}H-NMR** (300 MHz, DMSO-d_6) δ 7.73 (d, *J* = 8.2 Hz, 2H), 7.64 (dd, *J* = 6.6, 3.1 Hz, 2H), 7.44 – 7.37 (m, 2H), 7.35 (d, *J* = 8.0 Hz, 2H), 2.36 (s, 3H).

2-(4-methyl)-5-phenyl-6H-1,3,4-oxadiazin-6-one (2.12) was synthesized using a previously developed procedure described in general procedure A.[13] The product was obtained in 64% yield. **^{1}H-NMR** (600 MHz, $CDCl_3$): δ 8.26 – 8.21 (m, 2H), 8.08 (d, 2H), 7.43 (dt, 3H), 7.25 (d, *J* = 8.1 Hz, 2H), 2.36 (s, 3H). **^{13}C-NMR** (150 MHz, $CDCl_3$): δ 157.9, 152.4, 148.3, 144.8, 131.9, 131.1, 129.9, 128.9, 128.6, 128.2, 124.7, 21.9.

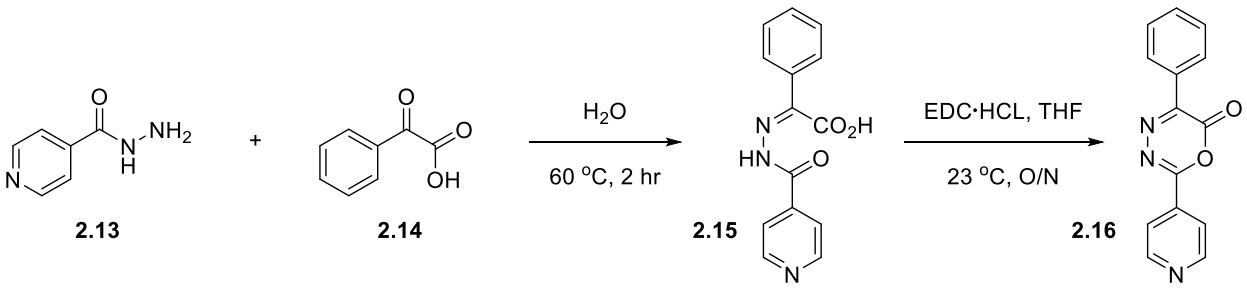

2.13 2.14 2.15 2.16

2-[2-(4-pyridinyl)hydrazinylidene]-benzeneacetic acid (2.15) was synthesized using a previously developed procedure described in general procedure A. The product was obtained in 75% yield. **^{1}H-NMR** (400 MHz, DMSO-d_6) δ 12.94 (br, 1H), 8.82 (d, *J* = 5.1 Hz, 2H), 7.77 (dd, *J* = 5.1 Hz, 3H), 7.45 (s, 4H). Spectral data are as reported in the literature.[13]

5-phenyl-2-(4-pyridinyl)-6H-1,3,4-oxadiazin-6-one (2.16) was synthesized using a previously developed procedure described in general procedure A.[13] the product was obtained in 42% yield. **^{1}H-NMR** (600 MHz, $CDCl_3$): δ 8.86 (d, 2H), 8.33 (d, 2H), 8.08 (dt, *J* = 4.5, 1.5 Hz, 2H), 7.55 (dt, 3H). **^{13}C-NMR** (150 MHz, $CDCl_3$): δ 155.8, 154.2, 151.0, 147.39, 135.2, 132.7, 130.5, 129.3, 128.8, 121.1.

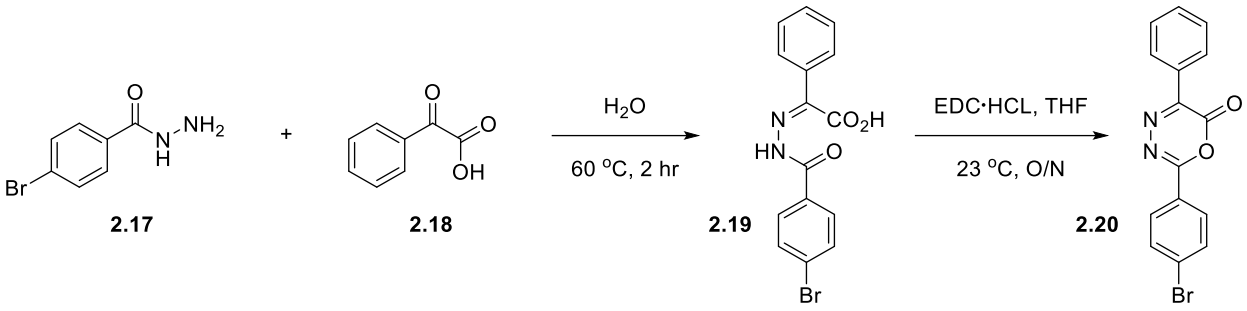

2-(p-bromophenylhydrazinylidene)-benzeneacetic acid (2.19) was synthesized using a previously developed procedure described in general procedure A. The product was obtained in 79% yield. **^{1}H-NMR** (400 MHz, DMSO-d_6) δ 12.85 (s, 1H), 7.75 (s, 4H), 7.68 – 7.56 (m, 2H), 7.45 – 7.37 (m, 3H). Spectral data are as reported in literature.[13]

2-(4-bromophenyl)-5-phenyl-6H-1,3,4-oxadiazin-6-one (2.20) was synthesized using a previously developed procedure described in general procedure A.[13] The product was obtained in 70% yield. **^{1}H-NMR** (600 MHz; $CDCl_3$): δ 8.28 – 8.23 (m, 2H), 8.11 – 8.05 (m, 2H), 7.66 – 7.60 (m, 2H), 7.53 – 7.43 (m, 3H). **^{13}C-NMR** (150 MHz, $CDCl_3$): δ 157.0, 153.0, 147.9, 132.56, 132.2, 130.9, 129.6, 129.1 (d, *J* = 2.6 Hz), 128.7, 126.5.

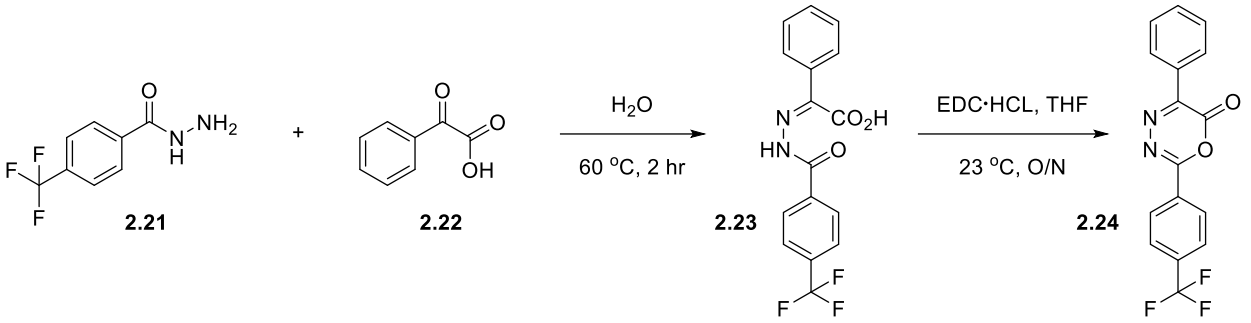

2.21 2.22 2.23 2.24

2-(p-trifluoromethylphenylhydrazinylidene)-benzeneacetic acid (2.23) was synthesized using a previously developed procedure described in general procedure A. The product was obtained in 69% yield. **^{1}H-NMR** (400 MHz, CD_3OD) δ 8.09 (dd, *J* = 8.0 Hz, 2H), 7.89 – 7.73 (m, 4H), 7.59 – 7.37 (m, 3H). Spectral data are as reported in literature.[13]

2-(4-trifluoromethylphenyl)-5-phenyl-6H-1,3,4-oxadiazin-6-one (2.24) was synthesized using a previously developed procedure described in general procedure A.[13] The product was obtained in 95% yield. **^{1}H-NMR** (600 MHz, $CDCl_3$): δ 8.33 (dd, *J* = 8.0, 0.8 Hz, 2H), 8.28 – 8.25 (m, 2H), 7.76 – 7.72 (m, 2H), 7.54 – 7.50 (m, 1H), 7.47 – 7.43 (m, 2H). **^{13}C-NMR** (150 MHz, $CDCl_3$): δ 156.3, 153.5, 147.7, 132.5, 130.9, 130.7, 129.4, 129.2, 128.8, 128.5, 126.1, 126.0, 124.4, 122.6.

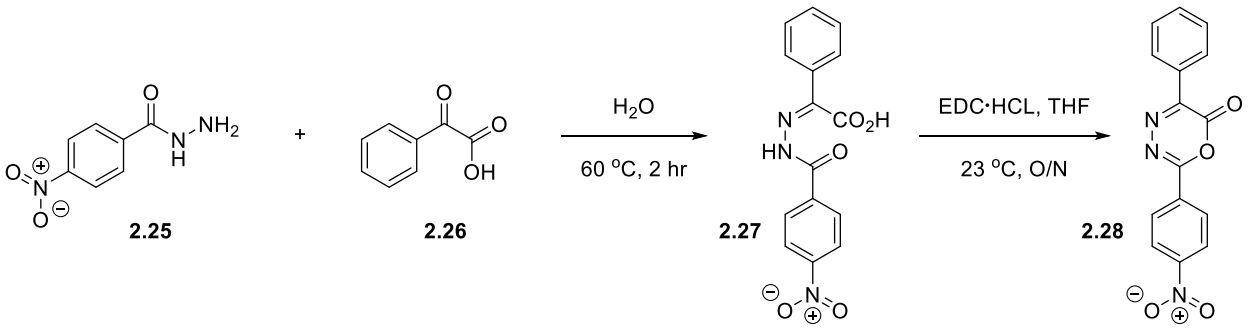

2.25 2.26 2.27 2.28

2-[2-(4-nitrophenyl)hydrazinylidene]-benzeneacetic acid (2.27) was synthesized using a previously developed procedure described in general procedure A. The product was obtained in 64% yield. **^{1}H-NMR** (400 MHz, DMSO-d_6) δ 12.93 (s, 1H), 8.35 (d, *J* = 9.0 Hz, 2H), 8.09 – 8.01 (m, 2H), 7.66 (s, 2H), 7.42 (s, 3H). Spectral data are as reported in literature.[13]

5-(4-nitrophenyl)-2-phenyl-6H-1,3,4-oxadiazin-6-one (2.28) was synthesized using a previously developed procedure described in general procedure A.[13] The product was obtained in 38% yield. **^{1}H-NMR** (600 MHz, $CDCl_3$): δ 8.44 – 8.38 (m, 2H), 8.36 – 8.31 (m, 2H), 8.31 – 8.26 (m, 2H), 7.58 – 7.52 (m, 1H), 7.50 – 7.44 (m, 2H). **^{13}C-NMR** (150 MHz, $CDCl_3$): δ 155.7, 153.7, 150.7, 147.4, 133.2, 132.7, 130.5, 129.3, 129.2, 128.8, 124.2.

2.5.2 Synthesis of Cyclooctenes

2.5.2.1 Synthesis of TCO

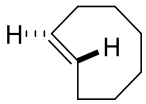

Trans-cyclooctene (2.30) Cis-cyclooctene (1.0 g, 9.1 mmol), methyl benzoate (3.3 g, 24.0 mmol), and 400 mL of a 1% mixture of Et_2O:Hexane were added to a 500 mL quartz flask and placed on the photochemical flow reactor described in general procedure B outlined in chapter 2.[14] The product was obtained in 63% yield. **^{1}H-NMR** (300 MHz, $CDCl_3$) δ 5.57 – 5.50 (m, 2H), 2.40 (dd, *J* = 11.4, 5.4 Hz, 2H), 2.08 – 1.78 (m, 6H), 1.56 – 1.33 (m, 2H), 0.92 – 0.74 (m, 2H). **^{13}C-NMR** (100 MHz, $CDCl_3$) δ 133.9, 35.8, 35.6, 29.2.

2.5.2.2 Synthesis of TCO-OH

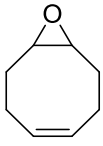

9-Oxabicyclo[6.1.0]non-4-ene (2.32) was synthesized by following a literature protocol.[15] The product was obtained in 51% yield. **^{1}H-NMR** (300 MHz, $CDCl_3$) δ 5.61 (tdd, *J* = 4.2, 1.9, 0.9 Hz, 2H), 3.07 (qd, *J* = 3.8, 2.4 Hz, 2H), 2.56 – 2.37 (m, 2H), 2.28 – 2.00 (m, 6H).

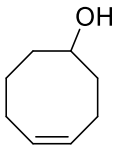

Cyclooct-4-enol (2.33) was synthesized by following a literature protocol.[15] The product was obtained in 66% yield. **^{1}H-NMR** (300 MHz, $CDCl_3$) δ 5.77 – 5.52 (m, 2H), 3.82 (dddd, *J* = 9.4, 8.3, 4.4, 1.1 Hz, 1H), 2.39 – 1.20 (m, 11H).

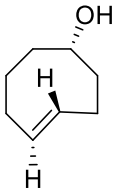

(E)-cyclooct-4-enol (3.34) cyclooct-4-enol (1 g, 7.92 mmol), methyl benzoate (1.07 g, 7.92 mmol) and 400 mL of a 1:10 mixture of Hex:EtO_2) were added to a 500 mL quartz flask and placed on the photochemical flow reactor described in general procedure B.[14] The major product was obtained in 23% yield. **^{1}H-NMR** (300 MHz, $CDCl_3$) δ 5.61 (ddd, *J* = 15.1, 10.2, 4.5 Hz, 1H), 5.42 (ddd, *J* = 16.0, 10.8, 3.6 Hz, 1H), 3.58 – 3.41 (m, 1H), 2.44 – 2.22 (m, 5H), 2.10 – 1.87 (m, 5H), 1.80 – 1.50 (m, 5H). **^{13}C-NMR** (100 MHz, $CDCl_3$) δ 135.1, 132.8, 77.8, 44.6, 41.1, 34.3, 32.7, 31.2.

2.5.2.3 Synthesis of s-TCO-OH

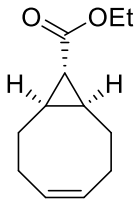

(1R,8S,9R,Z)-ethyl bicyclo[6.1.0]non-4-ene-9-carboxylate (2.35) was synthesized as reported in literature and match the reported ^{1}H NMR spectra.[6] The endo product was obtained in 38%

yield. **^{1}H-NMR** (300 MHz, $CDCl_3$) δ 5.69 – 5.53 (m, 2H), 4.12 (q, *J* = 7.1 Hz, 2H), 2.59 – 2.43 (m, 2H), 2.30 – 1.97 (m, 3H), 1.91 – 1.76 (m, 2H), 1.71 (t, 1H), 1.45 – 1.34 (m, 2H), 1.27 (t, *J* = 7.1 Hz, 3H).

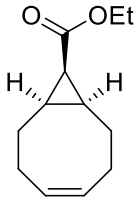

(1R,8S,9S, Z)-ethyl bicyclo[6.1.0]non-4-ene-9-carboxylate (2.36) was synthesized as reported in literature and match the reported ^{1}H NMR spectra.[6] The exo product was obtained in 49% yield. **^{1}H-NMR** (300 MHz, $CDCl_3$) δ 5.72 – 5.53 (m, 2H), 4.11 (q, *J* = 7.1, 4.9 Hz, 2H).

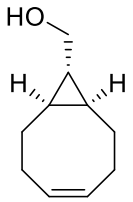

((1R,8S,9S,Z)-Bicyclo[6.1.0]non-4-en-9-yl)methanol (3.37) was synthesized as reported in literature and matched the reported ^{1}H NMR spectra.[6] The product was obtained in 94% yield. **^{1}H-NMR** (300 MHz, $CDCl_3$) δ 5.72 – 5.53 (m, 2H), 3.47 (d, *J* = 6.9 Hz, 2H), 2.38 – 1.98 (m, 4H), 1.41 (m, 4H), 1.31 – 1.20 (m, 1H), 0.83 – 0.58 (m, 3H).

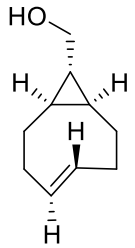

(rel-1R,8S,9R,4E)-bicyclo[6.1.0]non-4-ene-9-ylmethanol (3.38) was synthesized as reported according to literature with minor adjustments.[6] The ^{1}H NMR matches that reported in the literature.[6] ((1R,8S,9S,Z)-Bicyclo[6.1.0]non-4-en-9-yl)methanol (400 mg, 2.06 mmol), methyl benzoate (358 mg, 2.6 mmol) and 400mL of a 1:1 mixture of Hex:EtO_2) were added to a 500 mL quartz flask and placed on the photochemical flow reactor described in general procedure B found in chapter 2.[6] The $AgNO_3$ impregnated column was excessively flushed with Hexanes and Et_2O ~600 mL in place of the stated amount of 200 mL. The product was obtained in 13% yield. **^{1}H-NMR** (300 MHz, $CDCl_3$) δ 5.97 – 5.80 (m, 1H), 5.25 – 5.05 (m, 1H), 3.67 – 3.41 (m, 2H), 2.43 – 1.82 (m, 5H), 1.46 – 0.69 (m, 3H), 0.68 – 0.30 (m, 2H).

References

(1) Bird, R. E.; Lemmel, S. A.; Yu, X.; Zhou, Q. A. Bioorthogonal Chemistry and Its Applications. *Bioconjugate Chemistry* **2021**, *32* (12), 2457-2479. DOI: 10.1021/acs.bioconjchem.1c00461.

(2) Nguyen, S. S.; Prescher, J. A. Developing bioorthogonal probes to span a spectrum of reactivities. *Nature Reviews Chemistry* **2020**, *4* (9), 476-489. DOI: 10.1038/s41570-020-0205-0.

(3) Walker, R.; Conrad, R. M.; Grubbs, R. H. The Living ROMP of trans-Cyclooctene. *Macromolecules* **2009**, *42* (3), 599-605. DOI: 10.1021/ma801693q.

(4) Selvaraj, R.; Fox, J. M. trans-Cyclooctene--a stable, voracious dienophile for bioorthogonal labeling. *Current opinion in Chemical Biology* **2013**, *17* (5), 753-760. DOI: 10.1016/j.cbpa.2013.07.031.

(5) Darko, A.; Wallace, S.; Dmitrenko, O.; Machovina, M. M.; Mehl, R. A.; Chin, J. W.; Fox, J. M. Conformationally strained trans-cyclooctene with improved stability and excellent reactivity in tetrazine ligation. *Chemical Science* **2014**, *5* (10), 3770-3776. DOI: 10.1039/C4SC01348D.

(6) Taylor, M. T.; Blackman, M. L.; Dmitrenko, O.; Fox, J. M. Design and Synthesis of Highly Reactive Dienophiles for the Tetrazine–trans-Cyclooctene Ligation. *Journal of the American Chemical Society* **2011**, *133* (25), 9646-9649. DOI: 10.1021/ja201844c.

(7) Barber, J. Harnessing the Reactivity of Strained Intermediates and Biosynthetic Machinery. University of California, Los Angeles, United States, 2019.

(8) Lambert, W. D.; Fang, Y.; Mahapatra, S.; Huang, Z.; am Ende, C. W.; Fox, J. M. Installation of Minimal Tetrazines through Silver-Mediated Liebeskind–Srogl Coupling with Arylboronic Acids. *Journal of the American Chemical Society* **2019**, *141* (43), 17068-17074. DOI: 10.1021/jacs.9b08677.

(9) Wu, H.; Yang, J.; Šečkutė, J.; Devaraj, N. K. In Situ Synthesis of Alkenyl Tetrazines for Highly Fluorogenic Bioorthogonal Live-Cell Imaging Probes. *Angewandte Chemie International Edition* **2014**, *53* (23), 5805-5809. DOI: 10.1002/anie.201400135.

(10) Mao, W.; Shi, W.; Li, J.; Su, D.; Wang, X.; Zhang, L.; Pan, L.; Wu, X.; Wu, H. Organocatalytic and Scalable Syntheses of Unsymmetrical 1,2,4,5-Tetrazines by Thiol-Containing Promotors. *Angewandte Chemie International Edition* **2019**, *131* (4), 1118-1121. DOI: 10.1002/ange.201812550.

(11) Qu, Y.; Sauvage, F. X.; Clavier, G.; Miomandre, F.; Audebert, P. Metal-Free Synthetic Approach to 3-Monosubstituted Unsymmetrical 1,2,4,5-Tetrazines Useful for Bioorthogonal Reactions. *Angewandte Chemie International Edition* **2018**, *57* (37), 12057-12061. DOI: 10.1002/anie.201804878.

(12) Yang, J.; Karver, M. R.; Li, W.; Sahu, S.; Devaraj, N. K. Metal-Catalyzed One-Pot Synthesis of Tetrazines Directly from Aliphatic Nitriles and Hydrazine. *Angewandte Chemie International Edition* **2012**, *51* (21), 5222-5225. DOI: 10.1002/anie.201201117.

(13) Ramirez, M.; Darzi, E. R.; Donaldson, J. S.; Houk, K. N.; Garg, N. K. Cycloaddition Cascades of Strained Alkynes and Oxadiazinones. *Angewandte Chemie International Edition* **2021**, *60* (33), 18201-18208, DOI:10.1002/anie.202105244.

(14) Royzen, M.; Yap, G. P. A.; Fox, J. M. A Photochemical Synthesis of Functionalized trans-Cyclooctenes Driven by Metal Complexation. *Journal of the American Chemical Society* **2008**, *130* (12), 3760-3761. DOI: 10.1021/ja8001919.

(15) Baalmann, M.; Neises, L.; Bitsch, S.; Schneider, H.; Deweid, L.; Werther, P.; Ilkenhans, N.; Wolfring, M.; Ziegler, M. J.; Wilhelm, J.; et al. A Bioorthogonal Click Chemistry Toolbox for

Targeted Synthesis of Branched and Well-Defined Protein–Protein Conjugates. *Angewandte Chemie International Edition* **2020**, *59* (31), 12885-12893, DOI: 10.1002/anie.201915079.

Chapter 3 - Reactivity of the cycloaddition between diazapyrones and BCN and s-TCO

3.1 Introduction

It is difficult for chemical reactions to occur within a cellular environment while still maintaining the stability of the living system. Because of this, there is an inherent need to expand the bioorthogonal toolbox. A bioorthogonal reaction needs to occur with a high yield and fast enough rate to ensure that the concentration of the reagents are minimal, thus lowering its toxicity and preventing extensive interference with the living system.[1,2] Currently, the fastest known bioorthogonal reaction exhibiting high versatility is the tetrazine ligation with second-order rate constants ranging from 10^1 to 10^6 $M^{-1}s^{-1}$.[3] That being said, the tetrazine is easily hydrolyzed in aqueous environments and is redox-sensitive. This drives the need for a similar molecule to tetrazine or an alternative reaction with similar rates that are more stable in a cellular environment.

3.1.1 IEDDA – The Tetrazine Ligation

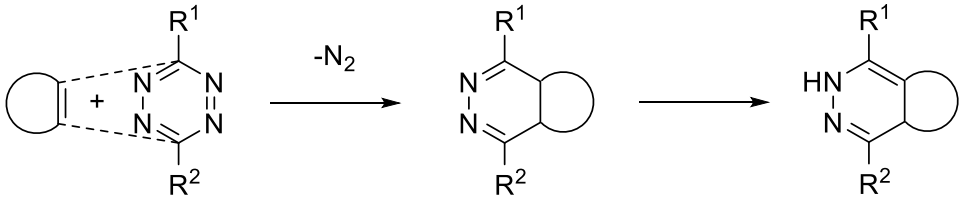

Scheme 3.8 The reaction between tetrazine and a cycloalkene via an inverse electron demand Diels alder reaction.

The tetrazine ligation is ideal for bioorthogonal chemistry due to its fast rates that allow for easy cell labelling at low concentrations and is not intrusive to the cell. The reaction also doesn't utilize metals and works at physiological pH, eliminating the cytotoxicity issue that other bioorthogonal

reactions such as CuAAC possess.[4] Mechanistically, the tetrazine ligation is a reaction that occurs between the 4π orbitals of tetrazine (diene) and the 2π orbitals of an alkene or alkyne (dienophile) through an IEDDA (**Scheme 3.1**).[5] The IEDDA reaction uses an electron-poor diene and an electron-rich dienophile, as opposed to the reverse case seen in typical Diels Alder cycloaddition reactions. This reaction is governed by the $HOMO_{dieneophile}$ and $LUMO_{diene}$ gap, where the smaller the gap, the faster the reaction will be.[6] One of the easiest ways to manipulate the HOMO-LUMO gap is with the electronics of tetrazine, which is controlled by adding electron-donating or withdrawing substituents on the molecule. For an IEDDA reaction, the diene is electron-poor therefore adding electron-withdrawing groups to the tetrazine will lower the HOMO-LUMO gap (**Figure 3.1**).

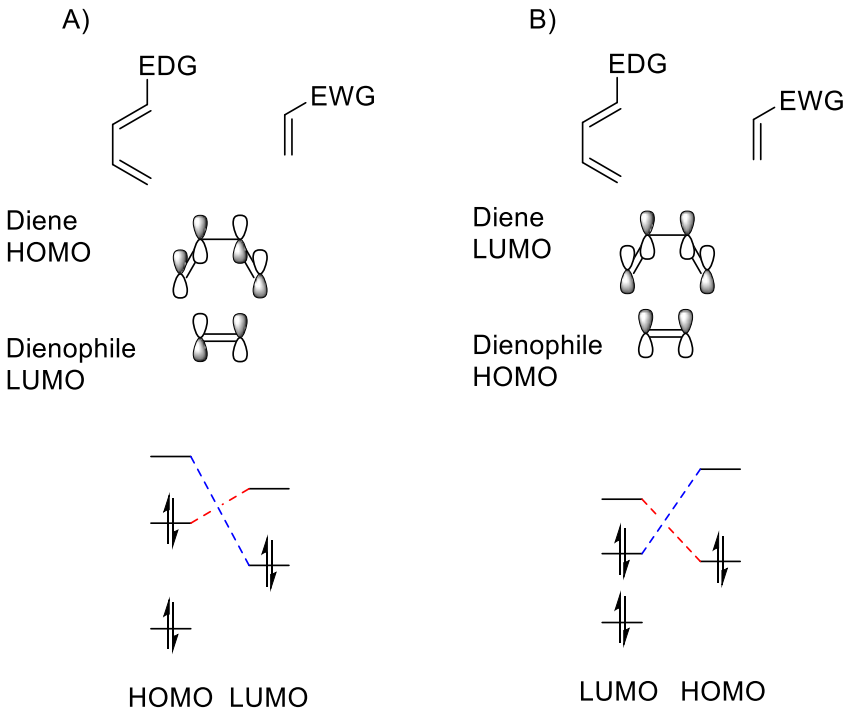

Figure 3.1 Electronic effect of electron-donating (EDG) and electron-withdrawing groups (EWG) on the HOMO and LUMO of the diene and dienophile of cycloaddition reactions.[5] Where A) is the reaction between the HOMO of the Diene and LUMO of the Dienophile and B) is the reaction between the HOMO of the dienophile and the LUMO of the Diene.

Another way the HOMO-LUMO gap can be manipulated is by using a dienophile that contains ring strain. The added ring strain increases the energy of the HOMO, therefore, decreasing the HOMO-LUMO gap. An example of this is cyclooctyne which is the smallest ring that can accommodate the triple bond and has ~18 kcal/mol of ring strain.[7] Another example is trans-cyclooctene (TCO) developed by the Fox group and others.[8] Compared to the cis-conformer of cyclooctene (CCO), TCO has second-order rate constants that are 7-fold larger. This is further increased with strained trans-cyclooctene (s-TCO) which have second-order rate constants that are 160 times faster than the reaction with TCO.[9,10] The increase in reactivity when comparing TCO and sTCO is due to the pseudo-chair conformation of the molecules (**Figure 3.2**). TCO can adopt either the "crown" or "half chair" conformation and then react with a dienophile. The half-chair

conformation has an addition of 5.6 kcal/mol of energy, due to strain, compared to the "crown" conformation. sTCO on the other hand can only adopt the "half-chair" conformation due to the fused cyclopropane ring. This destabilizes the ground state of the molecule and forces sTCO to be in a conformation more similar to the transition state.[11] This allows reactions with sTCO to have faster rates than reactions with TCO. Overall, the strain provided by the diene (cyclooctynes, TCO, s-TCO) pre-distorts the diene allowing for less distortion energy to be used to reach the transition state which subsequently allows for a faster reaction that is ideal for bioorthogonal chemistry.[2]

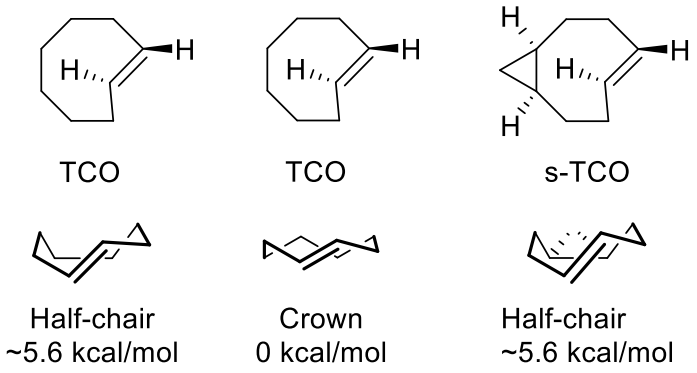

Figure 3.2 The strain effect on the conformation of trans-cyclooctenes. From left to right the molecules are trans-cyclooctene (where the molecule can adopt the crown or half-chair conformations) and strained trans-cyclooctene (where the half-chair is the only available conformation).

The tetrazine ligation can also be manipulated by sterics. The premise of this is that the less steric hindrance present in the reaction, the faster the reaction will be. For example, Devaraj discovered that an IEEDA reaction with a monosubstituted tetrazine is 30 times faster than a disubstituted tetrazine.[12] This is due to the added steric bulk from the disubstituted tetrazine. This is further proven when comparing a methylated tetrazine to an unsubstituted tetrazine. The methylated tetrazine adds 6 kcal/mol of distortion energy to the reaction causing a slower rate compared to the unsubstituted tetrazine.[13]

Finally, the tetrazine ligation can be manipulated by solvent effects. Protic solvents increase the rate of the tetrazine ligation by increasing the hydrophobic interactions between the reactants and stabilizing the interaction between the reaction and water.[14] In terms of the HOMO-LUMO gap, the protic solvent allows for H-bonding between the tetrazine complex and water. This increases the polarity and, in turn, decreases the HOMO-LUMO gap which then increases the overall rate of reaction.[14, 15]

3.1.2 Alternatives to Tetrazine

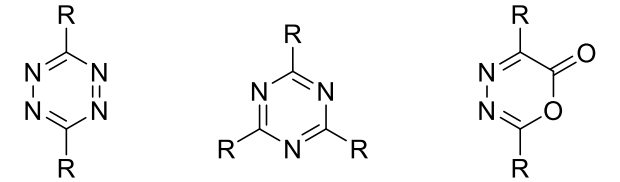

Figure 3.3 The structure of tetrazine and its alternatives triazine and diazapyrones.

Due to tetrazine redox sensitivity and hybridizability, an alternative to tetrazine is the key to the expansion of the bioorthogonal chemistry toolbox. This particularly becomes a problem with the more electron-withdrawing tetrazines that are more reactive due to the decreased energy of the LUMO of the diene but also their increased susceptibility to hydrolysis and redox reactions.[16] To combat this issue, tetrazines had been modified with thiols. However, this increases the size of the molecule to a point where it is no longer ideal for bioorthogonal chemistry.[17,18] One of the key alternatives for tetrazine has been triazines which have three nitrogen in their heterocyclic core rather than four (**Figure 3.3**).[19] This stabilizes the molecule and is less likely to hydrolyze in an aqueous environment. While this reaction has similar second-order rate constants to other bioorthogonal reactions, with a $k_2 \sim 10^{-2}$ $M^{-1}s^{-1}$, it is much slower than the tetrazine ligation.[20] Furthermore, triazine can only react with trans-cyclooctene molecules, limiting its versatility in

the application of biorthogonal chemistry. Another alternative to tetrazines are diazapyrones which are structurally similar to tetrazines, except two of the nitrogen in the heterocyclic core of tetrazine have been replaced by an ester group (**Figure 3.3**). This allows for either N_2 or CO_2 gas to be lost in the IEDDA reaction while maintaining the irreversibility of the tetrazine ligation. The addition of the carbonyl ester site adds the ability for modification to stabilize the molecule and form an ortho-ester without compromising the size of the molecule. The reaction between diazapyrones and benzyne and some cyclooctynes has been reported.[21] However, even with the evolution of the tetrazine ligation and the investigation of alternative dienes, tetrazine is still one of the most widely used molecules in bioorthogonal chemistry.

3.2 Objective

Based on Garg's work on the cycloaddition between diazapyrones and cyclohexenes, we aimed to find an alternative bioorthogonal reaction comparable to the fastest known bioorthogonal reaction, the tetrazine ligation. This was accomplished by studying reaction rates of various para-substituted diazapyrones, a similar adduct to tetrazine, with two different cycloadducts, BCN and s-TCO.

3.3 Results and Discussion

3.3.1 Kinetic Studies and Methodology – BCN

Kinetic studies procedure

The second-order rate constants (k_2) for the cycloaddition between various diazapyrones, BCN, and s-TCO were followed by using UV-Vis spectroscopy. These compounds were synthesized in Chapter 2. The reaction was studied under pseudo-first-order conditions where the cyclooctyne, BCN, was in a 10-50 fold excess (BCN). Each kinetic run was performed simultaneously in duplicate in acetonitrile at 25 ± 0.1 °C (n=2). The reaction was monitored by tracking the decrease of the diazapyrone peak specified in **Table 3.7.**

General procedure for the kinetic studies

To perform UV-Vis kinetics, a 4 mM stock solution of reach reagent was made. The excess reagent BCN was then serially diluted with ACN to a specified concentration **(Table 3.7)**. The excess reagent was then added to a clean cuvette followed by a calculated amount of diazapyrone. The cuvette was then capped, thoroughly mixed by inversion 5 times, and inserted into the UV-Vis spectrophotometer. Measurements were immediately obtained and collected every 60 seconds over 3 half-lives. The reaction was monitored by tracking the decrease of the diazapyrone peak stated in **Table 3.1.** The products were characterized using NMR and EI-MS.

Table 3.1 Reaction parameter of the cycloaddition reaction between BCN and various diazapyrones and the wavelength absorption (nm) of the corresponding decaying diazapyrone peak.

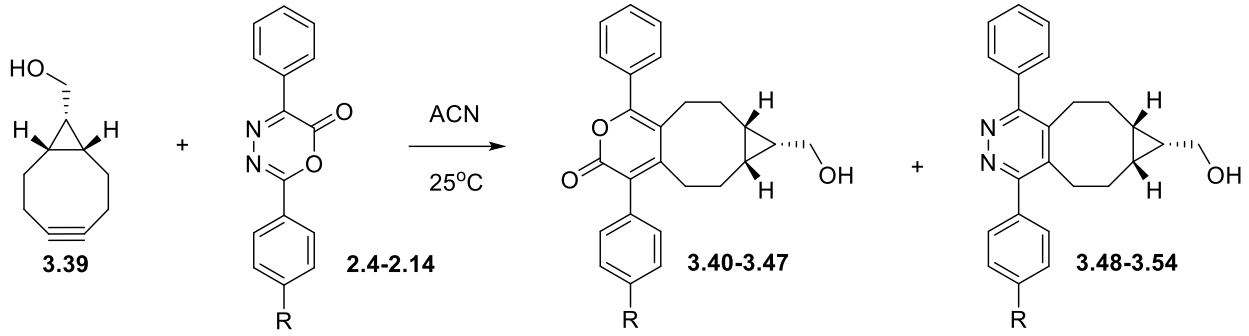

	Diazapyrone	Wavelength (nm)
2.2	R = H	344
2.4	R = OMe	372
2.6	R = Me	352
2.8	R = Py	333
2.10	R = Br	347
2.12	R = CF_3	340
2.14	R = NO_2	291

Data analysis of pseudo-first-order UV-Vis kinetic experiments. The UV-Vis data were analyzed by taking the natural log of the absorbance values of each diazapyrone and plotting them against time, for each excess concentration of BCN. The linear portion of these plots are used to obtain a negative slope that represents the k_{obs} values. The k_{obs} values for each duplicate run were averaged and used to determine k_2. To determine k_2, the positive average of k_{obs} values are plotted against each respective BCN concentration and analyzed using linear regression. The slope of the

linear regression is the k_2 rate constant. An example of this analysis can be seen **in Tables 3.2** and **3.4, Figures 3.4** and **3.5,** and **Appendix B**.

Table 3.2 Observed rate constants for the cycloaddition reaction between 5-methyl-2-phenyl-6H-1,3,4-oxadiazin-6-one (**2.6**) at 25 µM and endo BCN, with various concentrations of BCN in ACN at 25 ± 0.1 °C.

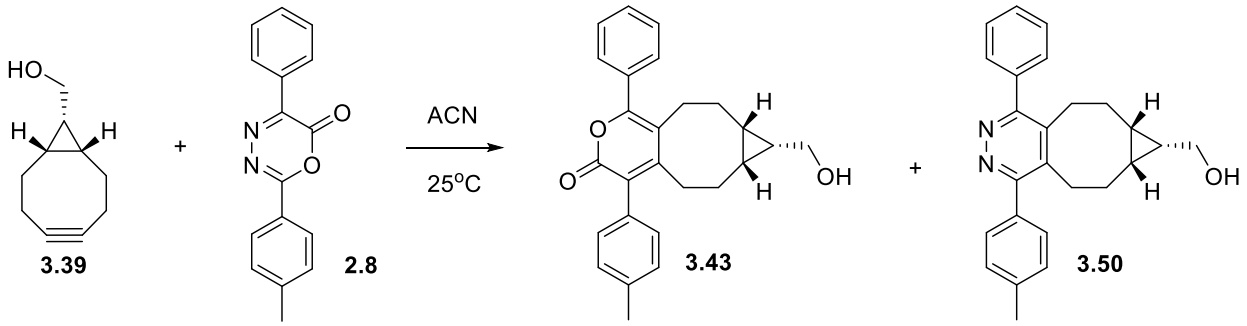

Diazapyrone	[BCN] (10^{-4} M)	k_{obs} (10^{-7} s^{-1})
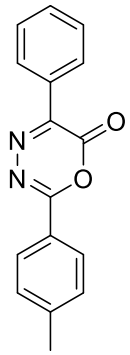	0.25	30.0 ± 2.00
	0.50	61.9 ± 1.00
	0.75	89.4 ± 0.200
	1.00	122 ± 5.00
	1.25	154 ± 4.00

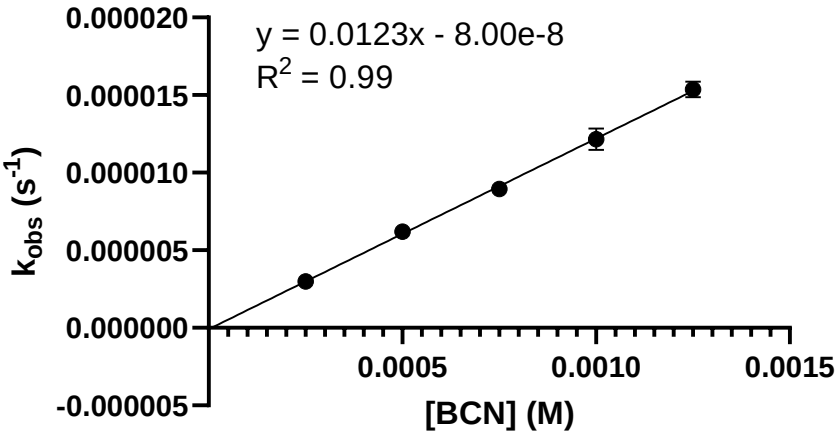

Figure 3.4 Pseudo first-order rate constant of the cycloaddition reaction between 5-methyl-2-phenyl-6H-1,3,4-oxadiazin-6-one (**2.6**) at 25 μM and endo BCN plotted against varying concentrations of BCN. These reactions were performed in ACN at 25 ± 0.1 °C. The error bars represent SD (n=2).

3.3.2 Kinetic Studies and Methodology – s-TCO-CO_2H

Kinetic studies procedure

The second-order rate constant (k_2) for the cycloaddition between various diazapyrones and s-TCO-CO_2H were determined by using UV-Vis spectroscopy. The reaction was studied under pseudo-first-order conditions where the cyclooctene, s-TCO, was in a 10-60 fold excess. Each kinetic run was performed in performed simultaneously in duplicate in ACN at 25 ± 0.1 °C (n=2). The reaction was monitored by tracking the decrease of the diazapyrone peak specified in **Table 3.3.**

To perform UV-Vis kinetics, a 4 mM stock solution of each reagent was made. The excess reagent s-TCO was then serially diluted with ACN to a specified concentration **(Table 3.7)**. The excess reagent was then added to a clean cuvette followed by a calculated amount of diazapyrone. The cuvette was then capped, thoroughly mixed by inversion 5 times, and inserted into the UV-Vis spectrophotometer. Measurements were immediately obtained and collected every 10 seconds.

The reaction was monitored by tracking the decrease of the diazapyrone peak stated in **Table 3.3.**

The products were characterized using NMR and EI-MS.

Table 3.3 Reaction scheme of the cycloaddition reaction between sTCO and various diazapyrones and the wavelength absorption (nm) of the corresponding decaying diazapyrone peak.

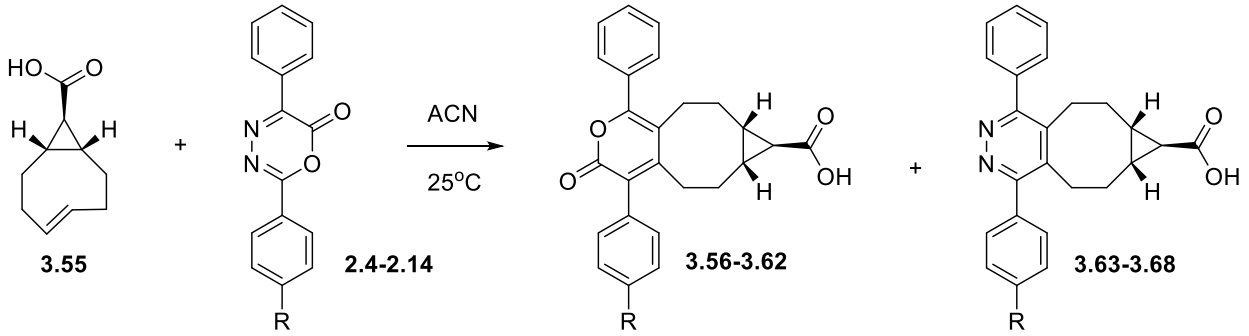

	Diazapyrone	Wavelength (nm)
2.2	R = Ph	350
2.4	R = OMe	371
2.6	R = Me	350
2.8	R = Py	340
2.10	R = Br	350
2.12	R = CF_3	345
2.14	R = NO_2	350

Data analysis of pseudo-first-order UV-Visible kinetic experiments.

Table 3.4 Observed rate constants for the cycloaddition reaction between 2,5-diphenyl-6H-1,3,4-oxadiazin-6-one (**2.2**) and s-TCO, with various concentrations of s-TCO in ACN at 25 ± 0.1 °C.

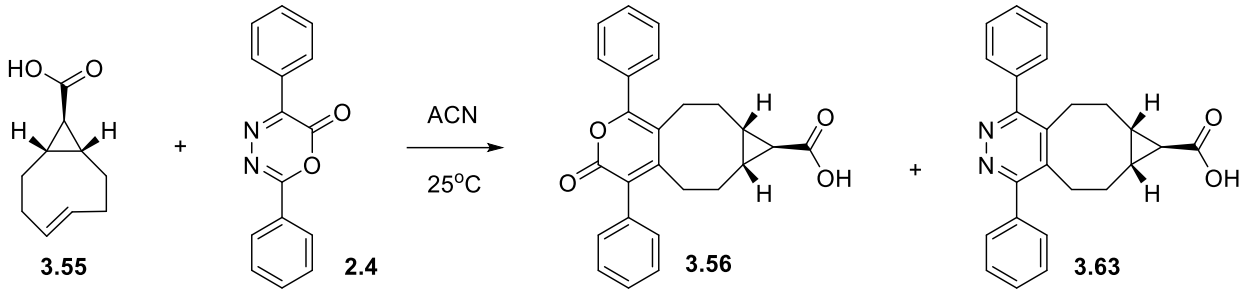

3.55 **2.4** **3.56** **3.63**

Diazapyrone	**[s-TCO] (10^{-4} M)**	**k_{obs} (10^{-5} s^{-1})**
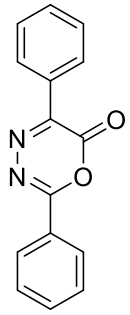	0.45	163 ± 0.10
	0.90	321 ± 0.08
	1.35	468 ± 3.00
	1.80	588 ± 0.30
	2.25	710 ± 9.00

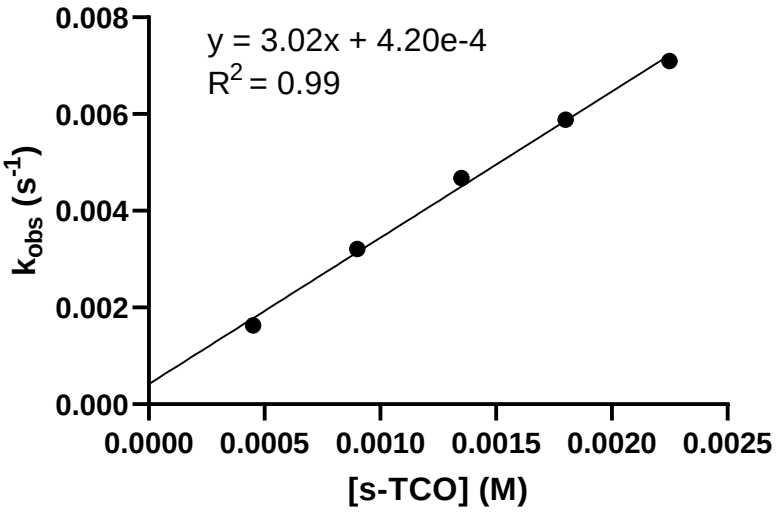

Figure 3.5 Pseudo first-order rate constant of the cycloaddition reaction between 2,5-diphenyl-6H-1,3,4-oxadiazin-6-one (**2.2**) and s-TCO plotted against varying concentrations of BCN. These reactions were performed in ACN at 25 ± 0.1 °C. The error bars represent SD (n=2).

3.3.3 Cycloadditions of BCN and s-TCO with Diazapyrones

Table 3.5 Kinetic results of the cycloaddition between BCN and various Diazapyrones studied under pseudo-first-order conditions.

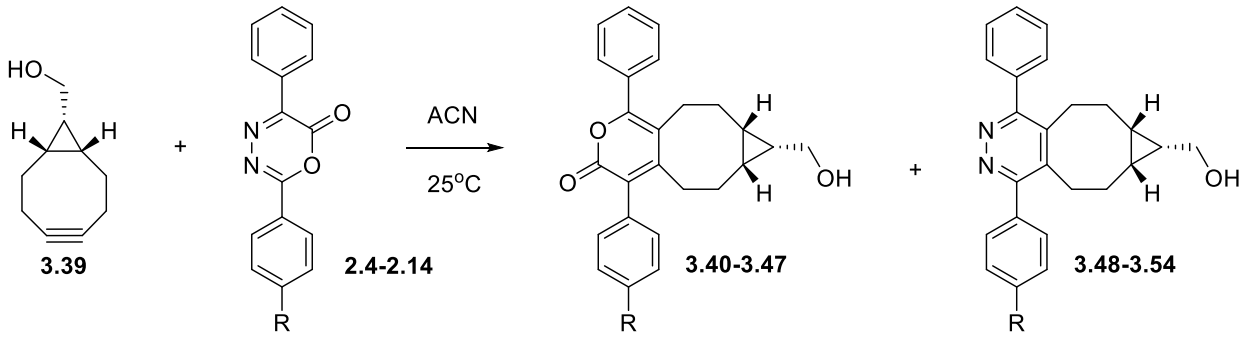

	Diazapyrone	k_2 (10^{-3} $M^{-1}s^{-1}$)
2.2	R = H	12 ± 0.80
2.4	R = OMe	14 ± 0.70
2.6	R = Me	12 ± 0.30
2.8	R = Py	22 ± 2.0
2.10	R = Br	19 ± 0.60
2.12	R = CF_3	28 ± 2.0
2.14	R = NO_2	18 ± 4.0

Table 3.6 Kinetic results of the cycloaddition between s-TCO and a variety of diazapyrones under pseudo-first-order conditions.

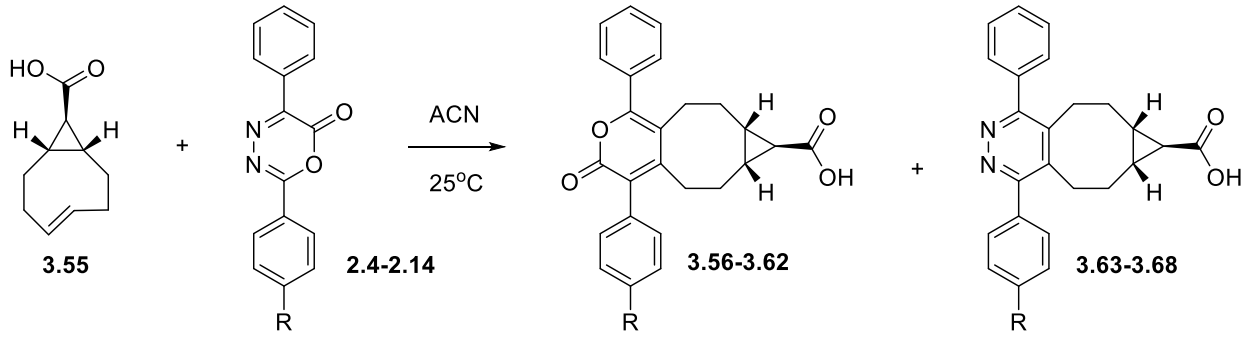

	Diazapyrone	k_2 (10^{-1} $M^{-1}s^{-1}$)
2.2	R = H	30 ± 0.70
2.4	R = OMe	16 ± 0.20
2.6	R = Me	24 ± 0.4
2.8	R = Py	95 ± 9.0
2.10	R = Br	40 ± 1.0
2.12	R = CF_3	40 ± 2.0
2.14	R = NO_2	83 ± 2.0

The para-substituted effect of various diazapyrones was studied by reacting diazapyrones (**2.2-2.14**) with BCN and s-TCO under pseudo-first-order conditions. The diazapyrones studied vary in electronics from being electron-rich to electron-poor. The rate of reaction increases as the diazapyrone becomes more electron-poor. Diels Alder cycloadditions occur best when the LUMO of the diene is electron-rich and the HOMO of the dienophile is electron-poor. However, this is not the case for this reaction. The diazapyrone (diene) is electron-poor while the BCN or s-TCO (dienophile) is electron-rich. This indicates that the reaction occurs more like an IEDDA, similar to the tetrazine ligation. The electron-withdrawing groups on the diazapyrones lower the energy

LUMO which decreases the gap between the HOMO and LUMO and increases the rate of the reaction.

When comparing these two reactions, the reaction between s-TCO and DAPs is 3 times faster than the BCN reaction. This is because the s-TCO molecules add the double strain effect to the reaction via the fused cyclopropane ring which causes an increase in strain. This makes it more favourable for the s-TCO molecule to react and release the strain.

3.3.4 Structure-Activity Relationships

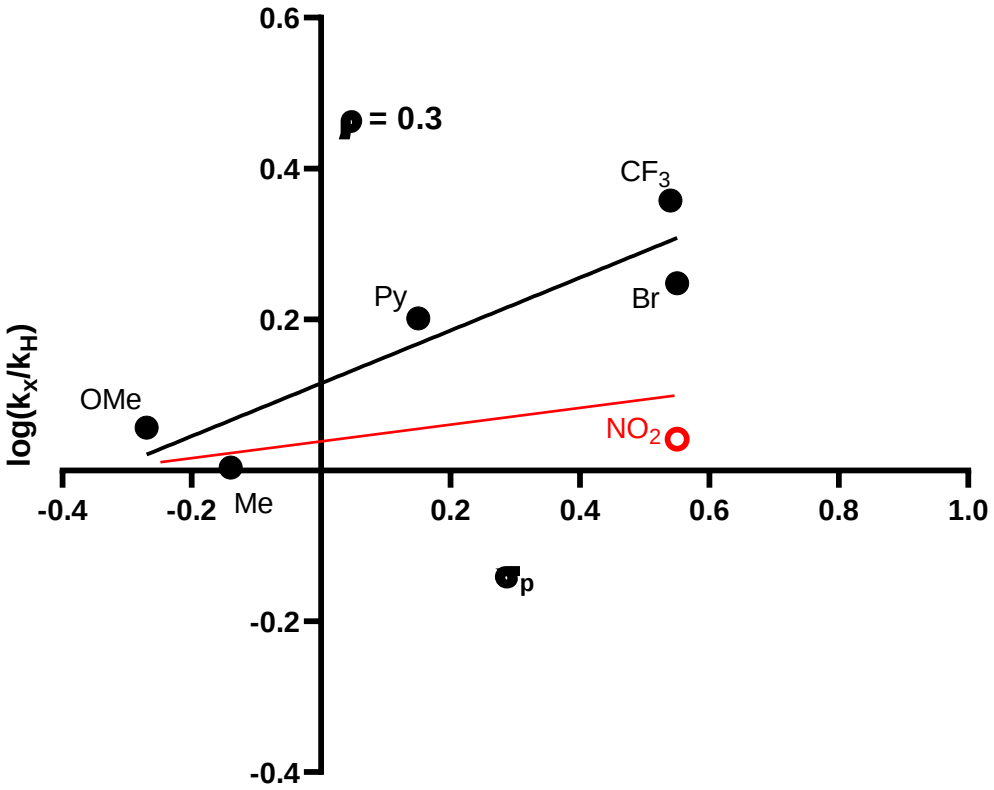

Figure 3.6 Hammett plot of the cycloaddition reaction between BCN and diazapyrones (**2.4-2.12**) evaluating the para-substituent effect of the rate of the reaction R^2 = 0.9. The red line represents the slope of the line where ρ = 0.1 when the NO_2 data point is taken into account (R^2=0.1).

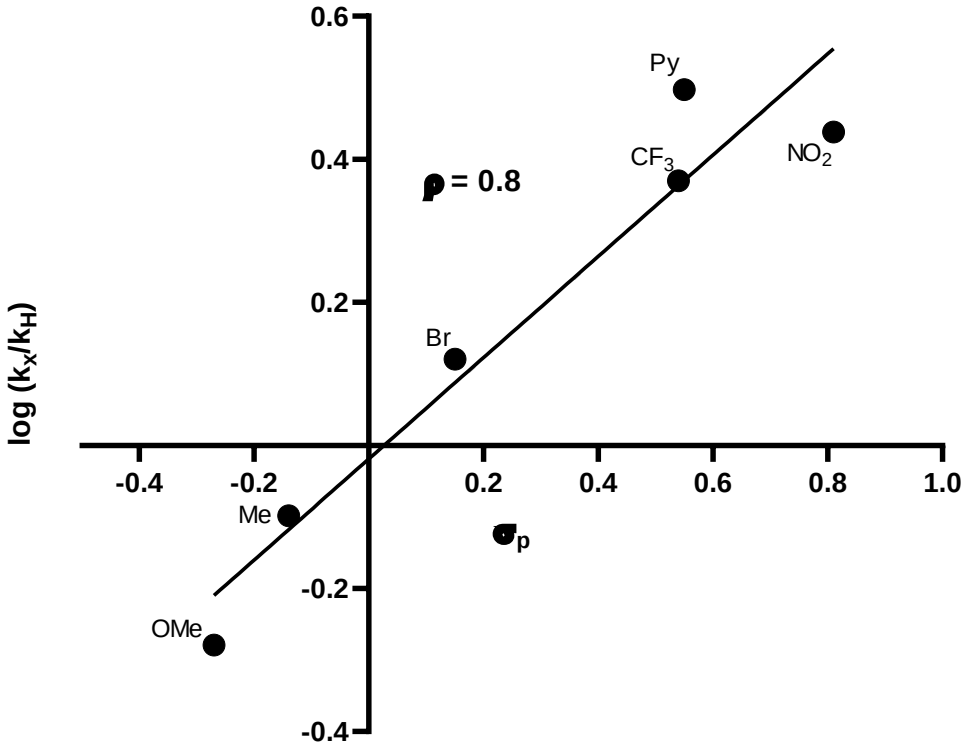

Figure 3.7 Hammett plot of the cycloaddition reaction between s-TCO and diazapyrones (**2.4-2.14**) evaluating the para-substituent effect of the rate of the reaction. $R^2 = 0.9$.

To further investigate the para-substituent effects, electron-donating and withdrawing substituents were added to the DAP. Two Hammett plots were constructed (**Figures 3.6** and **3.7**) to provide greater insight into how EWG and EDG affect the transition state or intermediates of the reaction. The resonance effect of the EWG and EDG can be seen in **Scheme 3.3.** The two Hammett plots represent the linear regression of the k_2 rate constants of diazapyrones (**2.4-2.14**) vs. the para-substituted sigma values (σ) which corresponds to the R group of each diazapyrone and are derived

from the pKa of acids. When the σ value is positive, the R group is more EWG and a stronger acid. The opposite is true for negative σ values where the R group is EDG and a weaker acid.

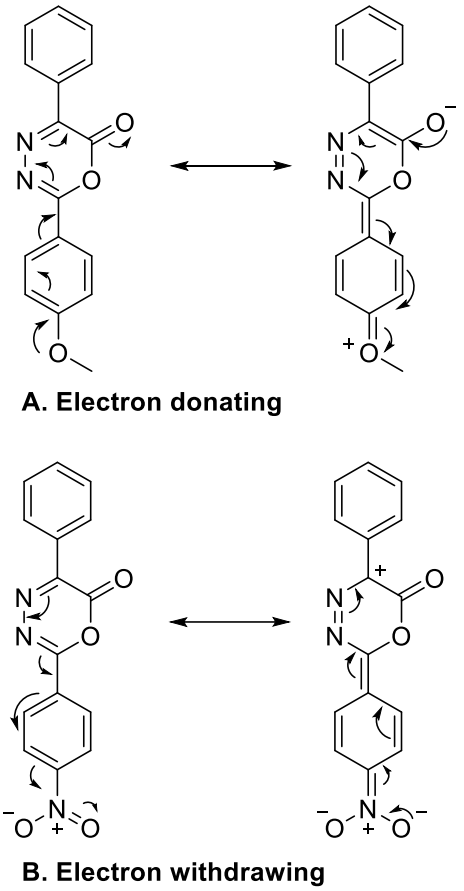

Scheme 3.9 Resonance effect of the para effect of a diazapyrone with (A) an electron-donating group and (B) an electron-withdrawing group.

The slope of the linear regression represents the ρ value. The ρ value indicates the reactions sensitivity and gives great insight into the rds. When the ρ value is larger and positive (i.e., 5 or higher) a negative charge is built up and electrons are delocalized. When the ρ values are between 2-4, there is a negative charge build up and electrons flow through the transition state. When the ρ values are -2 to -4, electrons flow out of the transition states and a positive charge is generated. When the ρ values are -5 and smaller, a positive charge is built up and delocalized. Finally, when

the ρ values are small (between -1 and 1) there are three possible scenarios. The first scenario is when the aromatic ring, where electrons are delocalized, is too far away to affect the ρ value. The second is when there are two ρ values that cancel each other out. An example of this is a hydrolysis of ethyl benzoates in acid, where the ρ value for the hydrolysis of the ester is +2.5 while the ρ value for the equilibrium protonation is -2.5.[12] The third is when the reaction is not dependent on electronics. This is the case for Diel-Alder reactions and for the shown IEDDA reactions with BCN and s-TCO, which display a ρ value of 0.4 ± 0.9 and 0.8 ± 0.9, respectively. It means the addition of EWD and EDG to the diazapyrone has little to no effect on the reaction. That being said, the positive values indicate a very small and negligible amount of negative charge is formed. The other significance of the ρ values obtained in **Figures 3.6** and **3.7** is that these values are small. This indicates that it is unlikely that the ester is hydrolyzing during the reaction and that the diazapyrone remained stable in the ACN environment. This is because the ρ value of an ester hydrolysis is ~ 2-3, involving a nucleophilic attack on the carbonyl at the rds, where excess electron delocalizes around the ring.

In terms of **Figure 3.6**, the ρ value is 0.4 ± 0.9 indicating that little negative charge buildup is occurring and that substituent affect does not have an appreciable effect on this reaction. This indicates that the reaction is occurring similarly to the reaction between sTCO and DAP. However, when the k_2 value for 5-(4-nitrophenyl)-2-phenyl-6H-1,3,4-oxadiazin-6-one (2.28) is taken into account, the k_2 value for DAP (2.28) is 0.0178 ± 0.004 $M^{-1}s^{-1}$, which lies outside the trend and is much lower than expected. This results in the ρ value being 0.1 ± 0.1. This indicates that the rates are insensitive to substituents. The low rate is likely due to the stability of DAP (2.14). When there is more EWG character in the DAP, the DAP is more reactive but also less stable. In this case, it is likely that the DAP is hydrolyzing in water. Despite the DAP stock being made fresh

prior to every kinetic run, ACN is used as the solvent and happens to be hygroscopic. It is likely the ACN solution used to prepare the 4 mM DAP stock was “old” and has accumulated enough water from the atmosphere to reduce the rate for the IEDDA reaction between the DAP and BCN. This is because most of the DAP would have already reacted via hydrolysis leaving less DAP to react with BCN. Another possibility is that the wrong wavelength was monitored or that a second product is forming. As the DAP peak decays, if there isa formation of another peak around the same wavelength that interferes with the monitoring of the decay the reaction will appear slower and an accurate rate would be difficult to obtain. An alternative method would be to use fresh ACN in conjunction with an instrument capable of monitoring the reaction chamber prior to the reagents being injected. This would ensure that the maximum amount of DAP would be left to react via a cycloaddition. Alternatively, the DAP can be modified with substituents to shift the UV-absorption wavelength. Therefore, if the additional peak is forming, there will be no interference.

Table 3.7 Rate parameter (ρ) obtained from the Hammett plots in **Figures 3.6** and **3.7** for the cycloaddition reaction between BCN and s-TCO and various diazapyrones.

Cycloaddition reaction	**Rate parameter (ρ)**
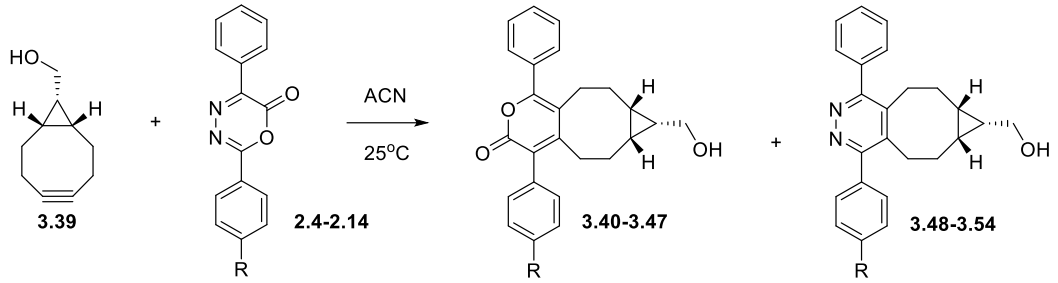	0.4 ± 0.9
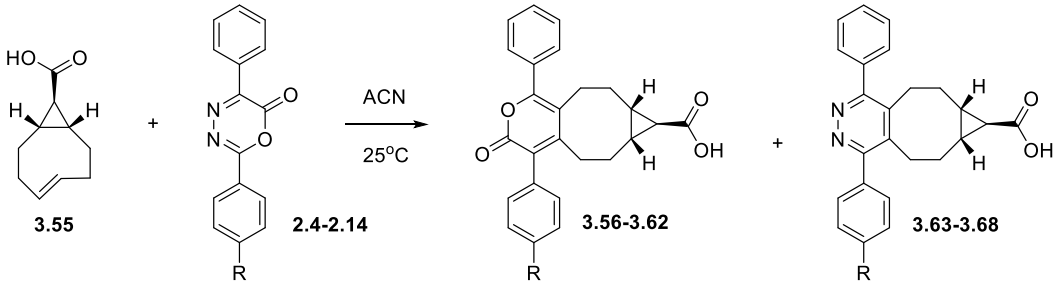	0.8 ± 0.9

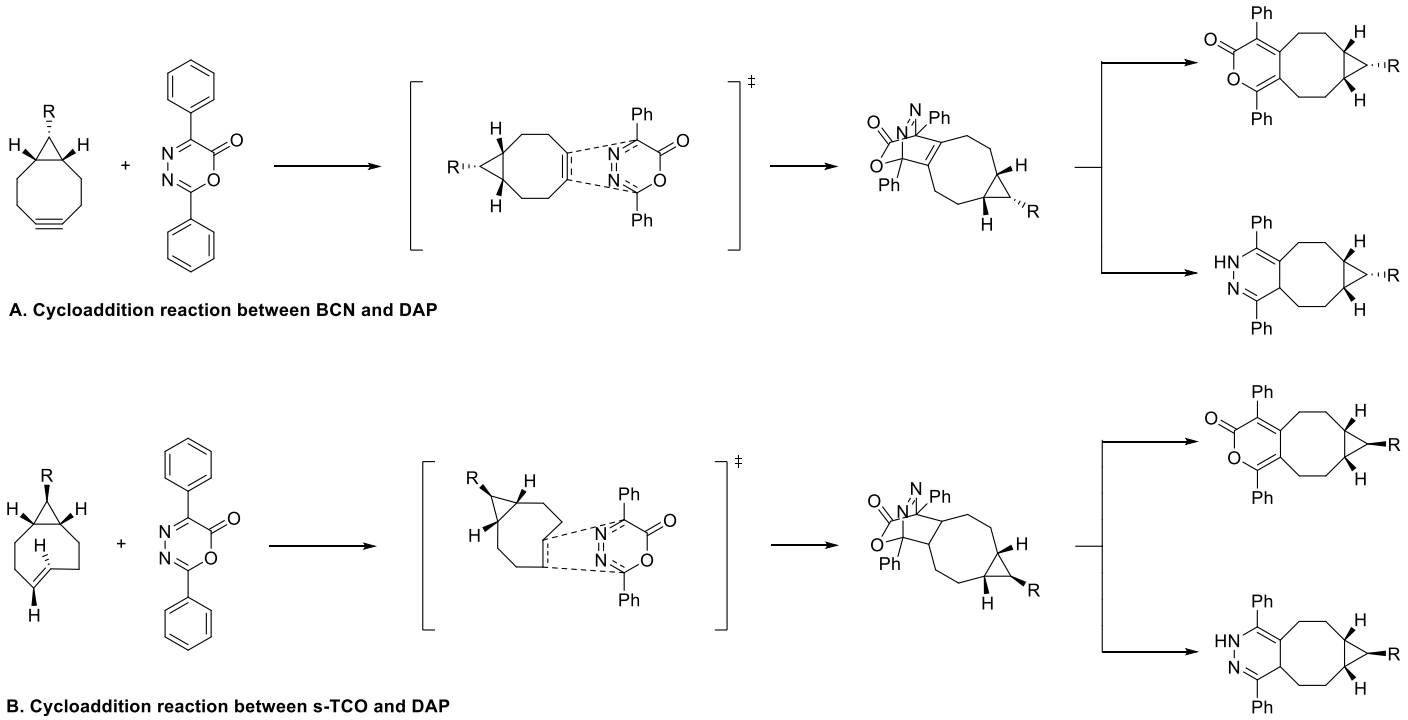

Scheme 3.10 Reaction between diazapyrone and (A) BCN or (B) s-TCO with transition state based on the Hammett plot with rate parameter ρ = 0.4 and 0.8, respectively.

From the Hammett plot, information about the reaction mechanism of the IEDDA reaction can be obtained. As stated previously, when the magnitude of the ρ value is large, there is a larger accumulation of charge. This indicates the reaction occurs via a reaction intermediate and that the reaction is step-wise. On the other hand, values of ρ with smaller magnitudes have a very small or negligible amount of charge build up and the reaction is concerted. Based on the ρ values obtained from **Figure 3.6** and **3.7** (ρ = 0.4 ± 0.9 and 0.8 ± 0.9, respectively) the reaction is likely concerted. From this information, the transition state for both these reactions can be determined (**Scheme 3.4**). However, to confirm this, quantum calculations would be required to study the transition state of the reaction. Quantum mechanics would also give insight into the synchronicity of the reaction (i.e., synchronous or asynchronous). A synchronous reaction occurs when the changes in the molecule, typically bonds forming and breaking, occur at the same rate to get to the transition state.

An asynchronous reaction on the other hand involves the formation and breaking of bonds independent of each other.

Based on this information, we proposed the following mechanism (**Scheme 3.11**) which results in the formation of three products. In the first step, BCN and a diazapyrone react via a [4+2] cycloaddition reaction. To reestablish stability in the molecule, a retro [4+2] cycloaddition occurs to either lose N_2 (**3.1**) or CO_2 gas (**3.2**). This gives two different products (**3.1** and **3.2**). Through mass spectrometry analysis, only the product containing carbon dioxide (**3.2**) was observed. From there, a double conjugation can occur. This is done by reacting the molecule obtained via the first cycloaddition reaction with another molecule of BCN via a [4+2] cycloaddition which will result in the loss of carbon dioxide. The doubly conjugated product (**3.3**) was also observed by mass spectrometry.

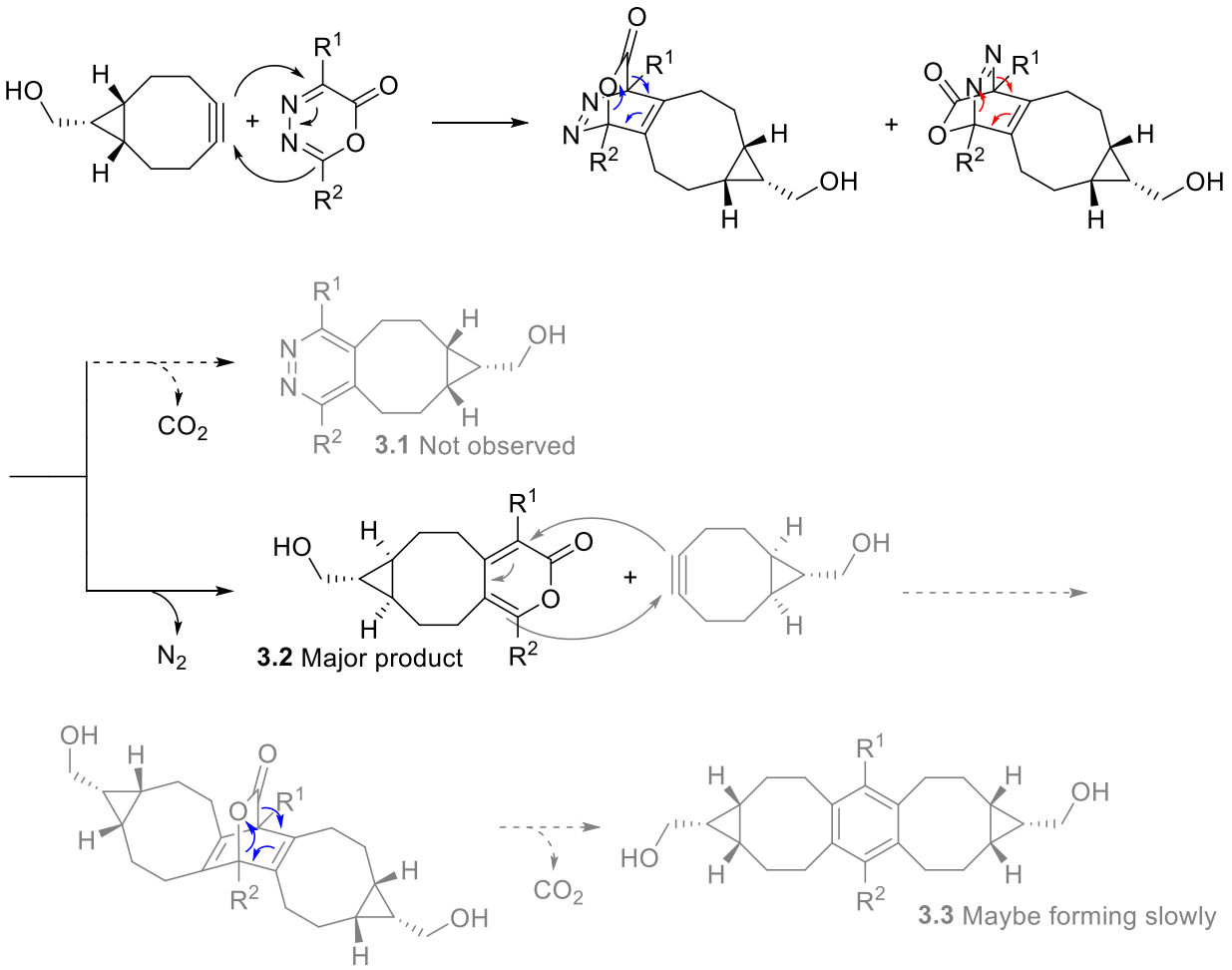

Scheme 3.11 Proposed reaction mechanism of a generic diazapyrone reacting with BCN. In the first step, BCN and a diazapyrone react via a [4+2] cycloaddition reaction. To reestablish stability in the molecule, a retro [4+2] cycloaddition could occur to either lose N_2 (**3.1**) or CO_2 gas (**3.2**). the two different pathways can give products **3.1** and **3.2**. Through mass spectrometry analysis, only the product containing carbon dioxide (**3.2**) was observed. From there, a double conjugation can occur. This is done by reacting the molecule obtained via the first cycloaddition reaction with another molecule of BCN via a [4+2] cycloaddition which will result in the loss of carbon dioxide. The doubly conjugated product (**3.3**) was also observed by mass spectrometry.

3.4 Conclusion

In summary, we studied the reactivity of diazapyrones in the context of bioorthogonal chemistry. We have demonstrated the reactivity between DAP, BCN, and s-TCO as an alternative to tetrazine thereby expanding upon the current bioorthogonal toolbox. The cycloaddition reactions of DAP

have a k_2 ranging from $10^{-3} – 10^{1}$ $M^{-1}s^{-1}$, and is comparable to those in the tetrazine ligation with cyclopropenes.

3.5 Materials and Methods

All commercially available reagents were purchased from Alfa Aesar and Sigma Aldrich and were used without further purification. Strained-trans cyclooctene ((1R,8S,9S, E)-bicyclo[6.1.0]non-4-ene-9-carboxylic acid) was received from the Fox group (Department of Chemistry at the University of Delaware, USA). All deuterated solvents were purchased from Cambridge Isotopes and were used as received, except for deuterated chloroform which was neutralized by passing through a pad of basic alumina. Thin-layer chromatography (TLC) was performed on Analtech Uniplate® silica gel (60 A F254, layer thickness 250 μm). The TLC plates were visualized using a UV lamp and potassium permanganate. Flash chromatography was performed using silica gel (60 A, particle size 40-63 μm). Mass spectra were obtained using the John L. Holmes Mass Spectrometry facility at the University of Ottawa. A Waters Synapt High-Definition Mass Spectrophotometer with TriWave using a quadrupole time-of-flight mass spectrometer was used with positive electrospray ionization (ESI+). The samples were prepared from a 4 mM stock solution in LCMS Optima grade ACN.

All ^{1}H and ^{13}C NMR spectra were obtained using 300 MHz, 400 MHz, and 600 MHz Bruker NMR spectrometers and processed using MestReNova NMR 4.2.0 software. The units of the NMR spectra peaks are ppm and referenced against the residual solvent peak. Multiplicity of peaks are recorded as abbreviated: s = singlet, d = doublet, t = triplet, m = multiplet or unresolved, br = broad and J = coupling constants in Hz.

3.5.1 Synthesis

General polycyclic aromatic ring synthesis

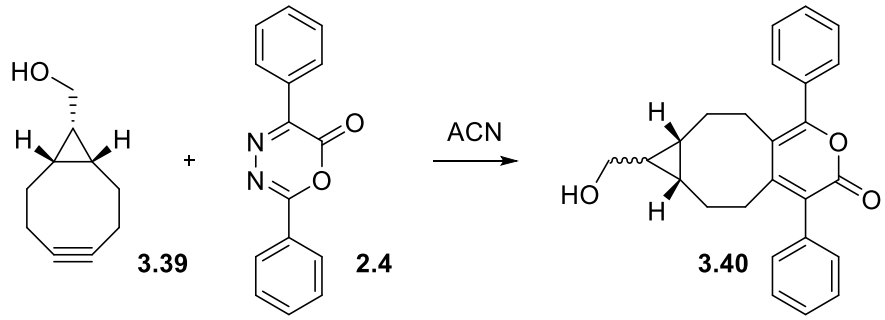

A RBF was dried and flushed with argon gas. BCN (70 mg, 0.47 mmol), 2,5-diphenyl-6H-1,3,4-oxadiazin-6-one (117 mg, 0.47 mmol) and 1.5 mL of ACN were then added and allowed to stir overnight. The reaction mixture was then filtered using a pasture pipette filled with ~4.0 cm of celite and flushed with 10 mL of EtOAc. The resulting mixture was then concentrated under reduced pressure. FCC 3:1 Hex:EtOAc to 1:1 Hex:EtOAc. The final product was obtained in 62% yield. **^{1}H-NMR** (600 MHz, $CDCl_3$) δ 7.45 (dt, *J* = 12.7, 4.1 Hz, 2H), 7.42 – 7.30 (m, 5H), 7.30 (s, 1H), 7.24 – 7.20 (m, 1H), 3.73 – 3.59 (m, 2H), 2.78 (t, *J* = 12.4 Hz, 1H), 2.73 – 2.59 (m, 1H), 2.59 – 2.53 (m, 1H), 2.30 (q, *J* = 11.1 Hz, 2H), 2.15 – 1.82 (m, 2H), 1.55 (s, 1H), 1.30 – 1.04 (m, 4H), 1.02 – 0.87 (m, 1H). **^{13}C-NMR** (151 MHz, $CDCl_3$) δ 162.3, 135.2, 135.0, 133.3, 133.2, 129.8, 129.7, 129.6,129.5, 129.0, 128.6, 128.4, 128.3, 128.0, 59.6, 31.4, 29.3, 28.1, 27.6, 25.9, 25.2, 24.6, 23.1, 21.9, 21.7, 21.3, 20.9, 20.6, 17.1, 16.2. **MS (EI)** m/z calculated for ($C_{25}H_{24}O_3$): 373.17 $[M+1]^+$, found 373.15, 395.17 $[M+Na]^+$, found 395.16**.**

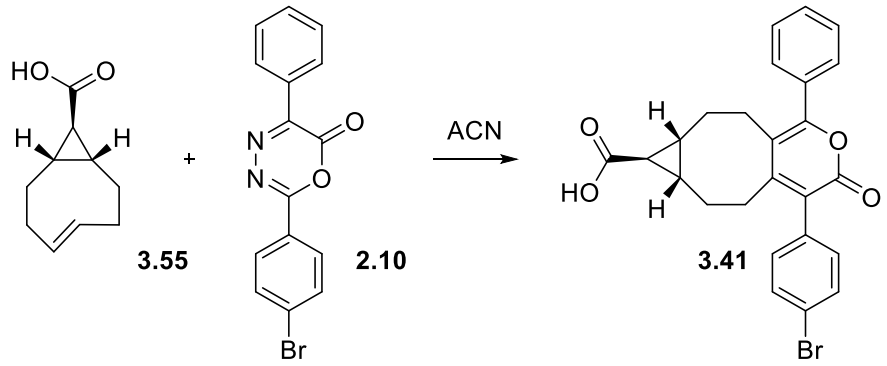

A RBF was dried and flushed with argon gas. 27.7 mg (0.16 mmol) of sTCO-CO_2H and 54.5 mg (0.16 mmol) of 2-(4-bromophenyl)-5-phenyl-6H-1,3,4-oxadiazin-6-one and 1.5 mL of ACN were then added and allowed to stir for 5 minutes. The reaction mixture was then concentrated under reduced pressure. FCC 3:1 Hex:EtOAc to 1:1 Hex:EtOAc. The final product was obtained in 71% yield. **^{1}H-NMR** (600 MHz, $CDCl_3$) δ 7.57-7.49 (dd, *J* = 13.0, 4.5 Hz, 2H), 7.37 – 7.32 (m, 3H), 7.30 (s, 1H), 7.23 – 7.17 (m, 4H), 2.10-1.94 (t, *J* =13.0 Hz, 4H), 1.85-1.76 (m, 2H), 1.71 (t, 1H), 1.20-1.07 (m, 4H). **MS (EI)** m/z calculated for ($C_{25}H_{21}BrO_4$): 465.06 $[M+1]^+$, found 465.51, 491.05 $[M+Na]^+$, found 491.11**.**

3.5.2 Kinetic procedures

Kinetic studies procedure

The second-order rate constant (k_2) for the cycloaddition between various diazapyrones and two different cycloadducts, s-TCO and BCN were determined by using UV-Vis spectroscopy. The reaction was studied under pseudo-first-order conditions where the cycloadduct reactant is in a 10-60 fold excess (s-TCO) and a 10-50 excess (BCN). Each kinetic run was performed in duplicate in acetonitrile at 25 ± 0.1 °C. The reaction was monitored by tracking the decrease of the diazapyrone peak specified in **Tables 3.1** and **3.3**.

4 mM Stock solutions of s-TCO/BCN and diazapyrone were prepared in screw cap vials in HPLC LCMS Optima grade ACN. Fresh stocks of diazapyrones were prepared and a serial dilution of s-TCO/BCN was prepared before each experiment. The cuvettes used were 1.5 mL quartz cuvettes with stoppers (10 mm pathlength). Before adding the prepared solutions to the cuvette, the UV-Vis cuvettes were cleaned with acetone 2 times and left to dry for 20 minutes. The cuvettes were then wiped with Kimwipes before reading to remove any residue on the outer surface. Before reactions, the UV-Vis spectrophotometer was blanked with 1 mL of acetonitrile and the spectrometer was set to scan the samples every 15 seconds (s-TCO) and every minute (BCN). Next, 1 mL of s-TCO/BCN from the serial dilution was added to the cuvette then followed by the quick addition of the diazapyrone. The cuvettes were then inverted three times to mix the reagents and inserted into the Cray spectrophotometer for absorbance readings. To choose a wavelength for product monitoring (**Table 3.1** and **3.3**), the spectra were obtained from 200 nm to 600 nm throughout the reaction.

Table 3.8 Sample preparation for the reaction between BCN, s-TCO and DAP using serial dilution.

Reaction	Dilution (dil) #	Volume and source of BCN (µL)	Vol. of ACN (µL)	Total Volume of serial dilution (µL)	Total Reaction volume (µL)
25 µM pyrone 1250 µM BCN	1	2625 µL of 4 mM stock BCN	4375	2000	1000
25 µM pyrone 1250 µM BCN	2	5000 µL of 1	1000	2000	1000
25 µM pyrone 1000 µM BCN	3	4000 µL of 2	1000	2000	1000
25 µM pyrone 750 µM BCN	4	3000 µL of 3	1000	2000	1000
25 µM pyrone 500 µM BCN	5	2000 µL of 4	1000	2000	1000
25 µM pyrone 250 µM BCN	6	1000 µL of 6	1000	2000	1000
Reaction	**Dilution (dil) #**	**Volume and source of s-TCO (µL)**	**Vol. of ACN (µL)**	**Total Volume of serial dilution (µL)**	**Total Reaction volume (µL)**
45 µM pyrone 2700 µM s-TCO	1	4860 of 4 mM stock s-TCO	2340	2000	1000
45 µM pyrone 2250 µM s-TCO	2	5000	1000	2000	1000
45 µM pyrone 1800 µM s-TCO	3	4000	1000	2000	1000
45 µM pyrone 1350 µM s-TCO	4	3000	1000	2000	1000
45 µM pyrone 900 µM s-TCO	5	2000	1000	2000	1000
45 µM pyrone 450 µM s-TCO	6	1000	1000	2000	1000

References

(1) Prescher, J. A.; Bertozzi, C. R. Chemistry in living systems. *Nature Chemical Biology* **2005**, *1* (1), 13-21. DOI: 10.1038/nchembio0605-13.

(2) Liu, F.; Liang, Y.; Houk, K. N. Theoretical Elucidation of the Origins of Substituent and Strain Effects on the Rates of Diels–Alder Reactions of 1,2,4,5-Tetrazines. *Journal of the American Chemical Society* **2014**, *136* (32), 11483-11493. DOI: 10.1021/ja505569a.

(3) Lang, K.; Davis, L.; Wallace, S.; Mahesh, M.; Cox, D. J.; Blackman, M. L.; Fox, J. M.; Chin, J. W. Genetic Encoding of Bicyclononynes and trans-Cyclooctenes for Site-Specific Protein Labeling in Vitro and in Live Mammalian Cells via Rapid Fluorogenic Diels–Alder Reactions. *Journal of the American Chemical Society* **2012**, *134* (25), 10317-10320. DOI: 10.1021/ja302832g.

(4) Fokin, V. V. CuAAC: The quintessential Click Reaction. *Chemical Information* **2013**, *44* (25). DOI: 10.1002/9783527664801.

(5) Oliveira, B. L.; Guo, Z.; Bernardes, G. J. L. Inverse electron demand Diels-Alder reactions in chemical biology. *Chemical Society Reviews* **2017**, *46* (16), 4895-4495. DOI: 10.1039/c7cs00184c.

(6) Boger, D. L.; Schaum, R. P.; Garbaccio, R. M. Regioselective Inverse Electron Demand Diels−Alder Reactions of N-Acyl 6-Amino-3-(methylthio)-1,2,4,5-tetrazines. *The Journal of Organic Chemistry* **1998**, *63* (18), 6329-6337. DOI: 10.1021/jo980795g.

(7) Gordon, C. G.; Mackey, J. L.; Jewett, J. C.; Sletten, E. M.; Houk, K. N.; Bertozzi, C. R. Reactivity of Biarylazacyclooctynones in Copper-Free Click Chemistry. *Journal of the American Chemical Society* **2012**, *134* (22), 9199-9208. DOI: 10.1021/ja3000936.

(8) Scinto, S. L.; Bilodeau, D. A.; Hincapie, R.; Lee, W.; Nguyen, S. S.; Xu, M.; am Ende, C. W.; Finn, M. G.; Lang, K.; Lin, Q.; et al. Bioorthogonal chemistry. *Nature Reviews Methods Primers* **2021**, *1* (1), 30. DOI: 10.1038/s43586-021-00028-z.

(9) Sauer, J.; Bäuerlein, P.; Ebenbeck, W.; Gousetis, C.; Sichert, H.; Troll, T.; Utz, F.; Wallfahrer, U. [4+2] Cycloadditions of 1,2,4,5-Tetrazines and Cyclopropenes − Synthesis of 3,4-Diazanorcaradienes and Tetracyclic Aliphatic Azo Compounds. *European Journal of Organic Chemistry* **2001**, *2001* (14), 2629-2638. DOI: 10.1002/1099-0690.

(10) Liu, F.; Paton, R. S.; Kim, S.; Liang, Y.; Houk, K. N. Diels–Alder Reactivities of Strained and Unstrained Cycloalkenes with Normal and Inverse-Electron-Demand Dienes: Activation Barriers and Distortion/Interaction Analysis. *Journal of the American Chemical Society* **2013**, *135* (41), 15642-15649. DOI: 10.1021/ja408437u.

(11) Taylor, M. T.; Blackman, M. L.; Dmitrenko, O.; Fox, J. M. Design and Synthesis of Highly Reactive Dienophiles for the Tetrazine–trans-Cyclooctene Ligation. *Journal of the American Chemical Society* **2011**, *133* (25), 9646-9649. DOI: 10.1021/ja201844c.

(12) Yang, J.; Liang, Y.; Šečkutė, J.; Houk, K. N.; Devaraj, N. K. Synthesis and Reactivity Comparisons of 1-Methyl-3-Substituted Cyclopropene Mini-tags for Tetrazine Bioorthogonal Reactions. *Chemistry – A European Journal* **2014**, *20* (12), 3365-3375. DOI: 10.1002/chem.201304225.

(13) Wagner, J. A.; Mercadante, D.; Nikić, I.; Lemke, E. A.; Gräter, F. Origin of Orthogonality of Strain-Promoted Click Reactions. *Chemistry (Weinheim an der Bergstrasse, Germany)* **2015**, *21* (35), 12431-12435. DOI: 10.1002/chem.201501727.

(14) Wijnen, J. W.; Zavarise, S.; Engberts, J. B. F. N.; Charton, M. Substituent Effects on an Inverse Electron Demand Hetero Diels−Alder Reaction in Aqueous Solution and Organic

Solvents: Cycloaddition of Substituted Styrenes to Di(2-pyridyl)-1,2,4,5-tetrazine. *The Journal of Organic Chemistry* **1996**, *61* (6), 2001-2005. DOI: 10.1021/jo9518563.

(15) Müller, K.; Sauer, J. Ketenacetale als dienophile: Reaktivität und regiospezifität bei (4+2)-cycloadditionen mit inversem elektronenbedarf. *Tetrahedron Letters* **1984**, *25* (24), 2541-2544. DOI: 10.1016/S0040-4039(01)81226-0.

(16) Šečkutė, J.; Devaraj, N. K. Expanding room for tetrazine ligations in the in vivo chemistry toolbox. *Current Opinion in Chemical Biology* **2013**, *17* (5), 761-767. DOI: 10.1016/j.cbpa.2013.08.004.

(17) Yang, J.; Liang, Y.; Šečkutė, J.; Houk, K. N.; Devaraj, N. K. Synthesis and Reactivity Comparisons of 1-Methyl-3-Substituted Cyclopropene Mini-tags for Tetrazine Bioorthogonal Reactions. *Chemistry : A European Journal* **2014**, *20* (12), 3365-3375. DOI: 10.1002/chem.201304225.

(18) Devaraj, N. K.; Weissleder, R. Biomedical applications of tetrazine cycloadditions. *Accounts of Chemical Research* **2011**, *44* (9), 816-827. DOI: 10.1021/ar200037t.

(19) Row, R. D.; Prescher, J. A. Constructing New Bioorthogonal Reagents and Reactions. *Accounts of Chemical Research* **2018**, *51* (5), 1073-1081. DOI: 10.1021/acs.accounts.7b00606.

(20) Jewett, J. C.; Sletten, E. M.; Bertozzi, C. R. Rapid Cu-Free Click Chemistry with Readily Synthesized Biarylazacyclooctynones. *Journal of the American Chemical Society* **2010**, *132* (11), 3688-3690. DOI: 10.1021/ja100014q.

(21) Ramirez, M.; Darzi, E. R.; Donaldson, J. S.; Houk, K. N.; Garg, N. K. Cycloaddition Cascades of Strained Alkynes and Oxadiazinones. *Angewandte Chemie International Edition* **2021**, *60* (33), 18201-18208. DOI:10.1002/anie.20210524

Chapter 4 – Future Directions

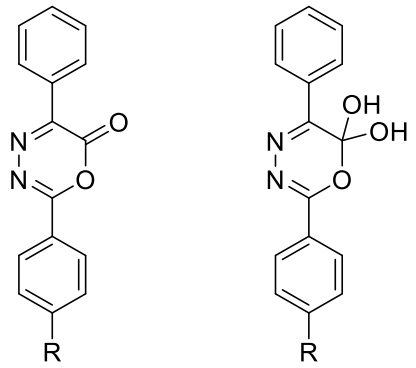

Figure 4.1 Comparison of Diazapyrone (right) and Orthoester structure of a diazapyrone (left).

In the future, these cycloaddition reactions will need further characterization which includes high-resolution mass spectrometry, and ^{15}N NMR to confirm if N_2 gas is lost during the reaction. In addition to that, quantum mechanics reaction simulation can be used to model the reaction which will give greater insight into the transition states of the reaction and can point towards a possible reaction mechanism. This can be done by doing density functional theory calculations using gaussian 16. For this reaction to be utilized in the field of click chemistry, the diazapyrones need to be modified to be more stable in water. This can be done by converting the carbonyl in the ester group of the diazapyrones into an ortho-ester (**Figure 4.1)**. The ortho-ester will act as a protecting group which will stabilize the molecule and prevent hydrolysis. If required, the ortho-ester can be easily converted back into a carbonyl via an acid catalyst. Another modification that can be done to the diazapyrone would be to change the O atom on the ester into a S atom. This can be accomplished by using the diazapyrone synthesis but replacing the hydrazine hydrate starting material with thiobenzhydrazide (**Scheme 4.1**). This will allow for sulfhydryl biotinylation (**Scheme 4.2)** which can be used for downstream biotin-streptavidin applications so that the

diazapyrone can act as a chemical tool to understand biology. This reaction could also potentially be used for other bioorthogonal applications such as cell labelling, identifying new targets, and peptide synthesis.

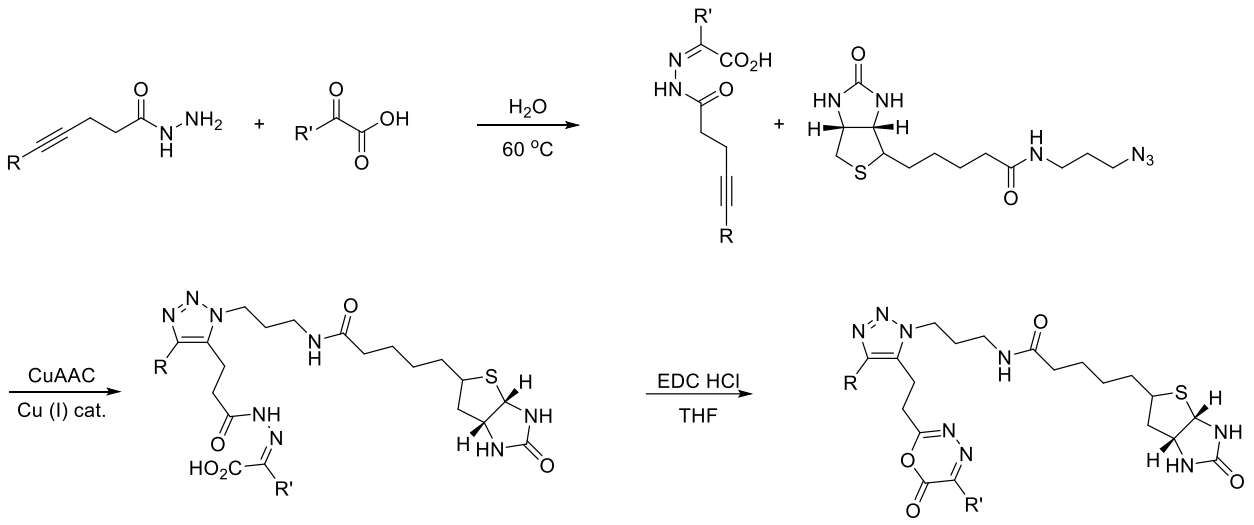

Scheme 4.6 Synthesis of 2,5-diphenyl-6H-1,3,4-thiasiazin-6-one.

Appendix A - NMR Spectra

1H NMR of Hydrazone intermediates

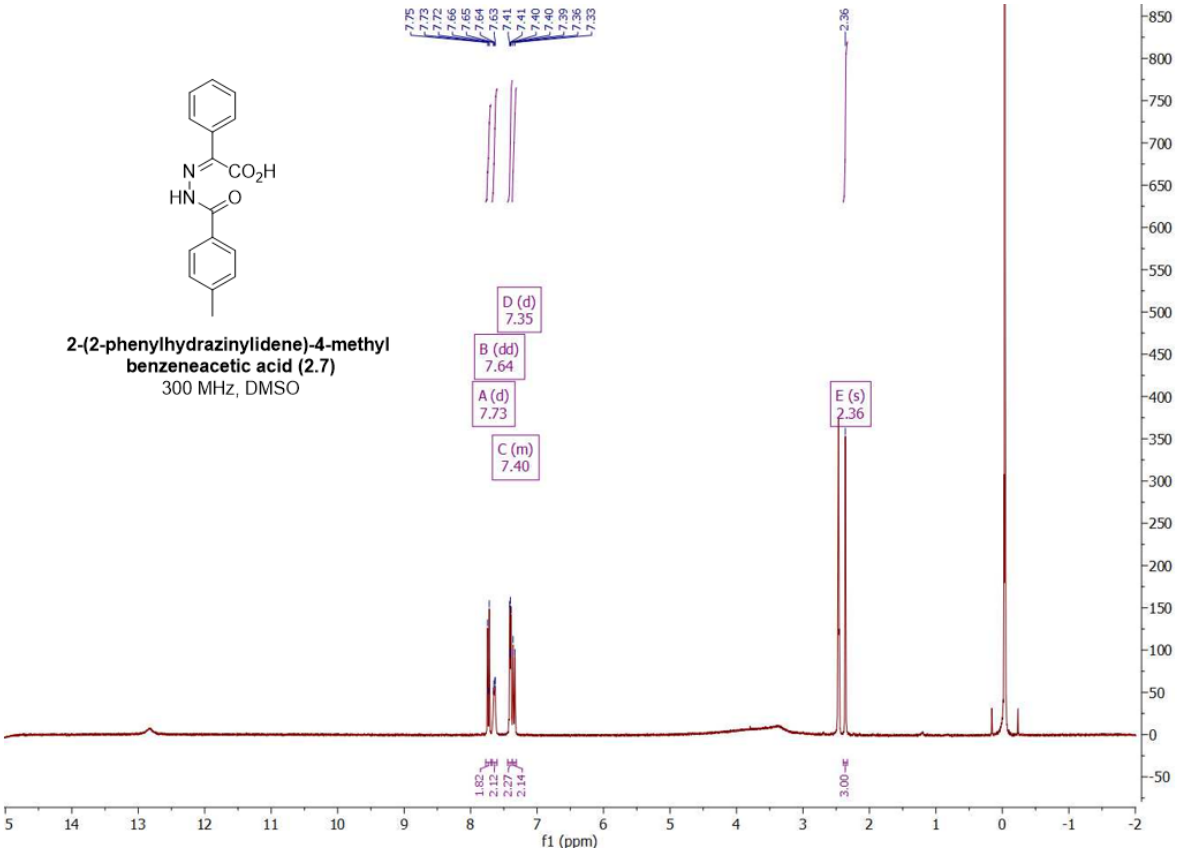

Figure A1. ^{1}H NMR of 2-(2-phenylhydrazinylidene)-4-methy1 benzeneacetic acid (**2.7**).

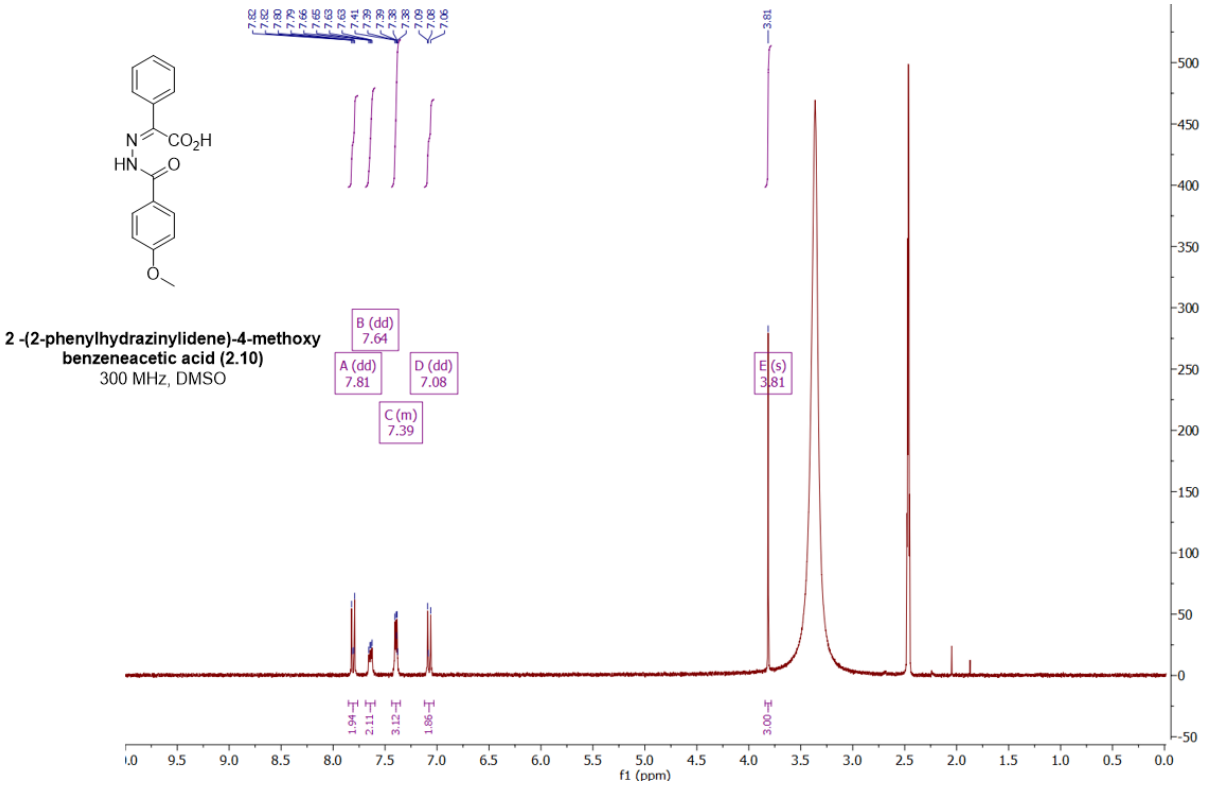

Figure A2. ^{1}H NMR of 2-(2-phenylhydrazinylidene)-4-methoxy benzeneacetic acid (**2.10**).

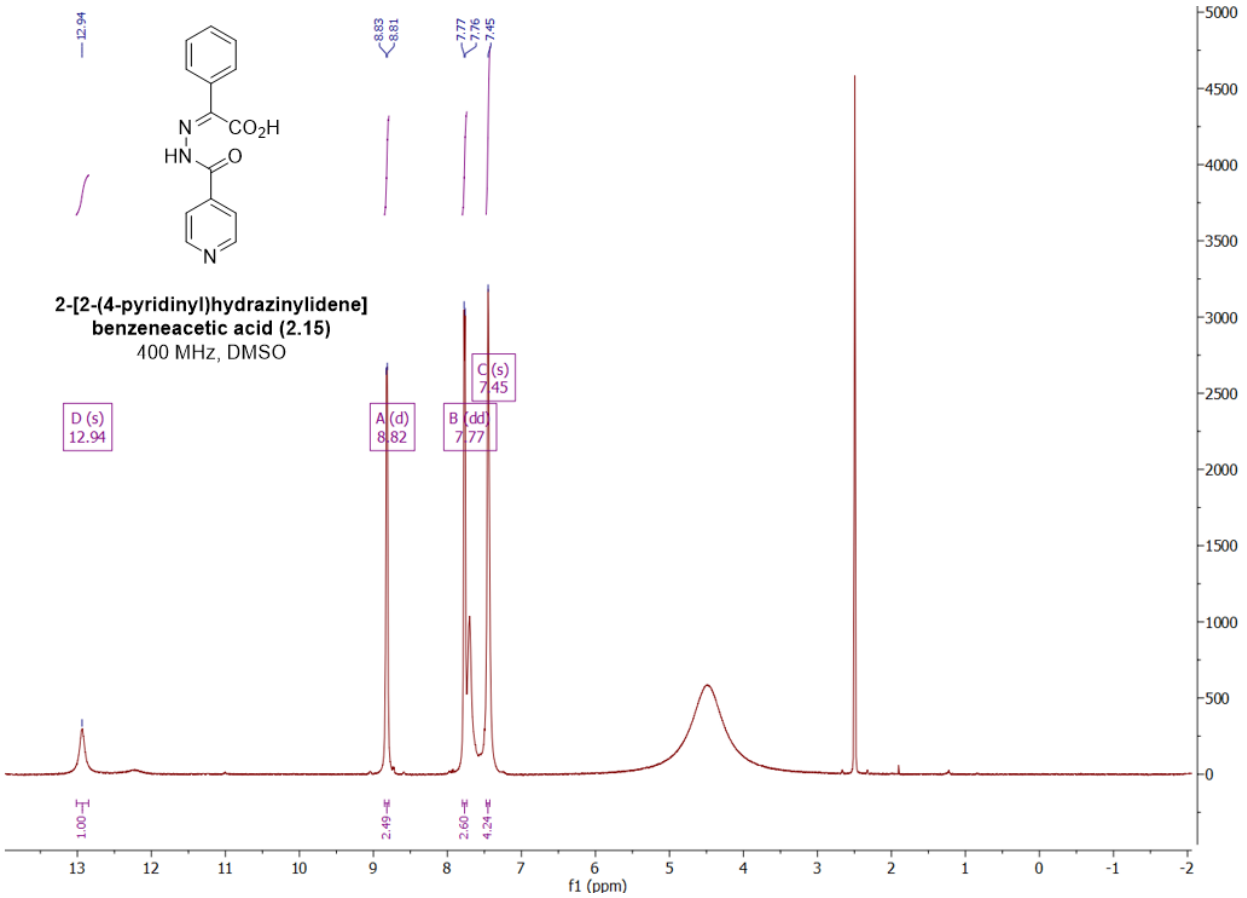

Figure A3. ^{1}H NMR of 2-[2-(4-pyridinyl)hydrazinylidene] benzeneacetic acid (**2.15**).

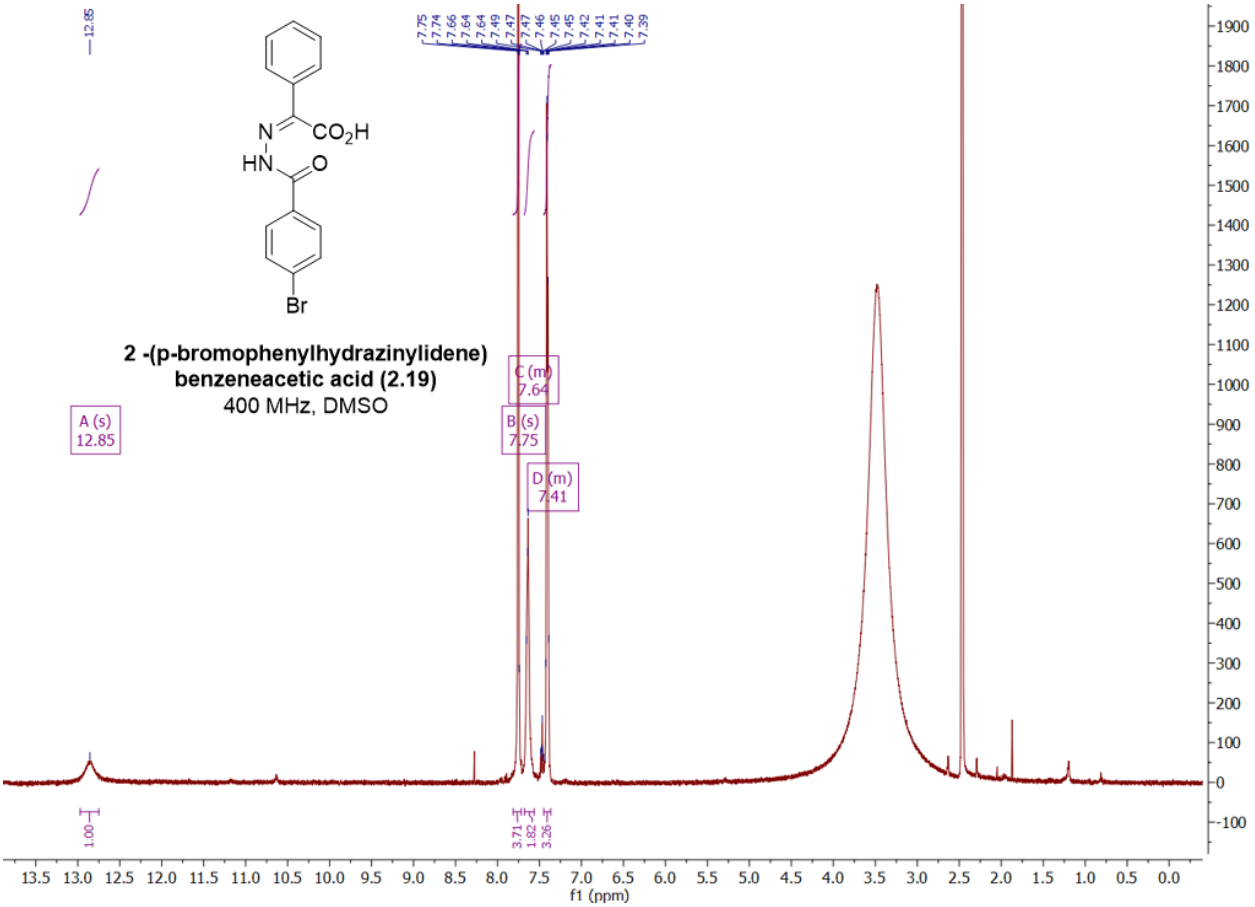

Figure A4. ^{1}H NMR of 2-(p-bromophenylhydrazinylidene) benzeneacetic acid (**2.19**).

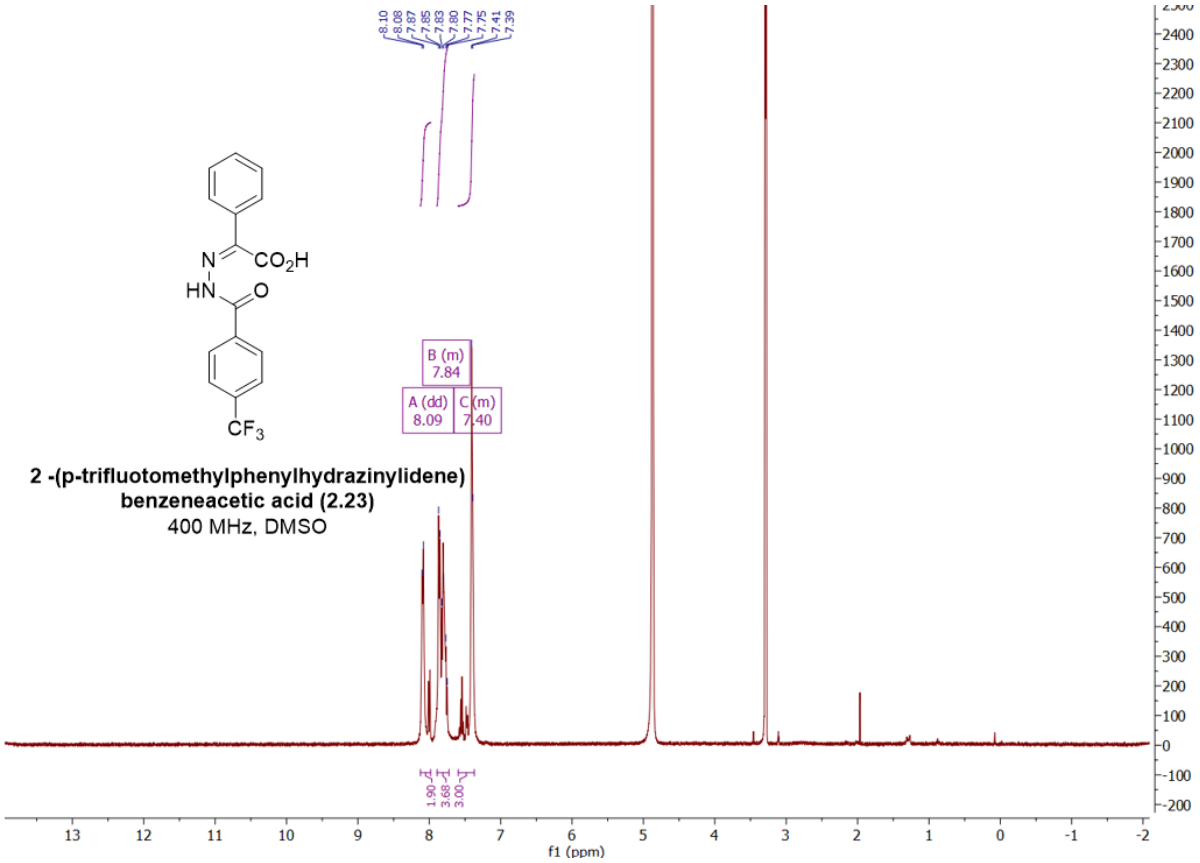

Figure A5. ^{1}H NMR of 2-(p-trifluoromethylphenylhydrazinylidene) benzeneacetic acid (**2.23**).

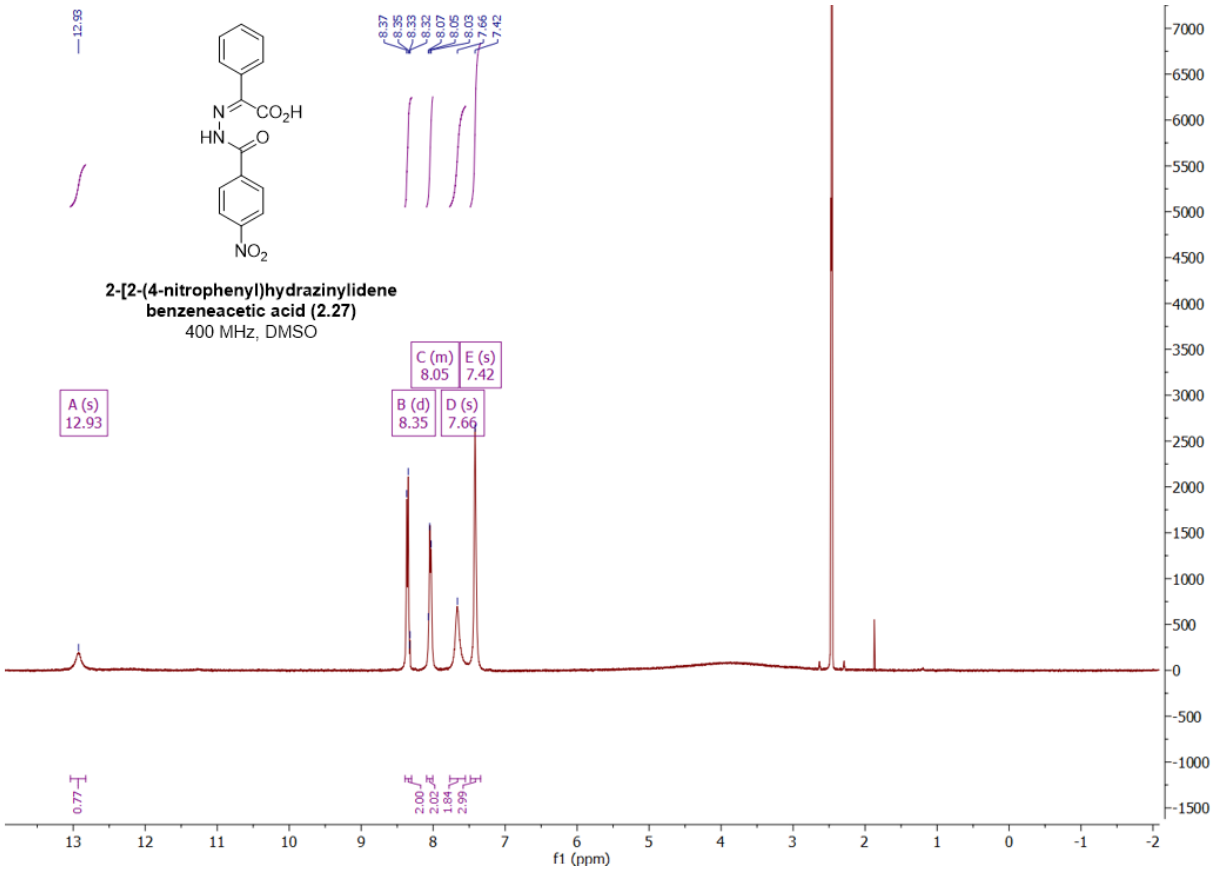

Figure A6. ^{1}H NMR of 2-[2(4-nitrophenyl)hydrazinylidene) benzeneacetic acid (**2.27**).

1H and 13C NMR of Diazapyrones

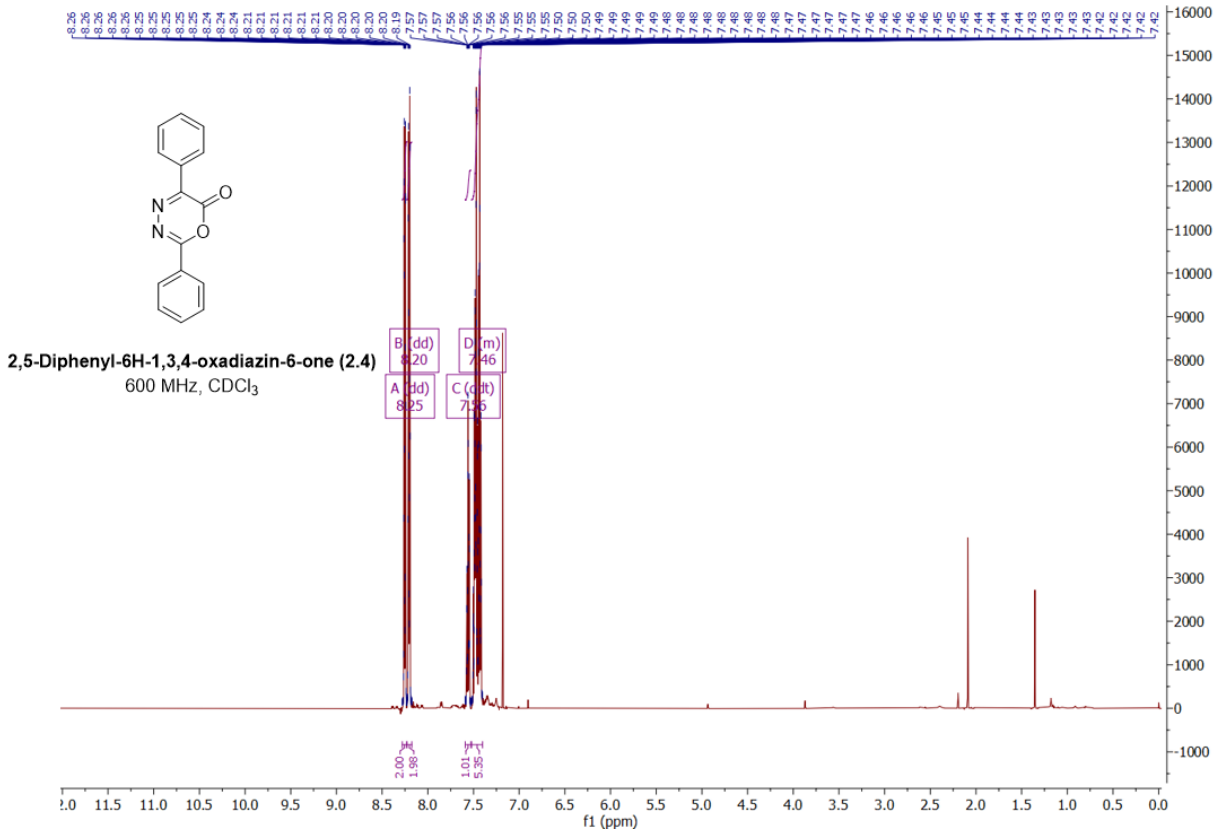

Figure A7. ^{1}H NMR of 2,5-diphenyl-6H-1,3,4-oxadiazin-6-one (**2.4**).

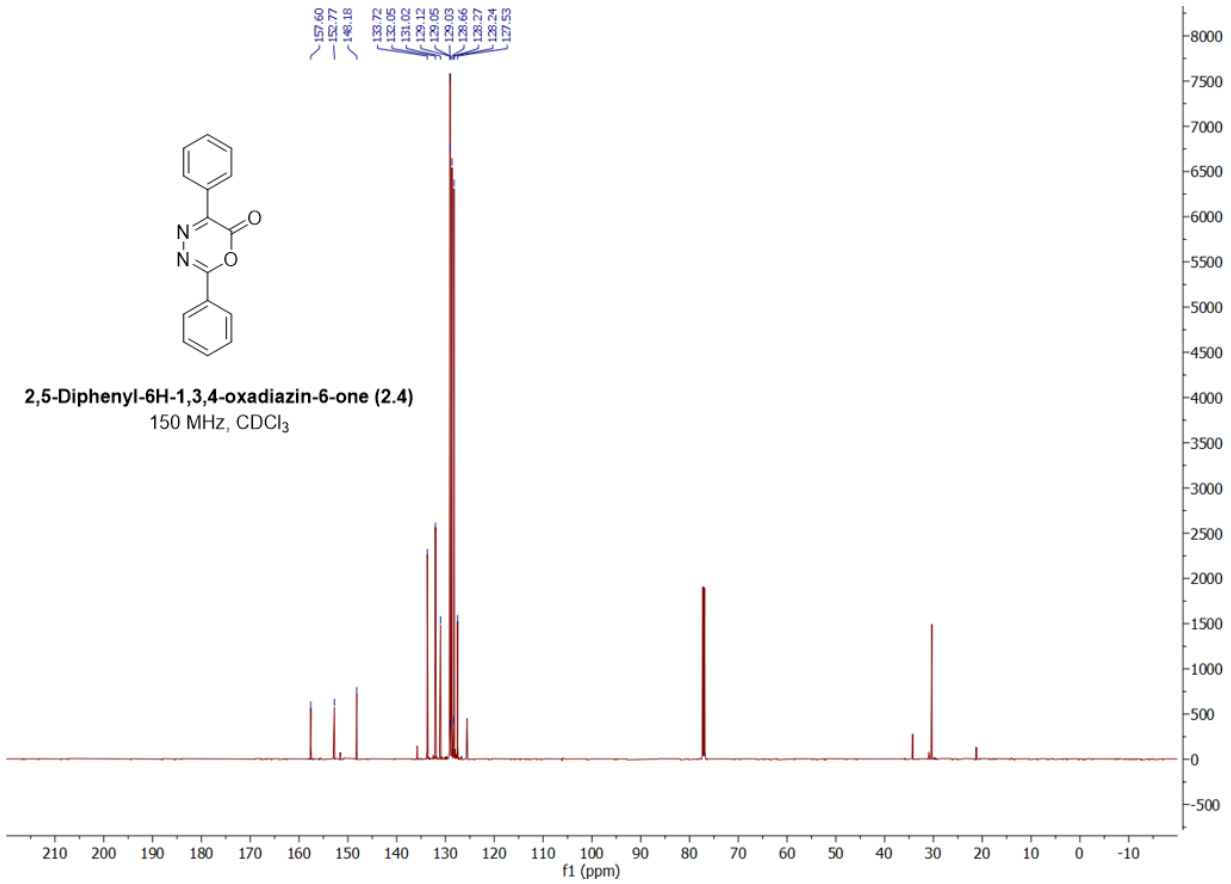

Figure A8. ^{13}C NMR of 2,5-diphenyl-6H-1,3,4-oxadiazin-6-one (**2.4**).

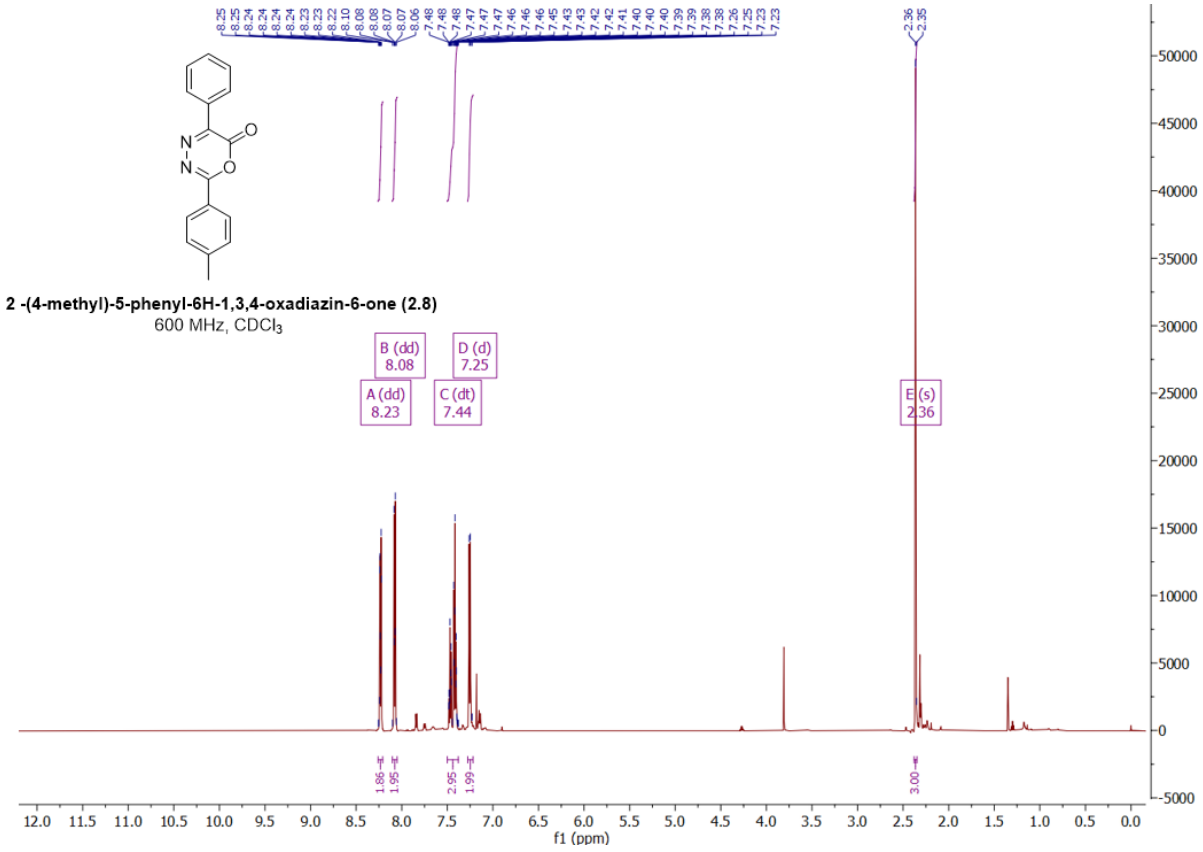

Figure A9. ^{1}H NMR of 2-(4-methyl)-5-phenyl-6H-1,3,4-oxadiazin-6-one (**2.8**).

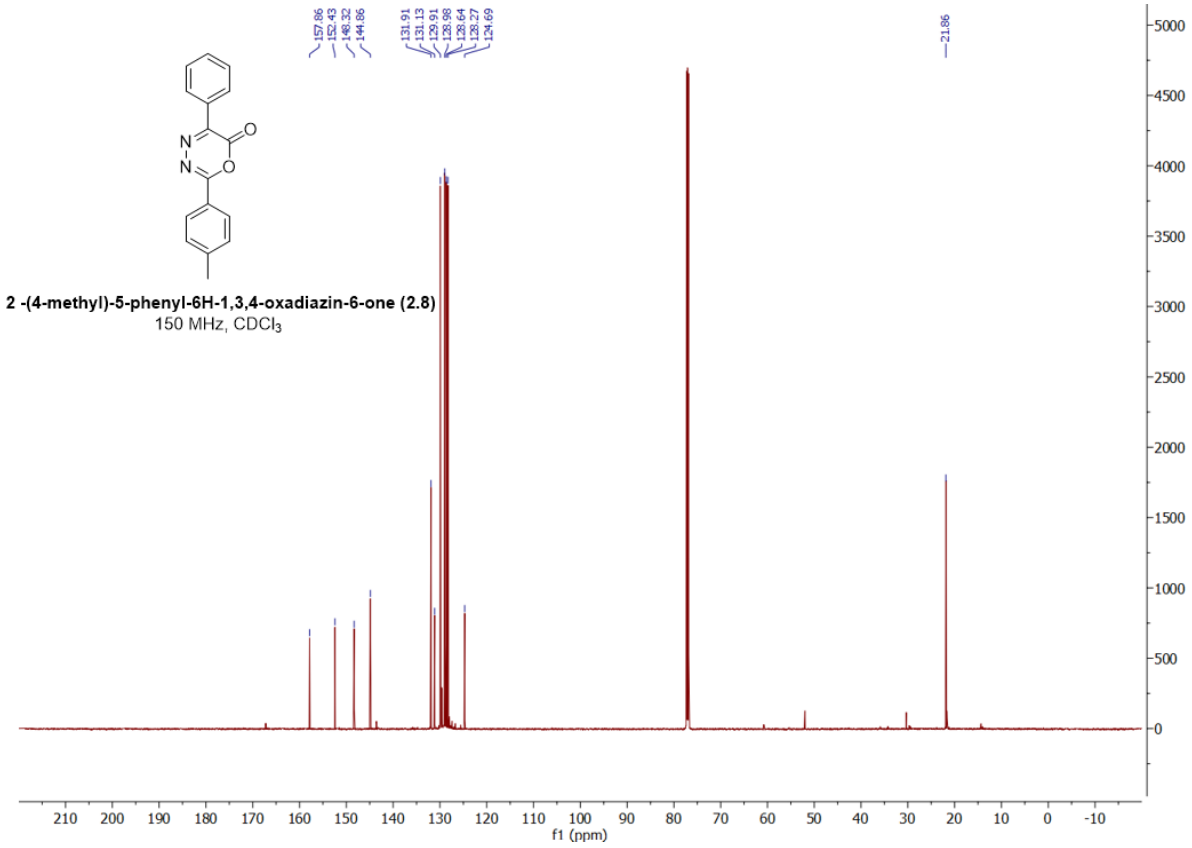

Figure A10. ^{13}C NMR of 2-(4-methyl)-5-phenyl-6H-1,3,4-oxadiazin-6-one (**2.8**).

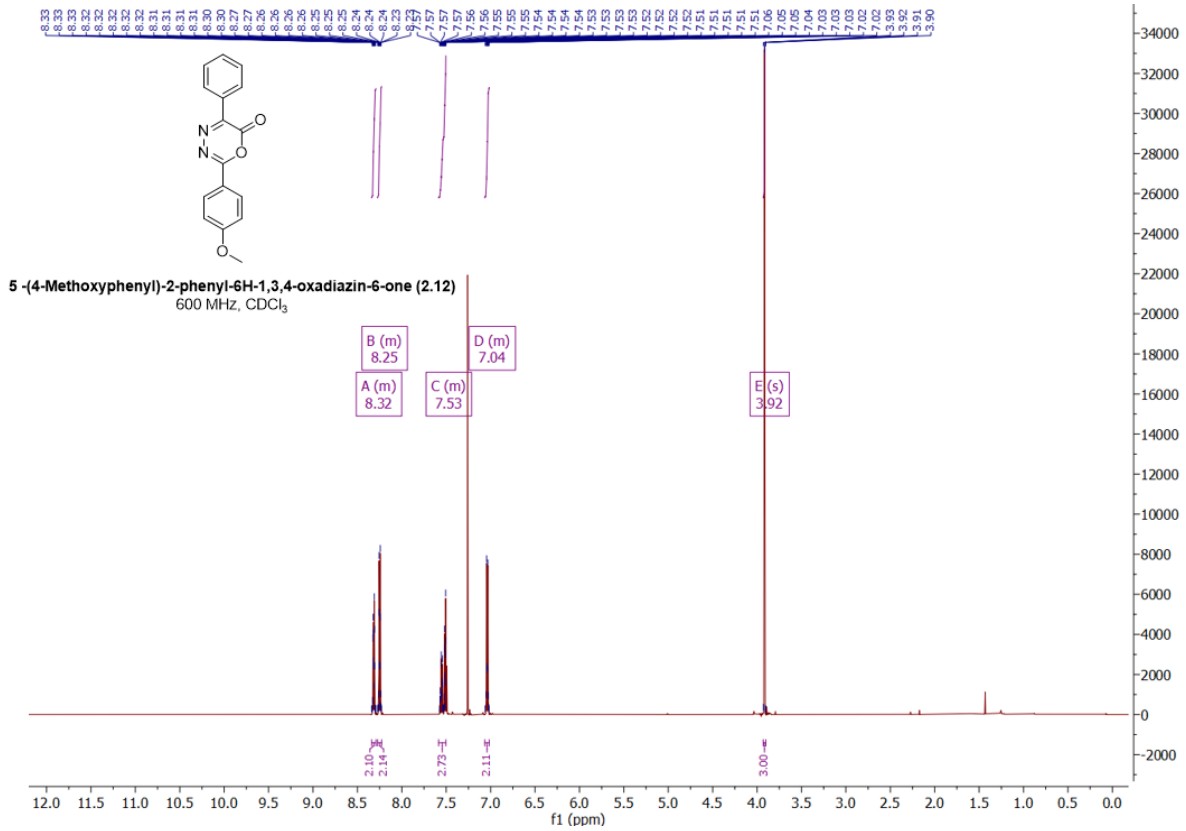

Figure A11. ^{1}H NMR of 5-(4-methoxyphenyl)-2-phenyl-6H-1,3,4-oxadiazin-6-one (**2.12**).

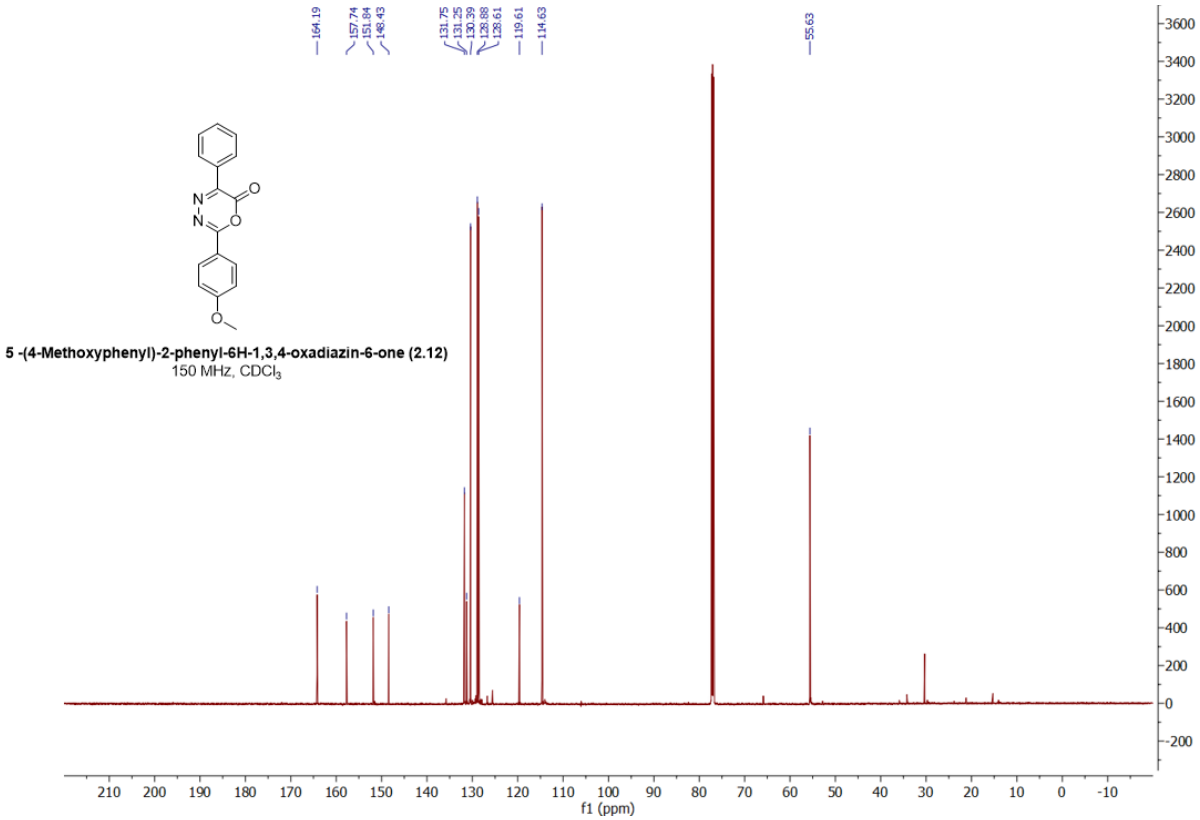

Figure A12. ^{13}C NMR of 5-(4-methoxyphenyl)-2-phenyl-6H-1,3,4-oxadiazin-6-one (**2.12**).

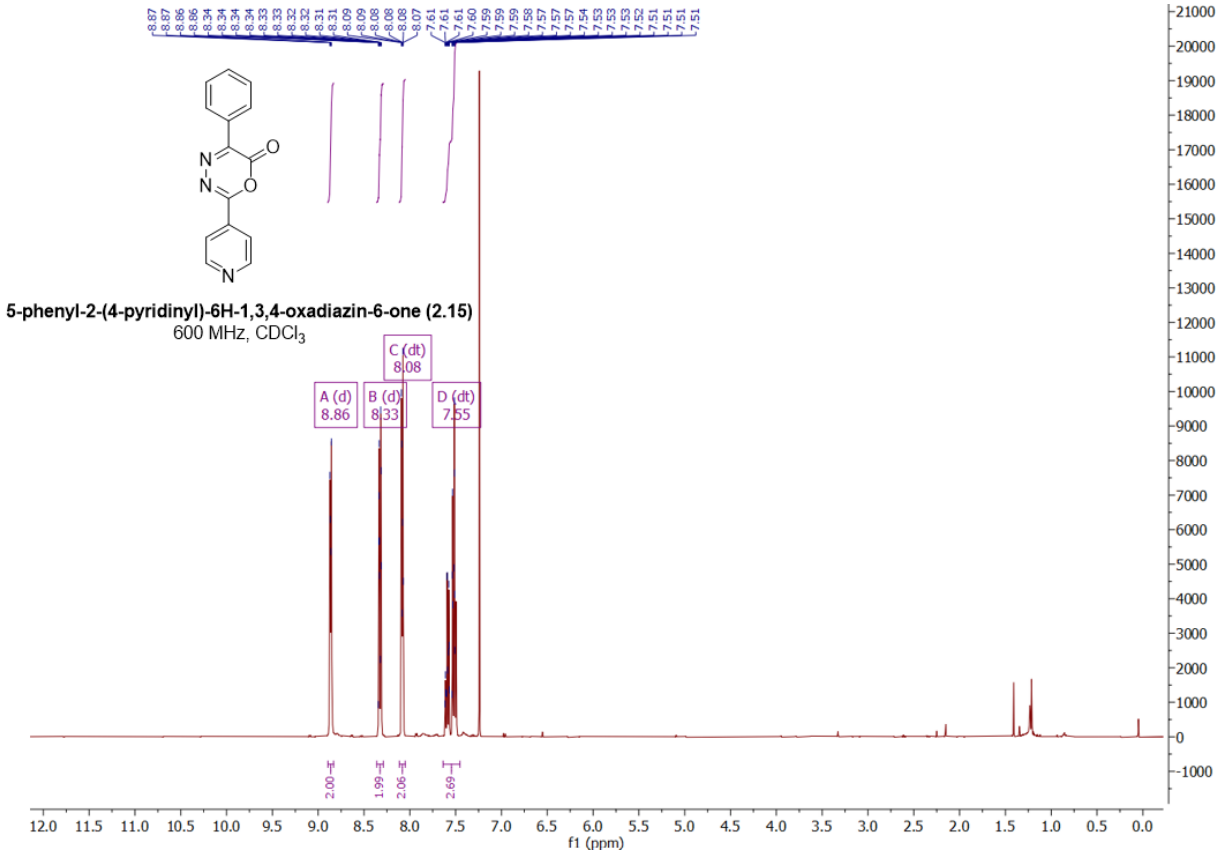

Figure A13. ^{1}H NMR of 5-phenyl-2(4-pyridinyl)-6H-1,3,4-oxadiazin-6-one (**2.16**).

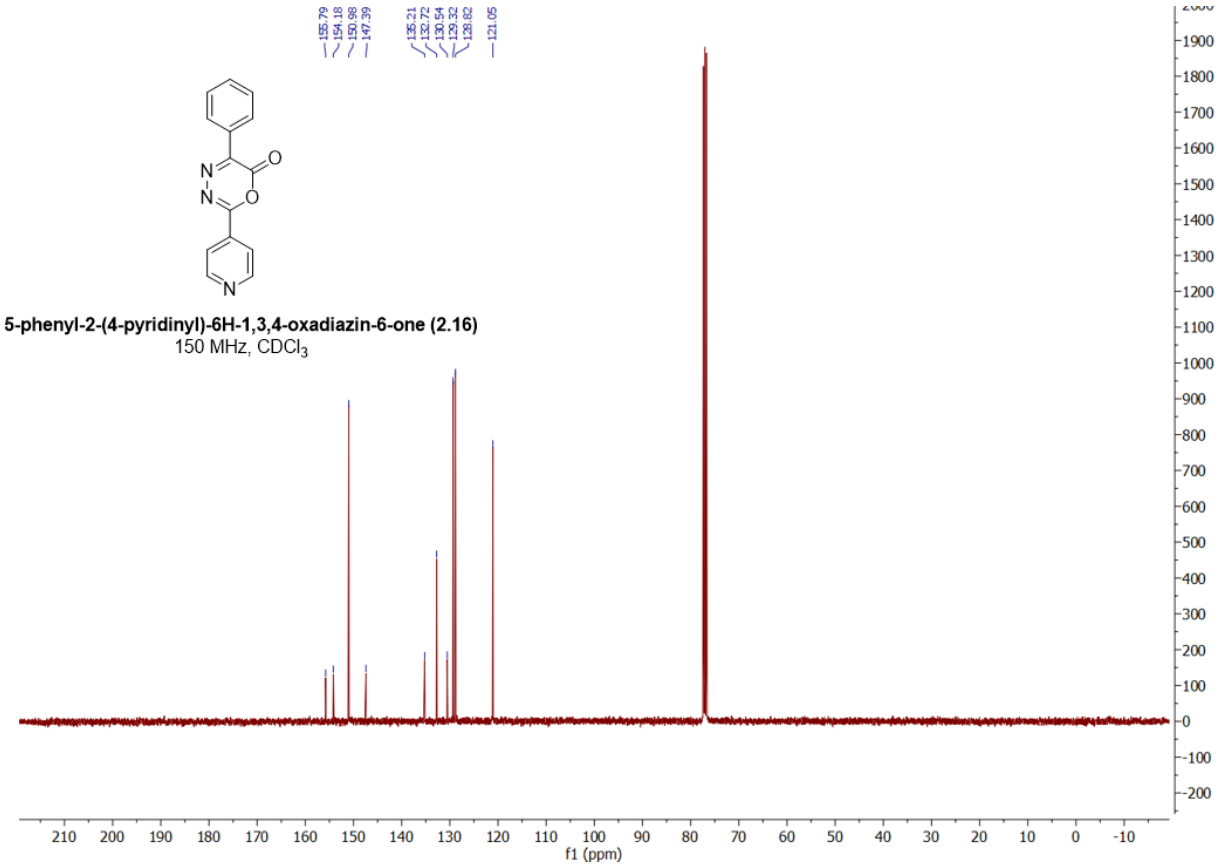

Figure A14. ^{13}C NMR of 5-phenyl-2(4-pyridinyl)-6H-1,3,4-oxadiazin-6-one (**2.15**).

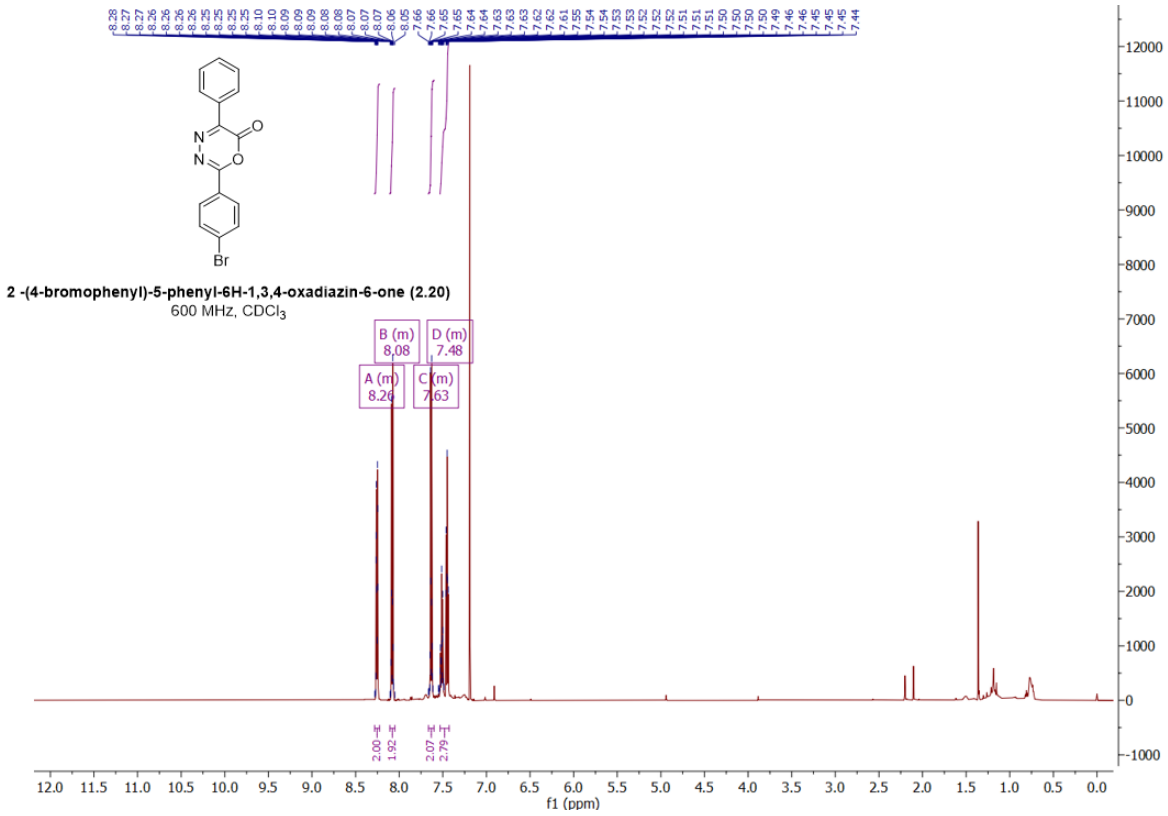

Figure A15. ^{1}H NMR of 2-(4-bromophenyl)-5-phenyl-6H-1,3,4-oxadiazin-6-one (**2.20**).

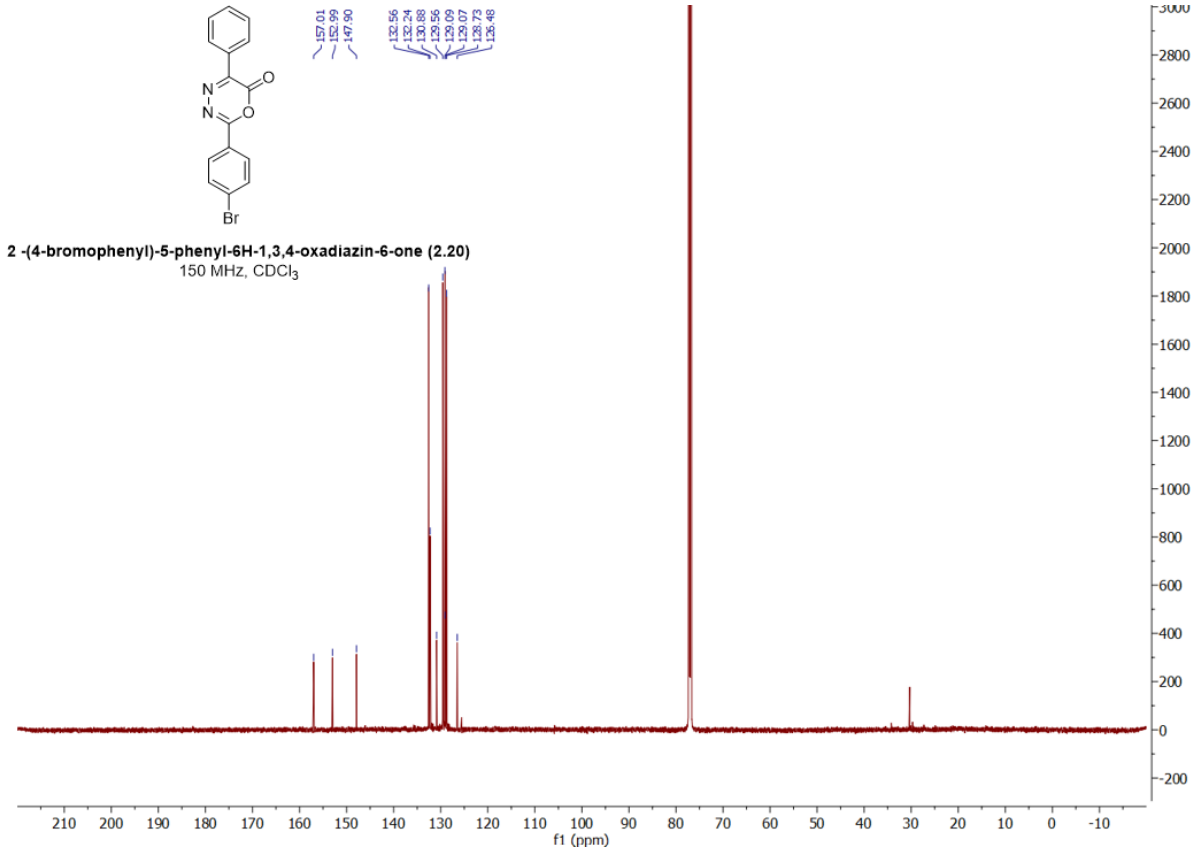

Figure A16. ^{13}C NMR of 2-(4-bromophenyl)-5-phenyl-6H-1,3,4-oxadiazin-6-one (**2.20**).

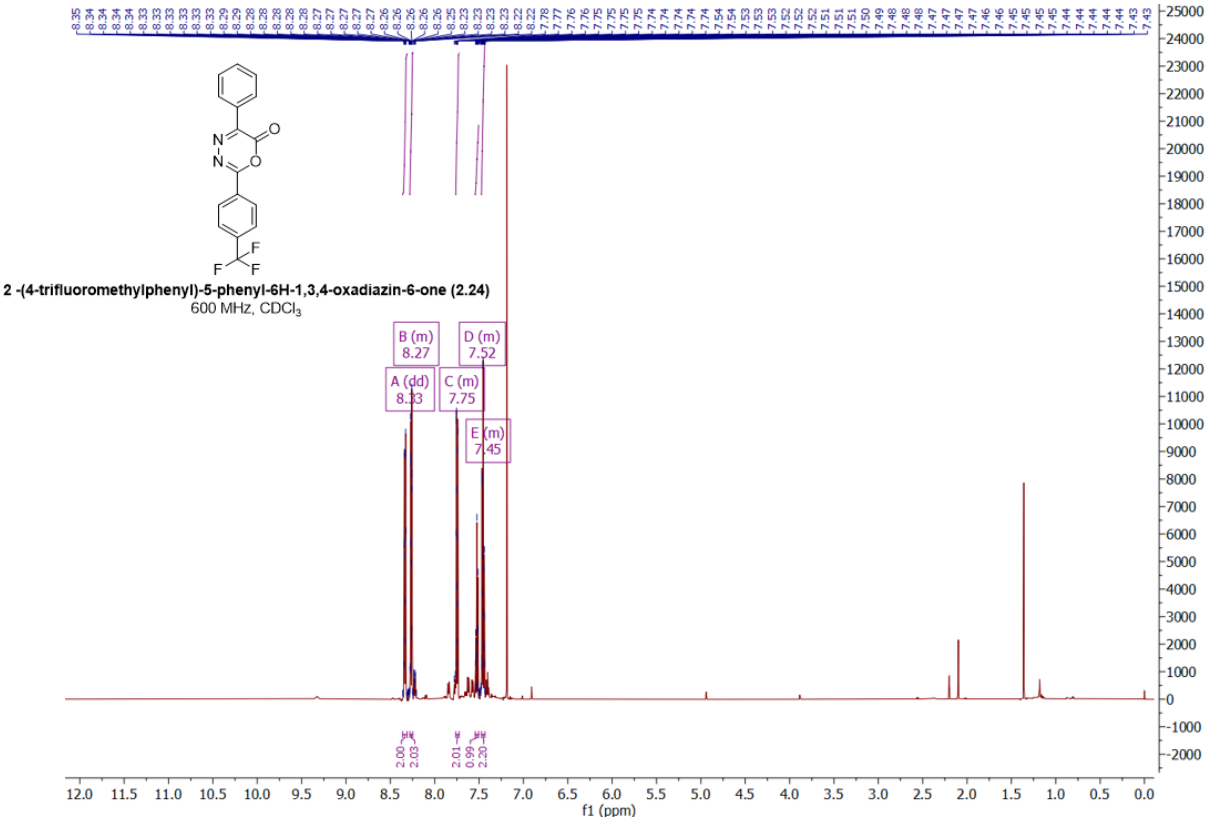

Figure A17. ^{1}H NMR of 2-(4-trifluoromethylphenyl)-5-phenyl-6H-1,3,4-oxadiazin-6-one (**2.24**).

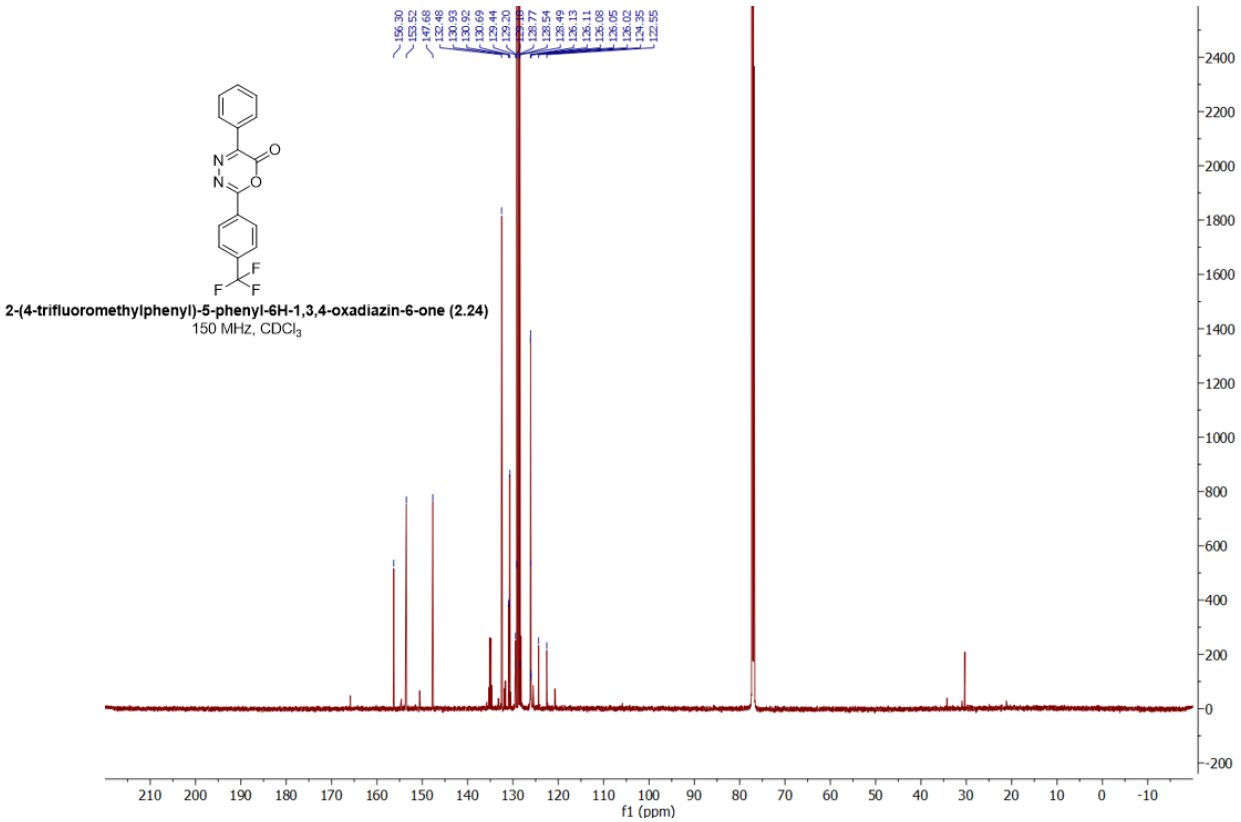

Figure A18. ^{13}C NMR of 2-(4-trifluoromethylphenyl)-5-phenyl-6H-1,3,4-oxadiazin-6-one (**2.24**).

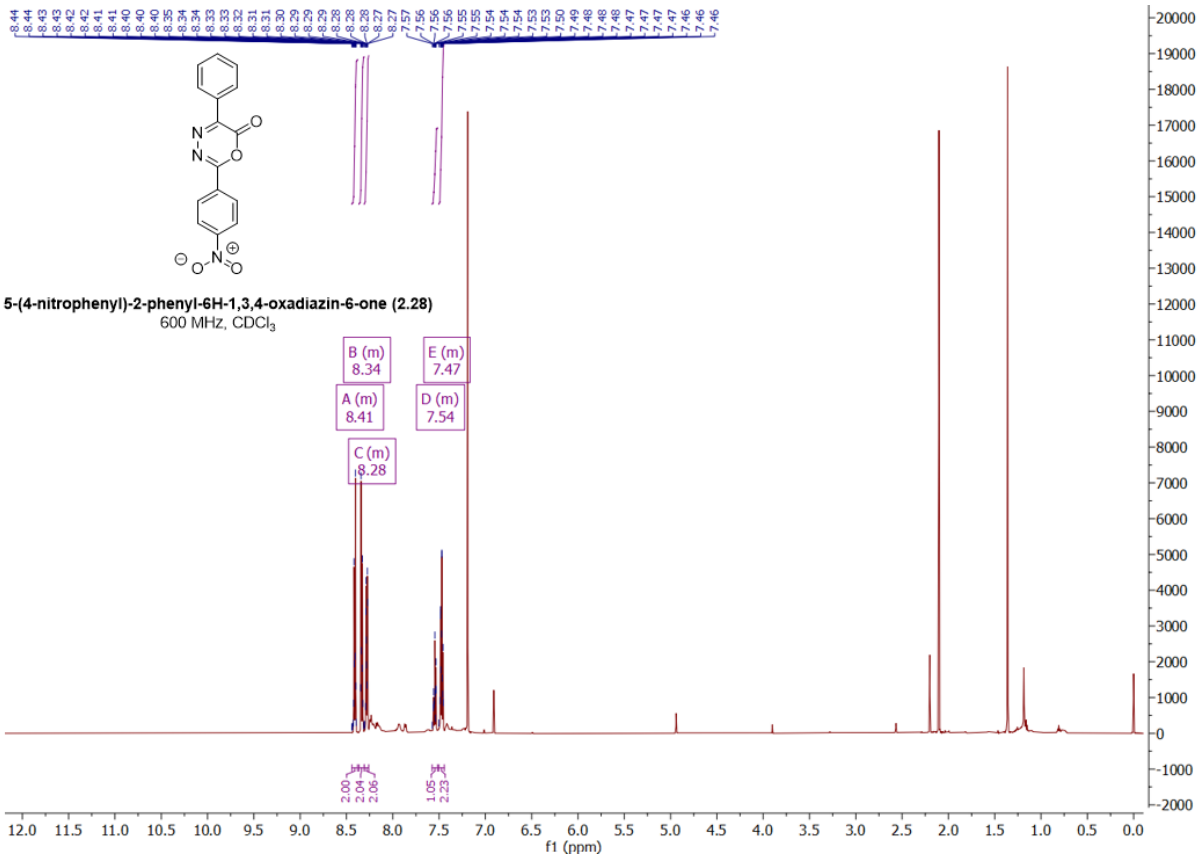

Figure A19. ^{1}H NMR of 5-(4-nitrophenyl)-2-phenyl-6H-1,3,4-oxadiazin-6-one (**2.28**).

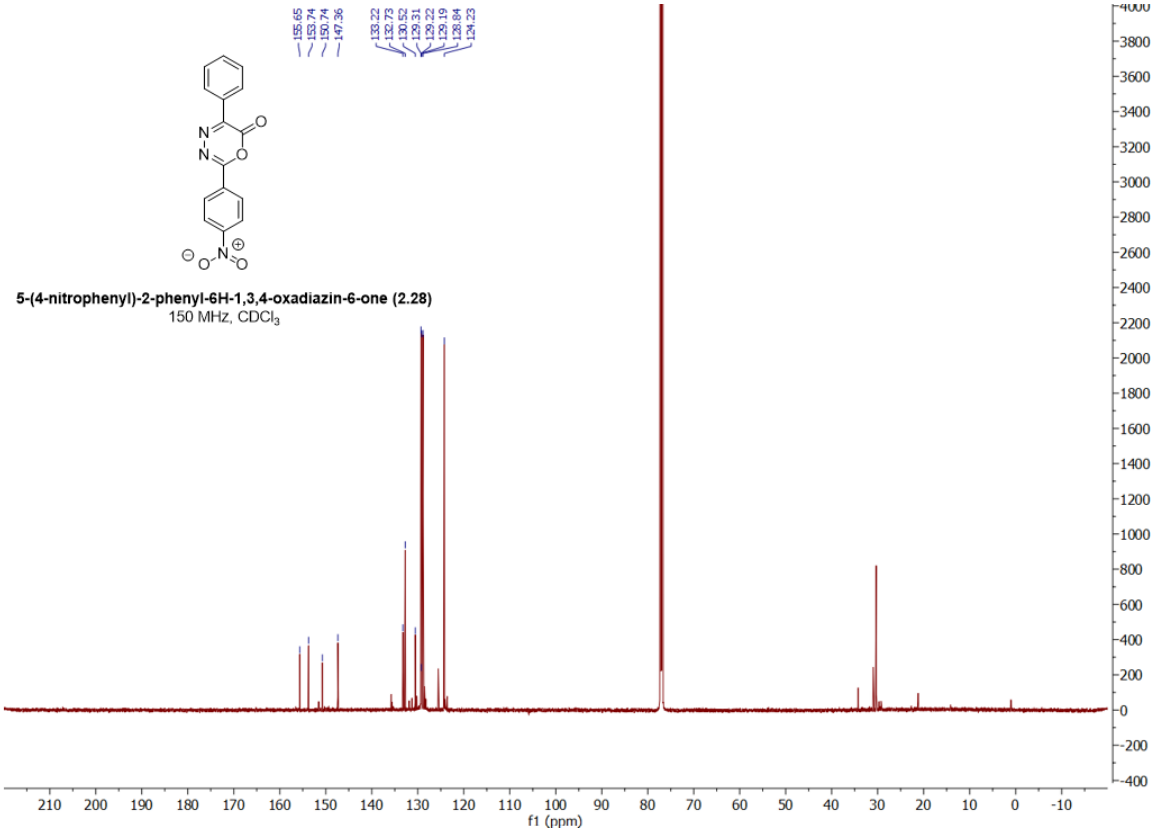

Figure A20. ^{13}C NMR of 5-(4-nitrophenyl)-2-phenyl-6H-1,3,4-oxadiazin-6-one (**2.28**).

1H and 13C of TCO

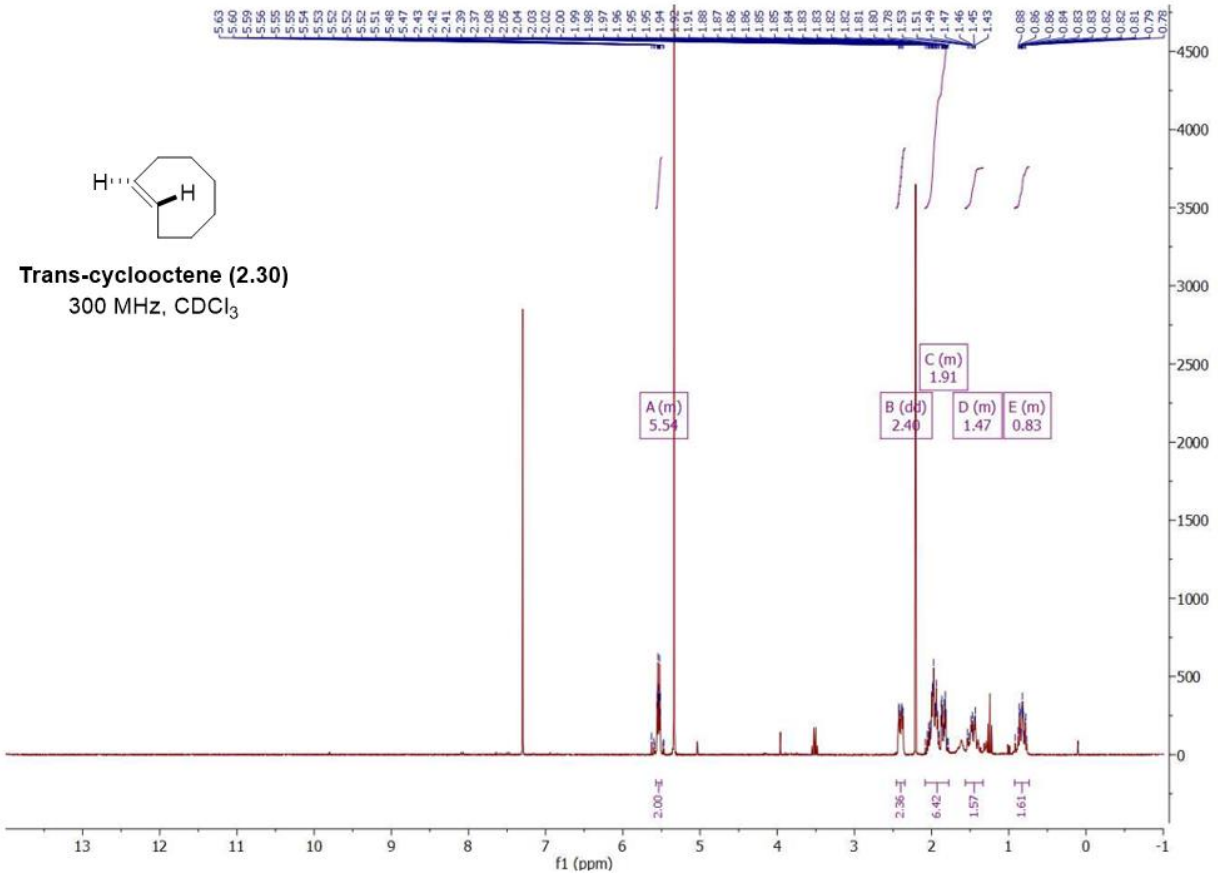

Figure A21. [1]H NMR of Trans-cyclooctene (**2.30**).

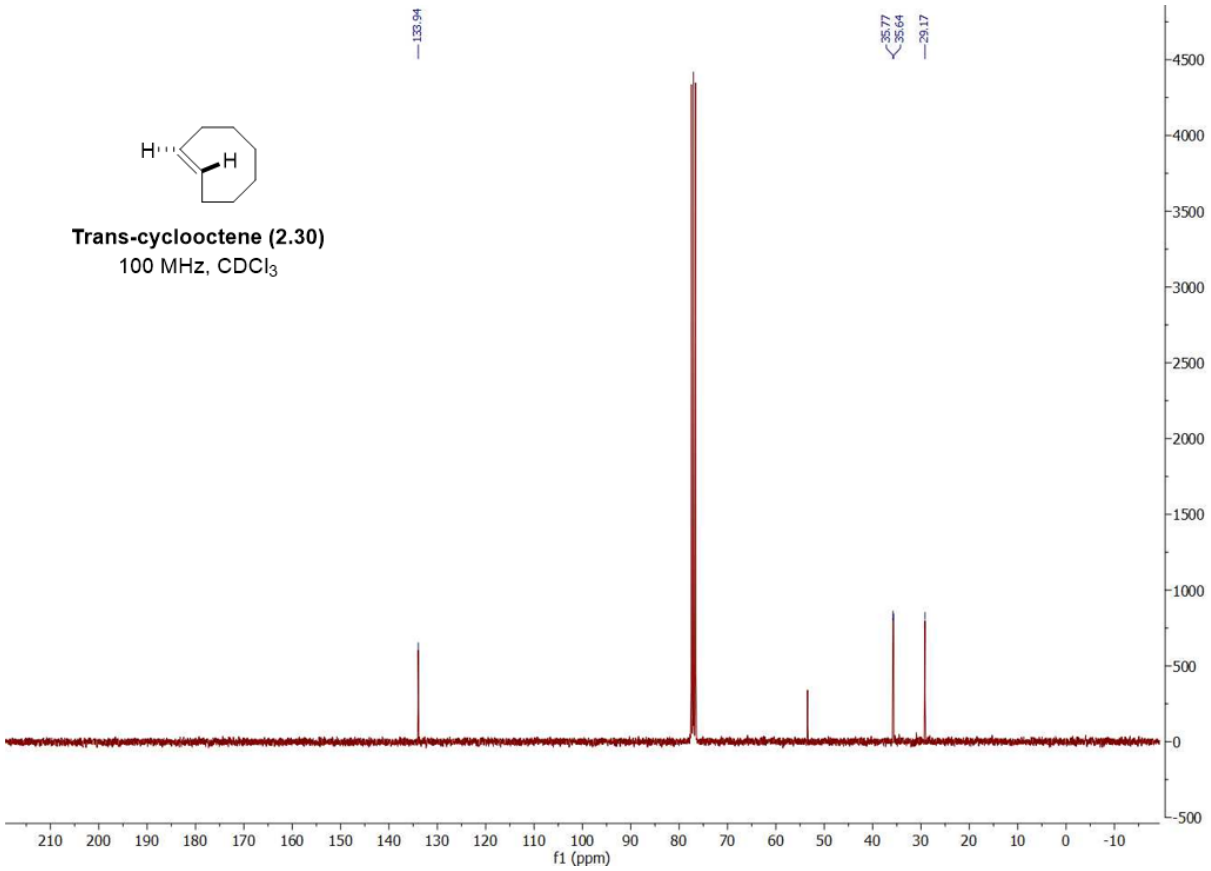

Figure A22. ^{13}C NMR of Trans-cyclooctene (**2.30**).

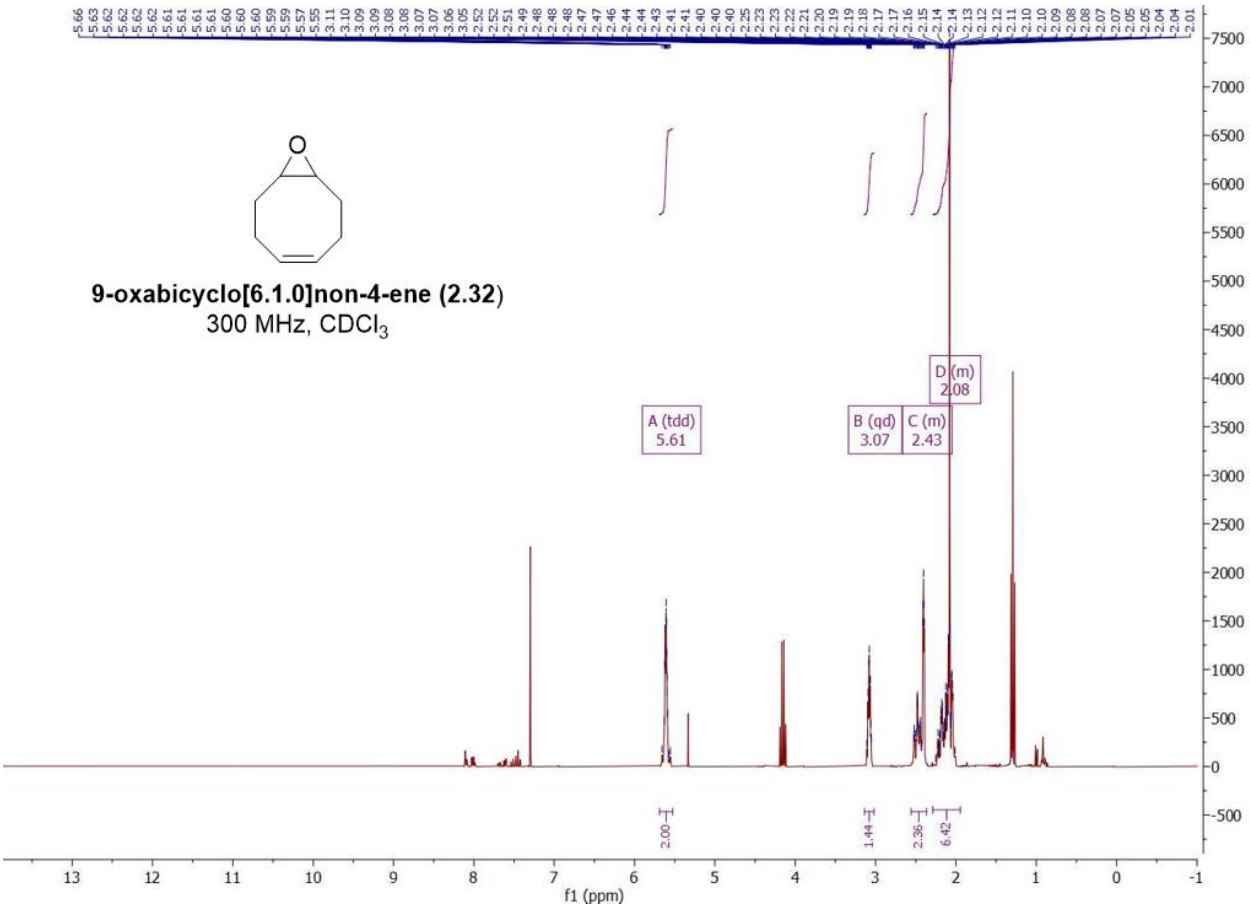

Figure A23. ^{1}H NMR of 9-oxabicyclo[6.1.0]non-4-ene (**2.32**).

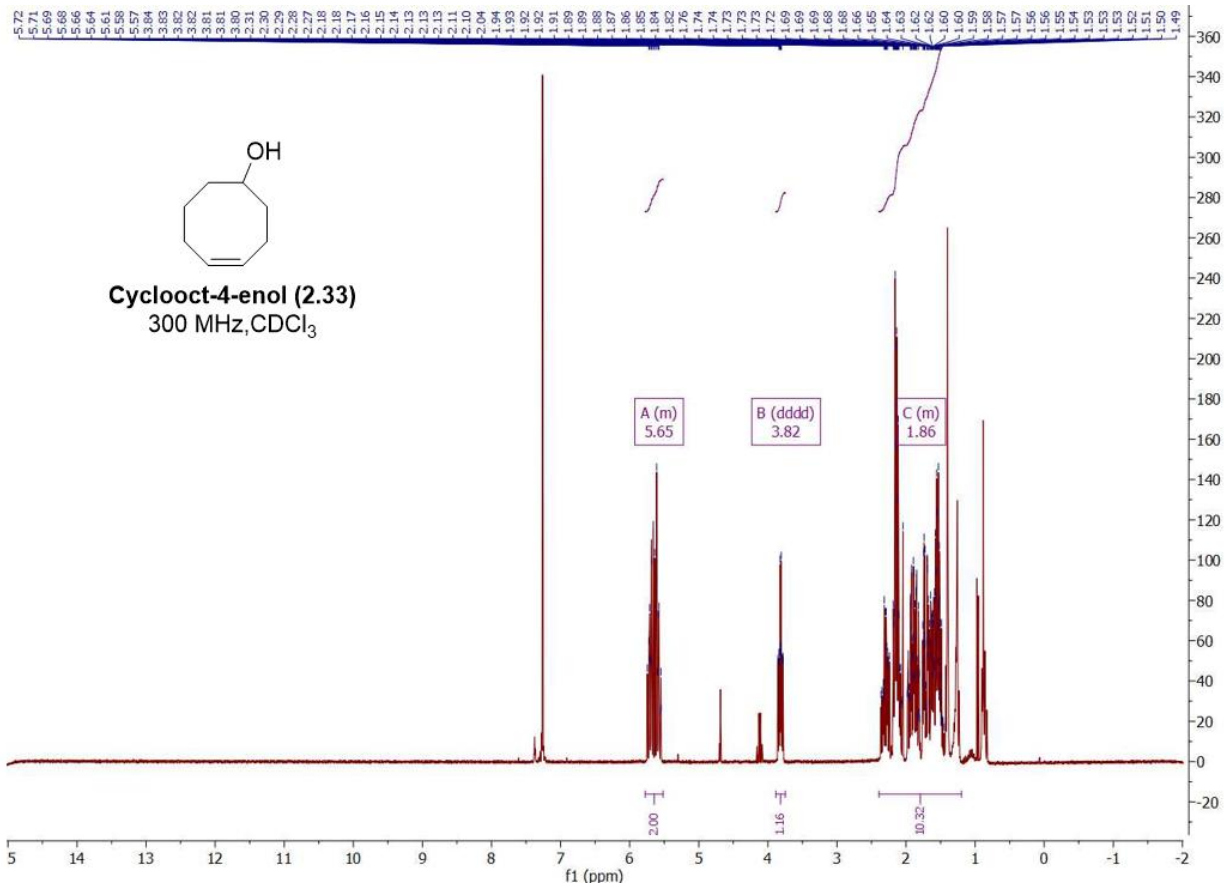

Figure A24. ^{1}H NMR of cyclooct-4-enol (**2.33**).

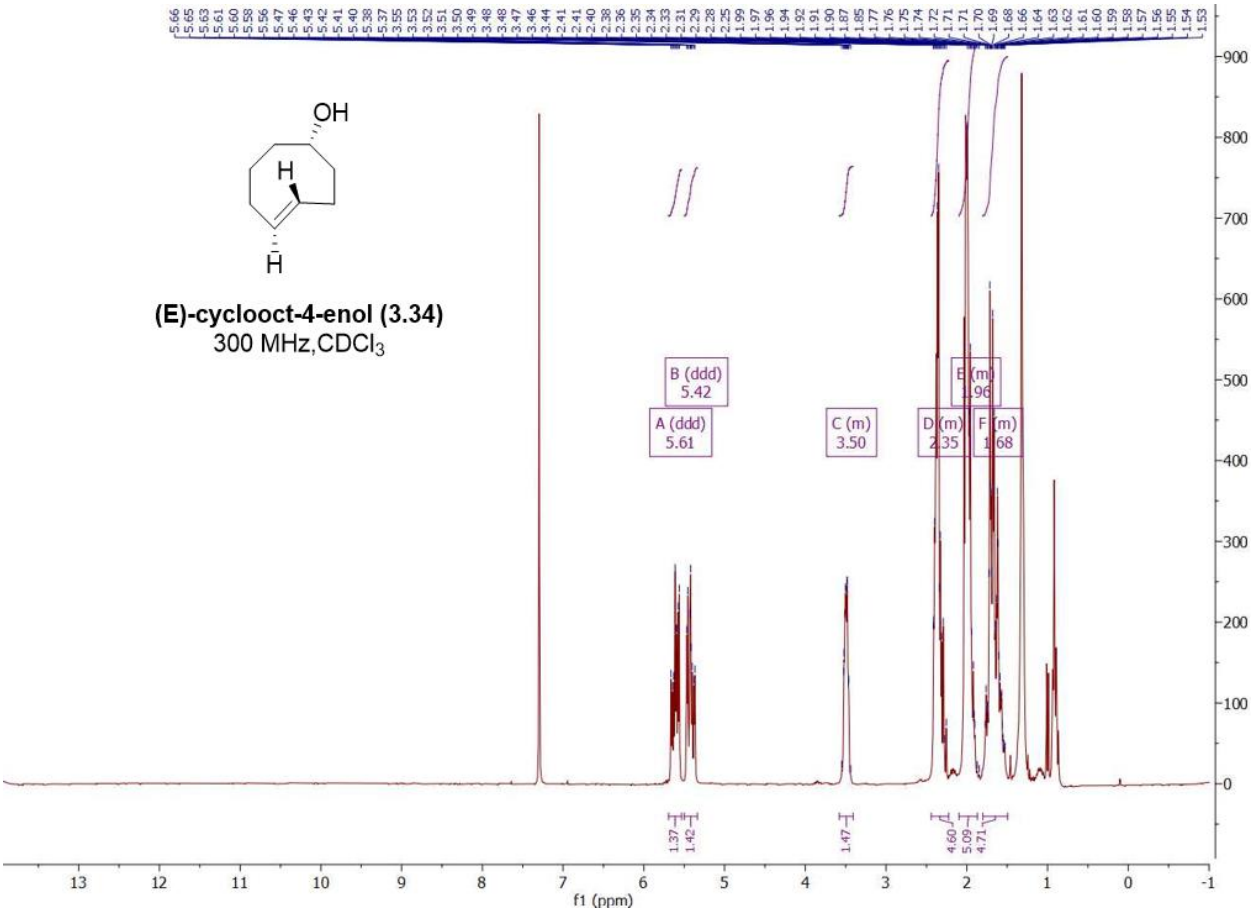

Figure A25. ^{1}H NMR of (E)-cyclooct-4-enol (**2.34**).

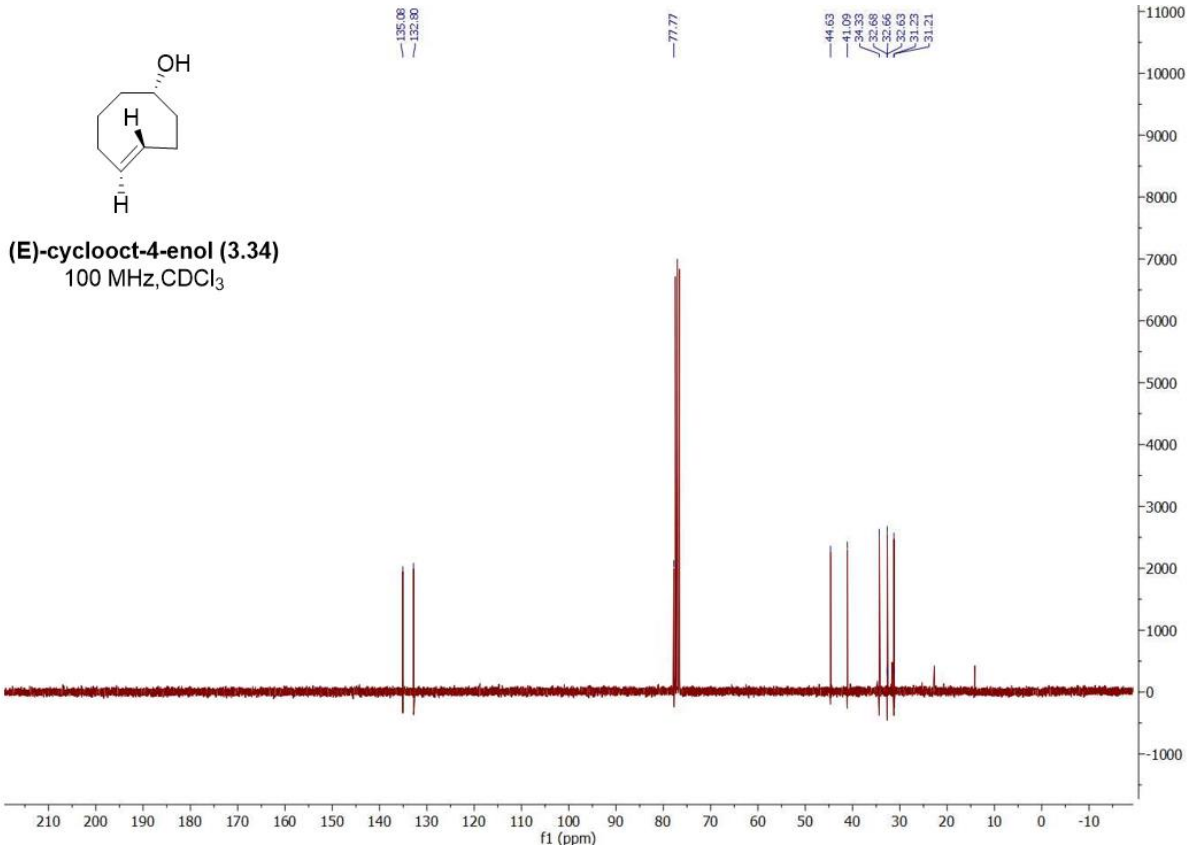

Figure A26. ^{13}C NMR of (E)-cyclooct-4-enol (**2.15**).

1H of s-TCO

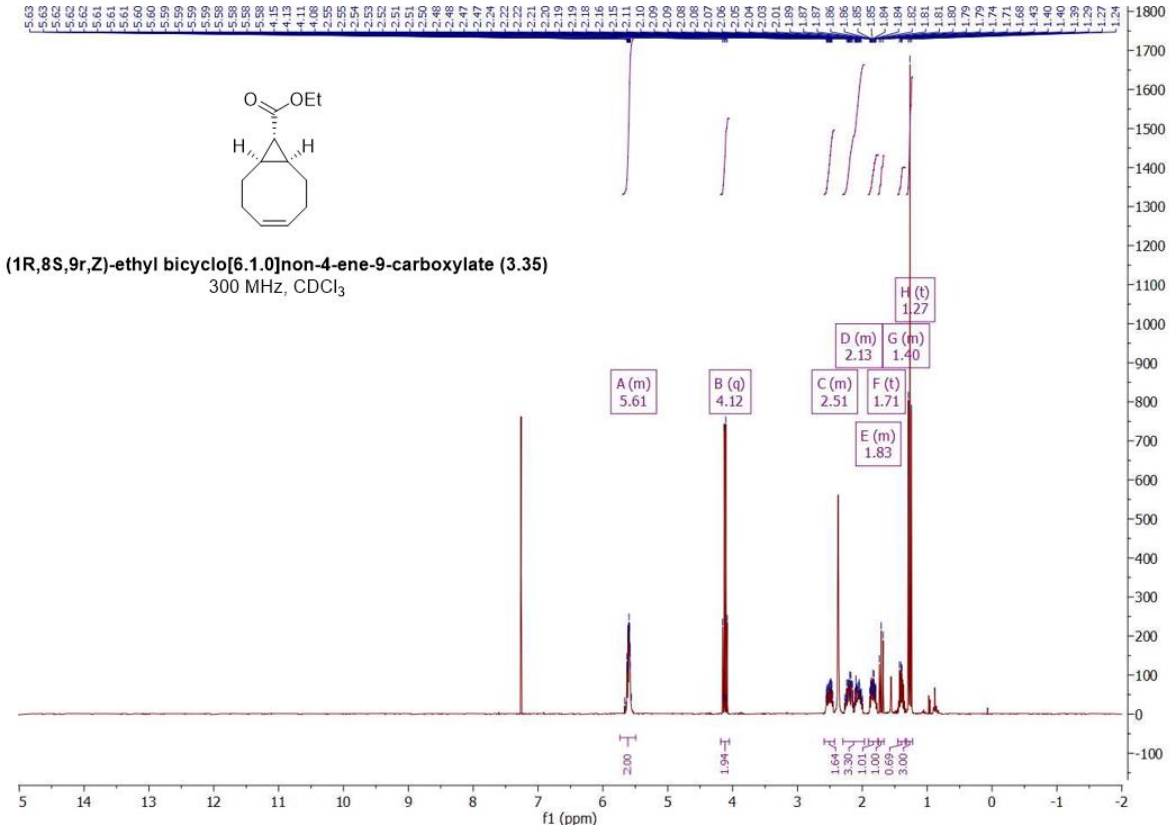

Figure A27. [1]H NMR of (1R, 8S,9R, Z) ethyl bicyclo[6.1.0]non-4-ene-9-carboxylate (**2.35**).

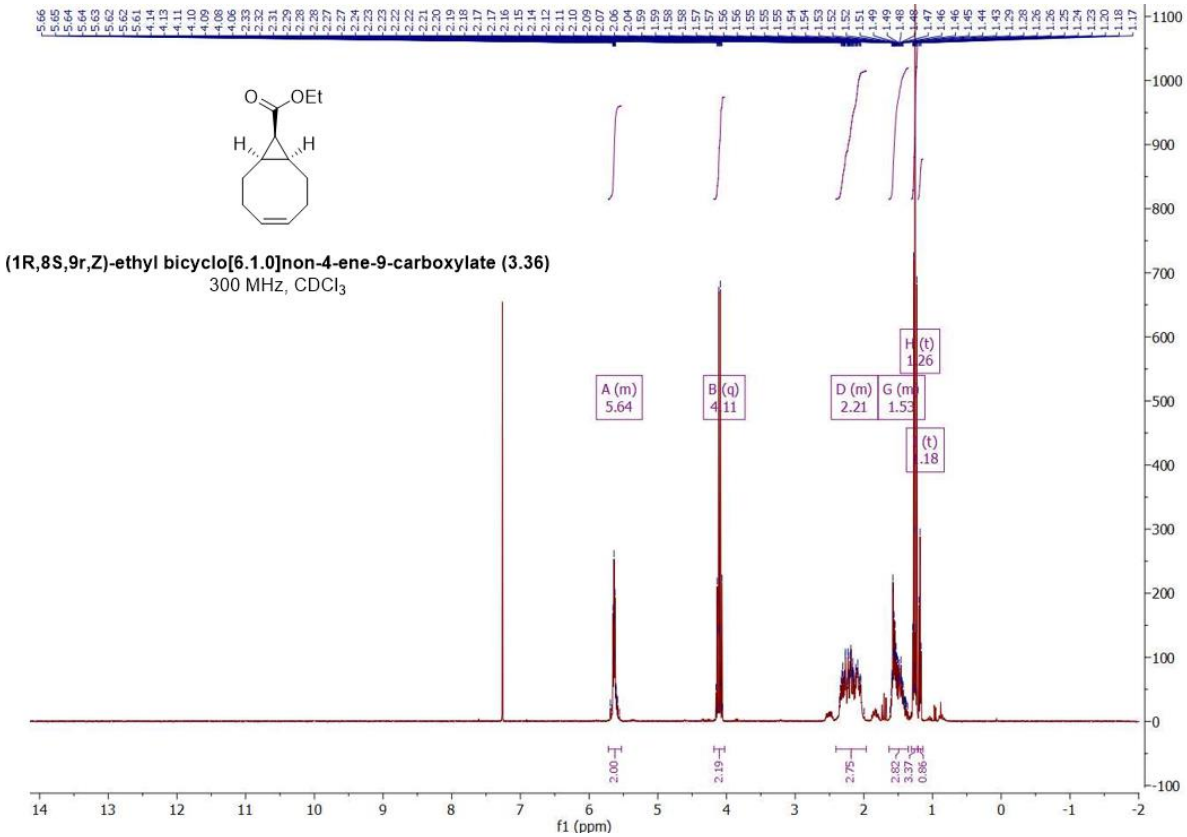

Figure A28. ^{1}H NMR of (1R,8S, 9R, Z) ethyl bicyclo[6.1.0]non-4-ene-9-carboxylate (**2.36**).

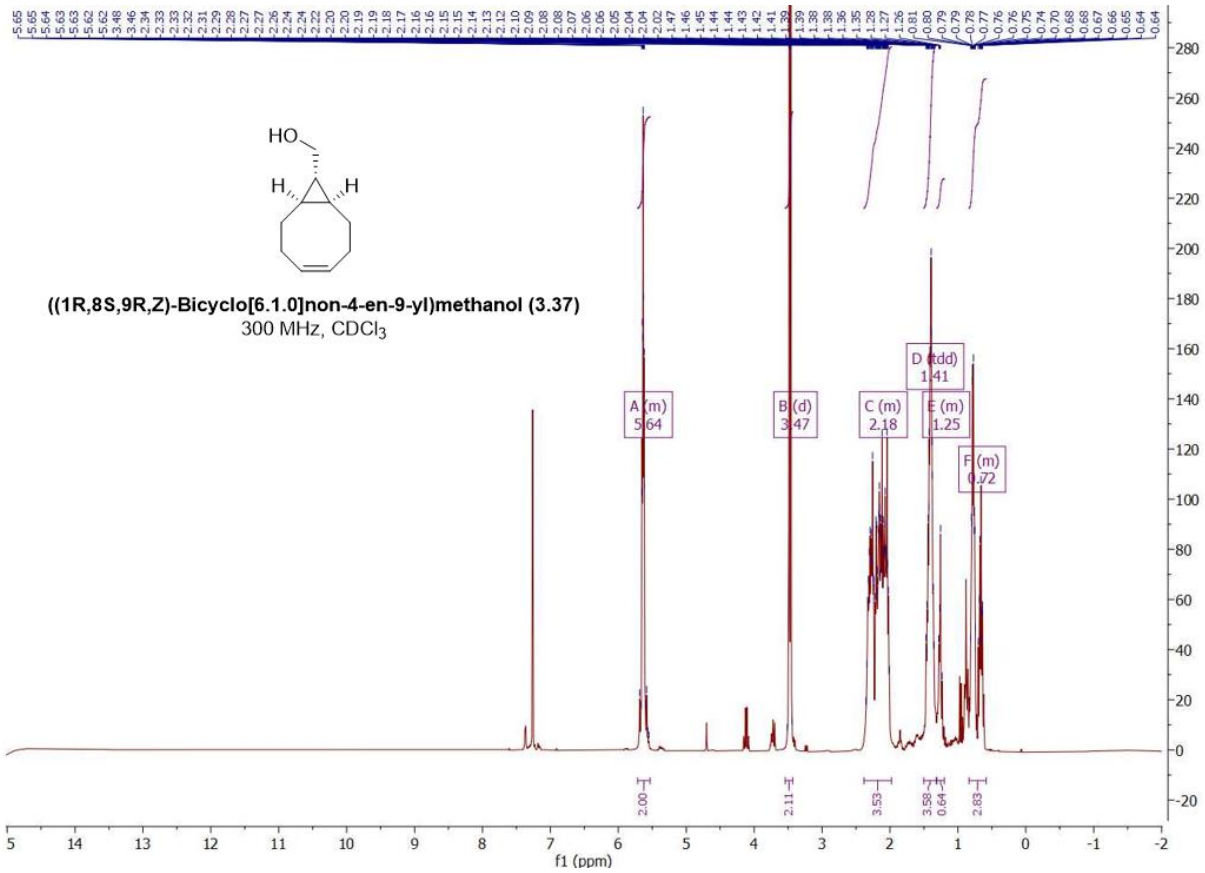

Figure A29. ^{1}H NMR of (1R, 8S, 9R, Z)-bicyclo[6.1.0]non-4-ene-9-yl)methanol (**2.37**).

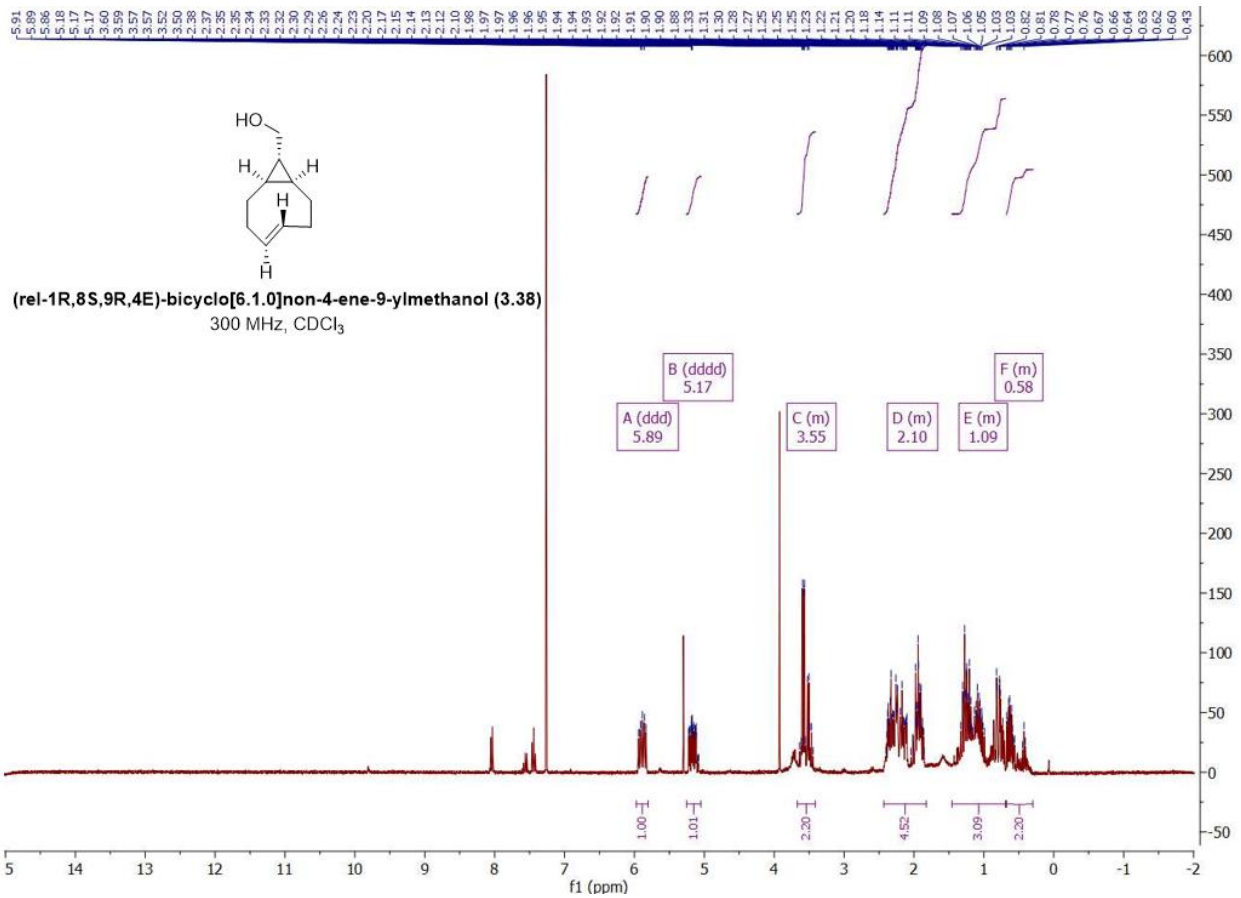

Figure A30. ^{1}H NMR of (rel-1R, 8S, 9R, E)-bicyclo[6.1.0]non-4-ene-9-yl)methanol (**2.38**).

Appendix B - Kinetic Analysis for Chapter 3

UV-Vis pseudo first-order kinetic analysis

Table B1. Observed rate constants for the cycloaddition reaction between 5-methyl-2-phenyl-6H-1,3,4-oxadiazin-6-one (**2.2**) and endo BCN, with various concentrations of BCN in ACN at 25 ± 0.1 °C.

Pyrone	Concentration of BCN (10^{-4} M)	k_{obs} (10^{-5} s^{-1})
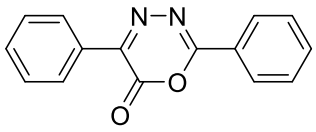 (2.4)	0.25	1.06 ± 0.00
	0.50	1.42 ± 0.05
	0.75	1.74 ± 0.07
	1.00	1.94 ± 0.00

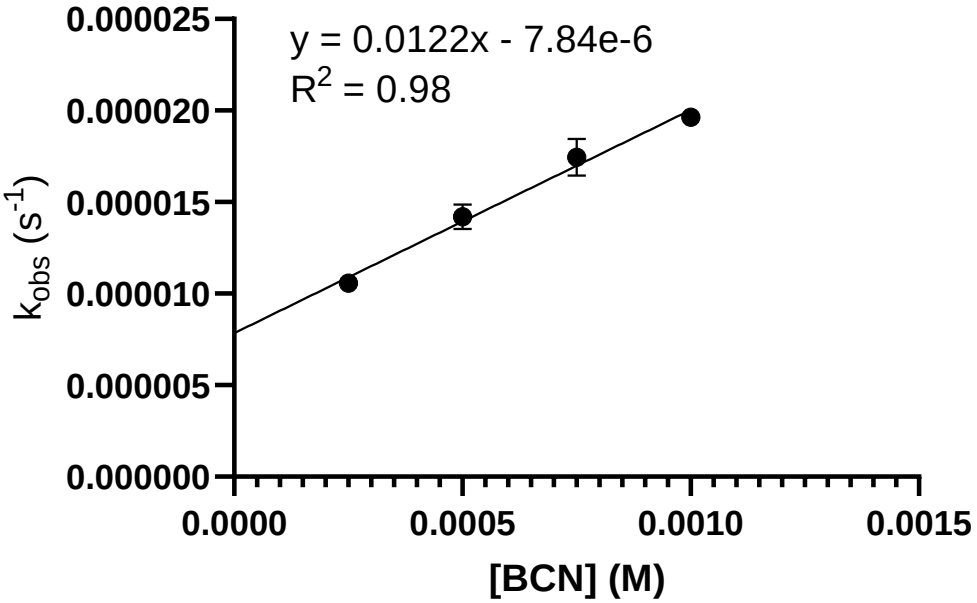

Figure B1. Pseudo first-order rate constant of the cycloaddition reaction between 5-methyl-2-phenyl-6H-1,3,4-oxadiazin-6-one (**2.2**) and endo BCN plotted against varying concentrations of BCN. These reactions were performed in ACN at 25 ± 0.1 °C. The error bars represent SD (n=2).

Table B2. Observed rate constants for the cycloaddition reaction between 5-(4-Methoxyphenyl)-2-phenyl-6H-1,3,4-oxadiazin-6-one (**2.4**) and endo BCN, with various concentrations of BCN in ACN at 25 ± 0.1 °C.

Pyrone	Concentration of BCN (10^{-4} M)	k_{obs} (10^{-6} s^{-1})
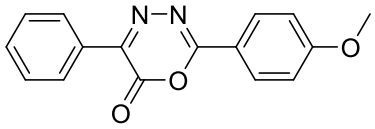 (2.11)	0.50	5.46 ± 0.00
	0.75	9.26 ± 0.12
	1.00	12.5 ± 0.08
	1.25	16.1 ± 0.00
	1.50	19.4 ± 0.05

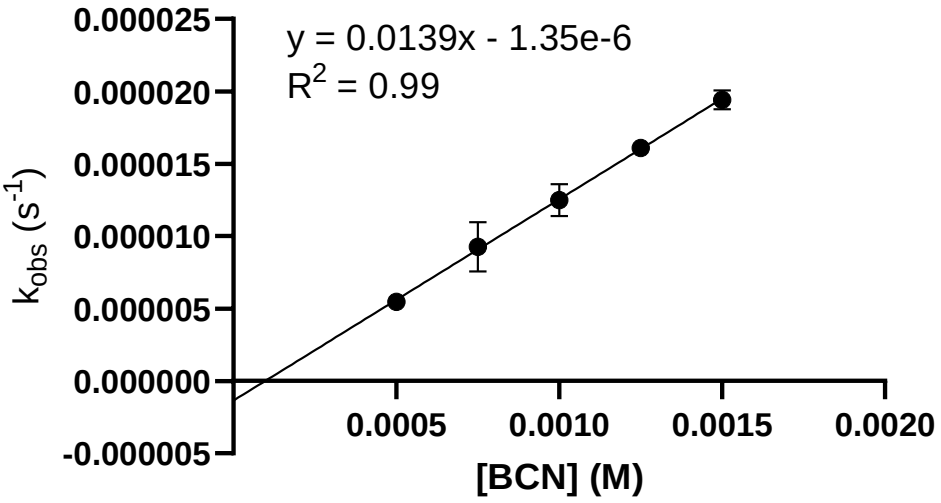

Figure B2. Pseudo first-order rate constant of the cycloaddition reaction between 5-(4-Methoxyphenyl)-2-phenyl-6H-1,3,4-oxadiazin-6-one (**2.4**) and endo BCN plotted against varying

concentrations of BCN. These reactions were performed in ACN at 25 ± 0.1 °C. The error bars represent SD (n=2).

Table B3. Observed rate constants for the cycloaddition reaction between 5-phenyl-2-(4-pyridinyl)-6H-1,3,4-oxadiazin-6-one (**2.8**) and endo BCN, with various concentrations of BCN in ACN at 25 ± 0.1 °C.

Pyrone	Concentration of BCN (10^{-4} M)	k_{obs} (10^{-5} s^{-1})
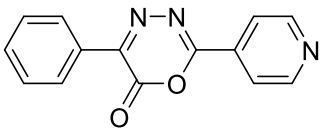 (2.15)	1	1.25 ± 0.10
	1.5	1.99 ± 0.02
	2	2.86 ± 0.60
	2.5	3.79 ± 0.17

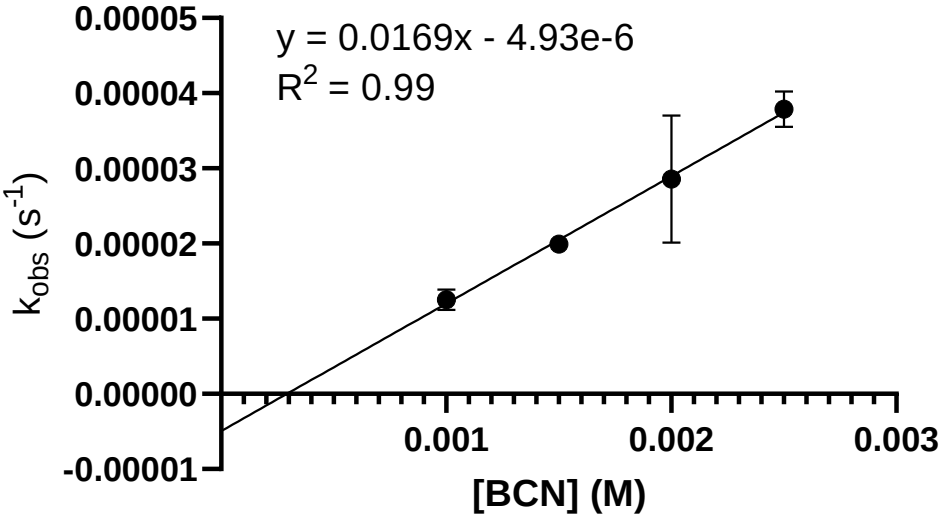

Figure B3. Pseudo first-order rate constant of the cycloaddition reaction between 5-phenyl-2-(4-pyridinyl)-6H-1,3,4-oxadiazin-6-one (**2.8**) and endo BCN plotted against varying concentrations

of BCN. These reactions were performed in ACN at 25 ± 0.1 °C. The error bars represent SD (n=2).

Table B4. Observed rate constants for the cycloaddition reaction between 2-(4-bromophenyl)-5-phenyl-6H-1,3,4-oxadiazin-6-one (**2.10**) and endo BCN, with various concentrations of BCN in ACN at 25 ± 0.1 °C.

Pyrone	Concentration of BCN (10^{-4} M)	k_{obs} (10^{-6} s^{-1})
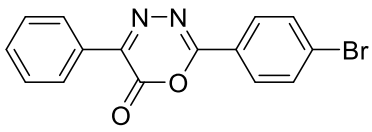 **(2.20)**	0.50	8.90 ± 0.00
	0.75	13.7 ± 0.00
	1.00	18.9 ± 0.00
	1.25	23.3 ± 0.07

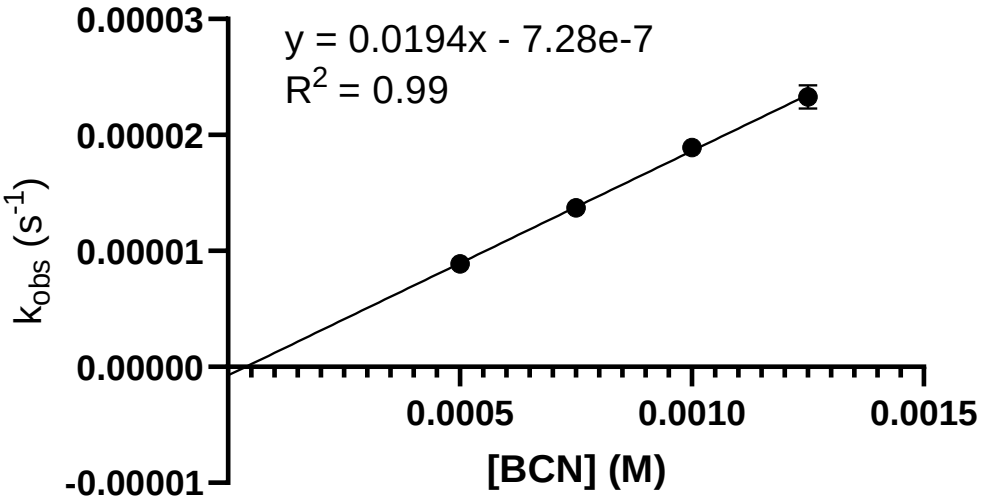

Figure B4. Pseudo first-order rate constant of the cycloaddition reaction between 2-(4-bromophenyl)-5-phenyl-6H-1,3,4-oxadiazin-6-one (**2.10**) and endo BCN plotted against varying concentrations of BCN. These reactions were performed in ACN at 25 ± 0.1 °C. The error bars represent SD (n=2).

Table B5. Observed rate constants for the cycloaddition reaction between 5-(4-triflouromethyl)-2-phenyl-6H-1,3,4-oxadiazin-6-one (**2.12**) and endo BCN, with various concentrations of BCN in ACN at 25 ± 0.1 °C.

Pyrone	Concentration of BCN (10^{-4} M)	k_{obs} (10^{-5} s^{-1})
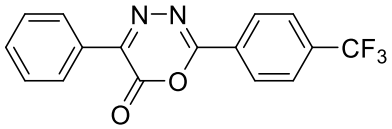 **(2.24)**	0.25	1.25 ± 0.00
	0.50	2.19 ± 0.13
	0.75	2.83 ± 0.00
	1.00	3.35 ± 0.07

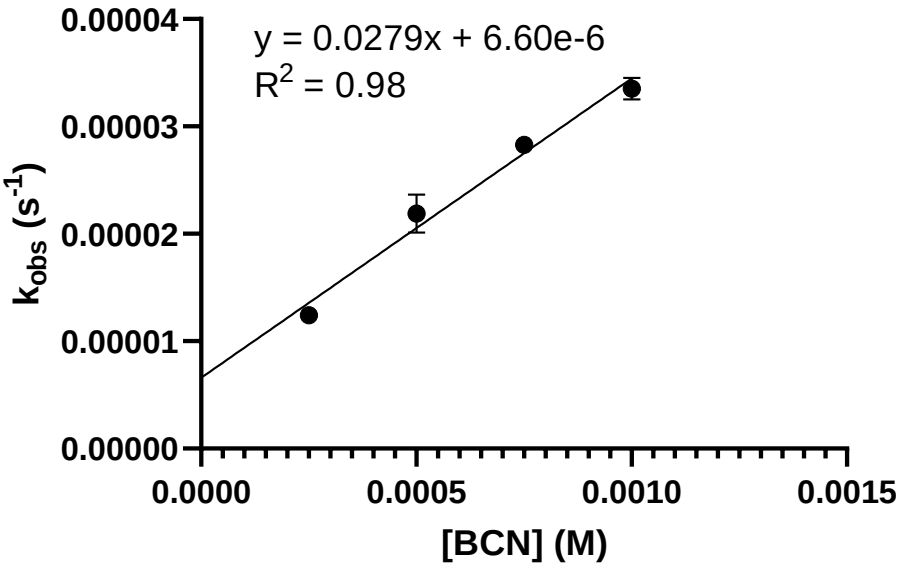

Figure B5. Pseudo first-order rate constant of the cycloaddition reaction between 5-(4-triflouromethyl)-2-phenyl-6H-1,3,4-oxadiazin-6-one (**2.12**) and endo BCN plotted against varying concentrations of BCN. These reactions were performed in ACN at 25 ± 0.1 °C. The error bars represent SD (n=2).

Table B6. Observed rate constants for the cycloaddition reaction between 5-(4-nitrophenyl)-2-phenyl-6H-1,3,4-oxadiazin-6-one (**2.14**) and endo BCN, with various concentrations of BCN in ACN at 25 ± 0.1 °C.

Pyrone	Concentration of BCN (10^{-4} M)	k_{obs} (10^{-6} s^{-1})
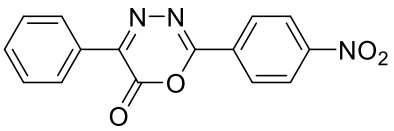 (2.28)	0.25	4.40 ± 2.26
	0.50	8.27 ± 1.46
	0.75	13.3 ± 1.39

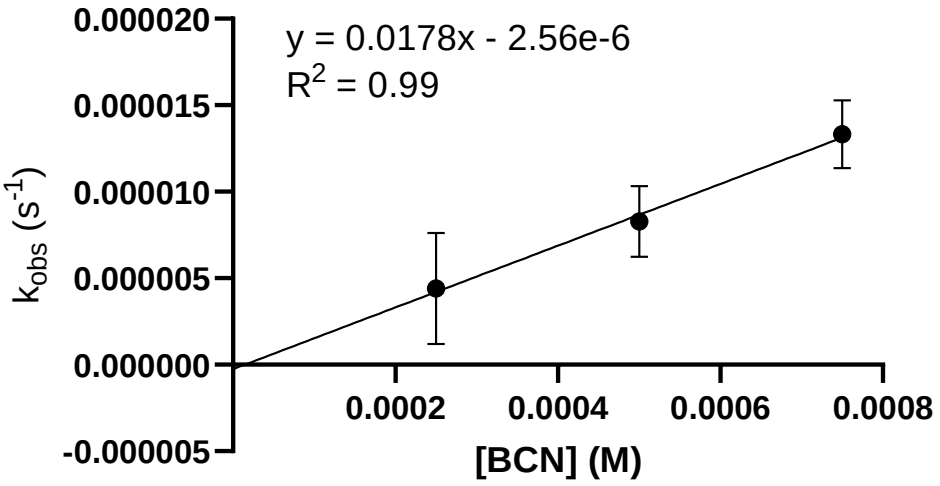

Figure B6. Pseudo first-order rate constant of the cycloaddition reaction between 5-(4-nitrophenyl)-2-phenyl-6H-1,3,4-oxadiazin-6-one (**2.14**) and endo BCN plotted against varying concentrations of BCN. These reactions were performed in ACN at 25 ± 0.1 °C. The error bars represent SD (n=2).

Table B7. Observed rate constants for the cycloaddition reaction between 5-(4-Methoxyphenyl)-2-phenyl-6H-1,3,4-oxadiazin-6-one (**2.4**) and s-TCO, with various concentrations of s-TCO in ACN at 25 ± 0.1 °C.

Pyrone	Concentration of BCN (10^{-4} M)	k_{obs} (10^{-4} s^{-1})
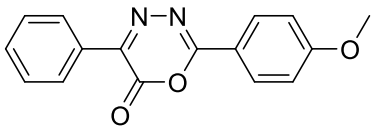 (2.12)	0.45	4.50 ± 0.00
	0.90	9.00 ± 0.00
	1.35	13.5 ± 0.00
	1.80	18.0 ± 0.00
	2.25	22.5 ± 0.00

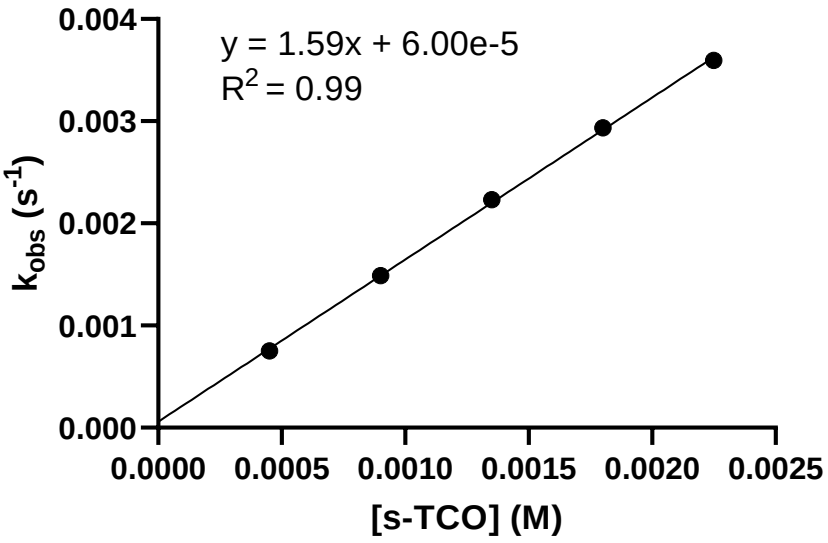

Figure B7. Pseudo first-order rate constant of the cycloaddition reaction between 5-(4-Methoxyphenyl)-2-phenyl-6H-1,3,4-oxadiazin-6-one (**2.4**) and s-TCO plotted against varying concentrations of s-TCO. These reactions were performed in ACN at 25 ± 0.1 °C. The error bars represent SD (n=2).

Table B8. Observed rate constants for the cycloaddition reaction between 5-methyl-2-phenyl-6H-1,3,4-oxadiazin-6-one (**2.6**) and endo s-TCO, with various concentrations of s-TCO in ACN at 25 ± 0.1 °C.

Pyrone	Concentration of BCN (10^{-4} M)	k_{obs} (10^{-3} s^{-1})
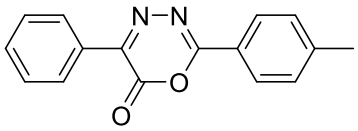 (2.8)	0.45	1.24 ± 0.00
	0.90	2.46 ± 0.00
	1.8	4.63 ± 0.00
	2.25	5.57 ± 0.00

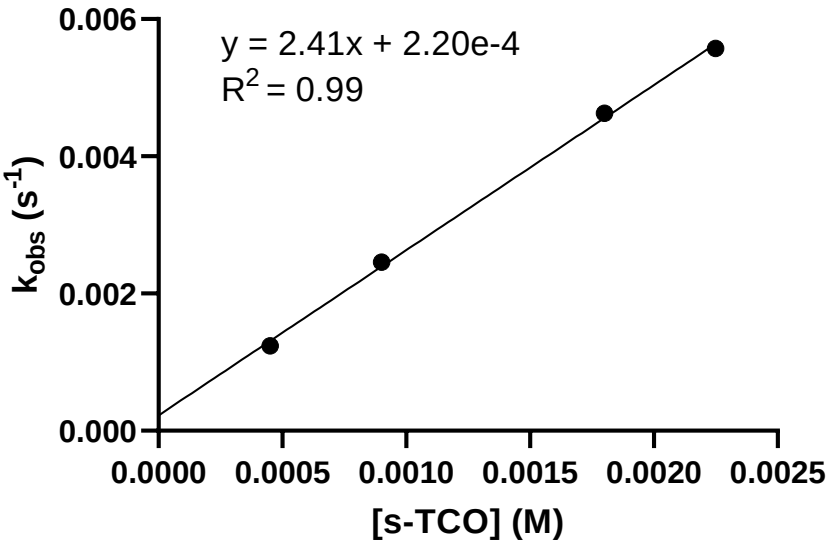

Figure B8. Pseudo first-order rate constant of the cycloaddition reaction between 5-methyl-2-phenyl-6H-1,3,4-oxadiazin-6-one (**2.6**) and s-TCO plotted against varying concentrations of s-TCO. These reactions were performed in ACN at 25 ± 0.1 °C. The error bars represent SD (n=2).

Table S9. Observed rate constants for the cycloaddition reaction between 5-phenyl-2-(4-pyridinyl)-6H-1,3,4-oxadiazin-6-one (**2.8**) and s-TCO, with various concentrations of s-TCO in ACN at 25 ± 0.1 °C.

Pyrone	Concentration of BCN (10^{-4} M)	k_{obs} (10^{-3} s^{-1})
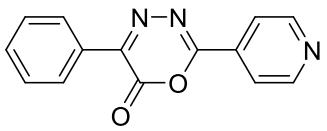 (2.16)	0.45	6.67 ± 0.00
	0.90	12.4 ± 0.00
	1.35	15.2 ± 0.03

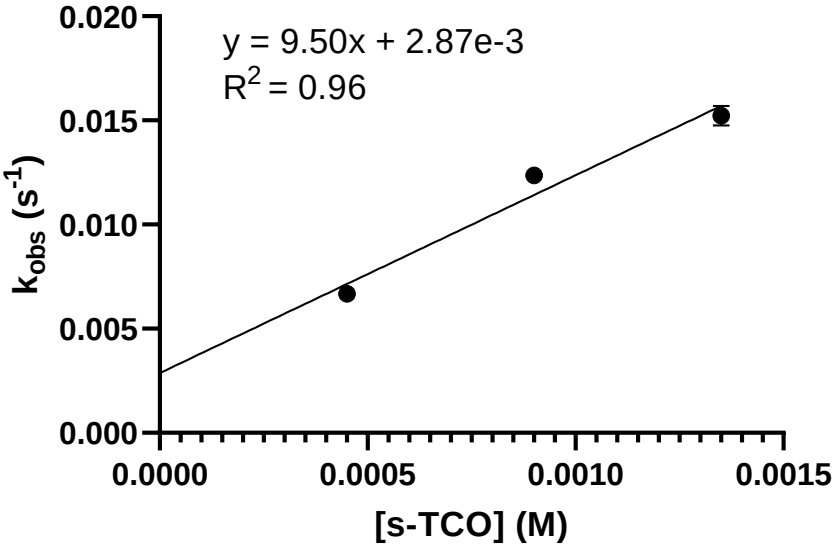

Figure B9. Pseudo first-order rate constant of the cycloaddition reaction between 5-phenyl-2-(4-pyridinyl)-6H-1,3,4-oxadiazin-6-one (**2.8**) and s-TCO plotted against varying concentrations of s-TCO. These reactions were performed in ACN at 25 ± 0.1 °C. The error bars represent SD (n=2).

Table B10. Observed rate constants for the cycloaddition reaction between 2-(4-bromophenyl)-5-phenyl-6H-1,3,4-oxadiazin-6-one (**2.10**) and s-TCO, with various concentrations of s-TCO in ACN at 25 ± 0.1 °C.

Pyrone	Concentration of BCN (10^{-4} M)	k_{obs} (10^{-3} s^{-1})
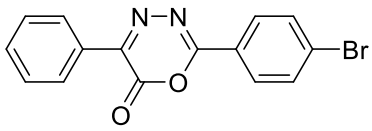 **(2.20)**	0.45	2.10 ± 0.00
	0.9	4.15 ± 0.00
	1.35	6.08 ± 0.00
	1.80	7.64 ± 0.17
	2.25	9.34 ± 0.00

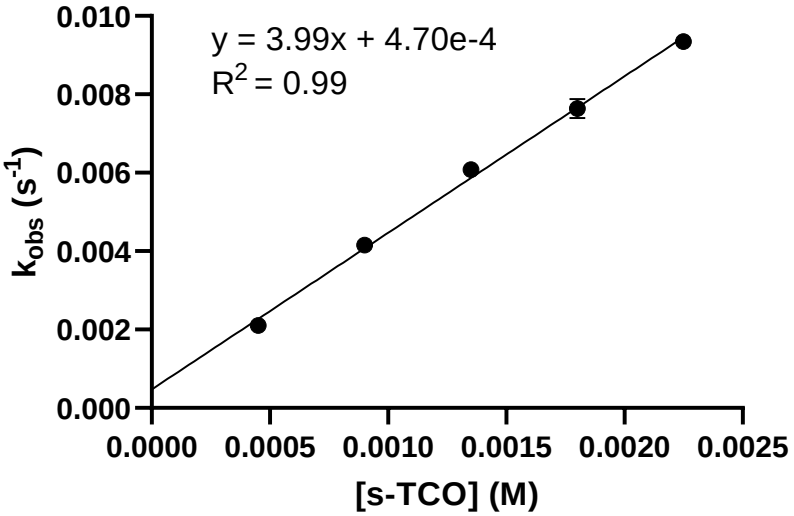

Figure B10. Pseudo first-order rate constant of the cycloaddition reaction between 2-(4-bromophenyl)-5-phenyl-6H-1,3,4-oxadiazin-6-one (**2.10**) and s-TCO plotted against varying concentrations of s-TCO. These reactions were performed in ACN at 25 ± 0.1 °C. The error bars represent SD (n=2).

Table B11. Observed rate constants for the cycloaddition reaction between 5-(4-triflouromethyl)-2-phenyl-6H-1,3,4-oxadiazin-6-one (**2.12**) and s-TCO, with various concentrations of s-TCO in ACN at 25 ± 0.1 °C.

Pyrone	Concentration of BCN (10^{-4} M)	k_{obs} (10^{-3} s^{-1})
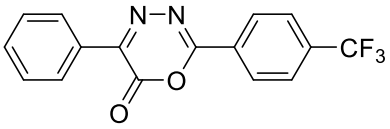 **(2.24)**	0.45	3.72 ± 0.00
	0.90	7.00 ± 0.00
	1.35	10.1 ± 0.00

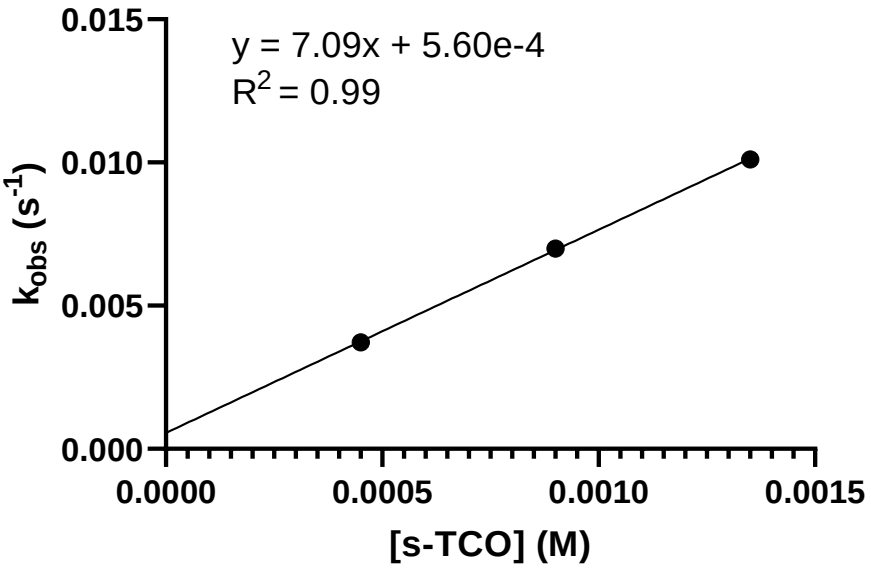

Figure B11. Pseudo first-order rate constant of the cycloaddition reaction between 5-(4-triflouromethyl)-2-phenyl-6H-1,3,4-oxadiazin-6-one (**2.12**) and s-TCO plotted against varying concentrations of s-TCO. These reactions were performed in ACN at 25 ± 0.1 °C. The error bars represent SD (n=2).

Table B12. Observed rate constants for the cycloaddition reaction between 5-(4-nitrophenyl)-2-phenyl-6H-1,3,4-oxadiazin-6-one (**2.14**) and s-TCO, with various concentrations of s-TCO in ACN at 25 ± 0.1 °C.

Pyrone	Concentration of BCN (10^{-4} M)	k_{obs} (10^{-3} s^{-1})
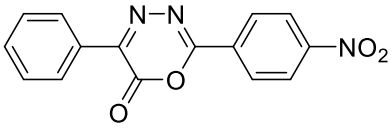 (2.28)	0.90	8.06 ± 0.00
	1.35	11.6 ± 0.00
	1.80	15.5 ± 0.00

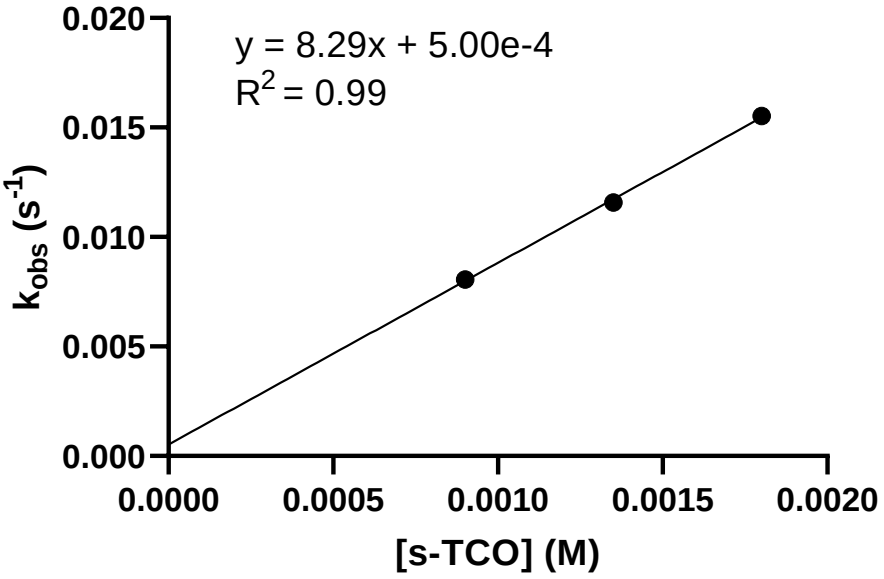

Figure B12. Pseudo first-order rate constant of the cycloaddition reaction between 5-(4-nitrophenyl)-2-phenyl-6H-1,3,4-oxadiazin-6-one (**2.14**) and s-TCO plotted against varying concentrations of s-TCO. These reactions were performed in ACN at 25 ± 0.1 °C. The error bars represent SD (n=2).